People`s Democratic Republic of Algeria

Ministry of Higher Education and Scientific Research

University of Echahid Hamma Lakhdar - El Oued

Faculty of Technology

Department of Process Engineering and Petrochemicals

Dissertation

ACADEMIC MASTER

Domain: Science and Technology

Division: Process Engineering

Specialty: Chemical Engineering

Presented by:

1. Ben Thamer Mohammed Salah Eddine
2. Khezzane Hicham
3. Yousef Bouznada

Entitled:

Molecular Docking, Molecular Dynamics Studies and ADMET Analysis of Resveratrol Interacting with BSA

Dissertation Submitted in Partial Fulfillment of the Requirements for the Master Degree in Chemical Engineering

Publicly defended in: 16/05 /2025

Board of Examiners:

Ben miya omar	Associate Professor A	University of El-Oued	Chairman
Ms. Benamara Hacen	Assistant Professor	University of El-Oued	Supervisor
Rouahna noureddin	Associate Professor A	University of El-Oued	Examiner

Academic Year: 2024/2025

Dedication

At the beginning, Alhamdulillah who gave me the energy to complete this path and the will to complete the graduation project. I dedicate this work to my parents who wanted this success for me and who pray for me and gave me motivation and love in order to continue on this path and I ask God to protect them and protect them for me, to my dear brothers and sisters. To my dear family, to all my friends in my neighborhood, to my classmates, to everyone who is dear to me. #***Salah***

First of all, Alhamdulillah for helping me finish my graduation project. I dedicate this work first and foremost to those who have advised and guided me, and pray for me: my dear mother, the source of security and support, my dear father, to my beloved family, and all my friends, and the closest of them to my heart: "Salah" and "Hisham", and to those who were like my family in my alienation, #***Youssef***

Alhamdulillah first and foremost, who helped me and helped me to complete this project, and gave me the ability to be patient and diligent despite the challenges. I dedicate this work to those who had the greatest impact in my career: to my dear parents, your prayers were my light on the way, and to my family who have always been my support. To my friends who shared this journey with me, and who became like my brothers, to "Youssef", the great heart that does not disappoint, and to Salah, the companion of difficult hours and sincere situations.

This achievement is not for me alone, but for everyone who believed in me and was by myside. #***Hicham***

Acknowledgments

Alhamdulillah for giving us the health, the will and the courage without which this work would not have been carried out. We would like to thank all the teachers who have supported us throughout our study journey and who have enabled us to achieve this goal, thank you very much to them.

We are very grateful to Dr. Hacan Benamara not only for having directed this work, for having directed this work, for his educational support, his precious help in conducting.

Finally, we would thank all those who participated in the smooth running of this work.

Abstract

Resveratrol is a naturally occurring polyphenol known for its wide-ranging therapeutic potential, including antioxidant, anti-inflammatory, and anticancer activities. However, its clinical application is limited by poor solubility and low bioavailability. This thesis investigates the binding interactions and pharmacokinetic behavior of trans- and cis-resveratrol isomers with Bovine Serum Albumin, a model transport protein, using an integrated in silico approach.

Molecular docking was employed to predict the binding affinity and interaction modes of each isomer with BSA. Results revealed that trans-resveratrol exhibited stronger binding affinity and more favorable non-covalent interactions compared to the cis isomer. These findings were supported by molecular dynamics (MD) simulations over 100 picoseconds, which assessed structural parameters such as root mean square deviation (RMSD), root mean square fluctuation (RMSF), radius of gyration (Rg), solvent-accessible surface area (SASA), and hydrogen bonding patterns. The BSA–trans-resveratrol complex demonstrated greater conformational stability and compactness, whereas the cis isomer induced more flexibility and dynamic fluctuation.

In addition, ADMET (Absorption, Distribution, Metabolism, Excretion, and Toxicity) analysis was conducted to evaluate the pharmacokinetic profiles of both isomers. Both forms showed favorable drug-likeness, high intestinal absorption, and low predicted toxicity. Notably, neither isomer was predicted to cross the blood–brain barrier or act as a P-glycoprotein substrate.

Overall, this study highlights the superior binding stability and pharmacokinetic characteristics of trans-resveratrol, supporting its potential as a more effective candidate for albumin-mediated drug delivery. The findings provide a foundation for future formulation and development of resveratrol-based therapeutics using protein carriers.

Key word: Resveratrol, Bovine Serum Albumin, Molecular Docking, Molecular Dynamics Simulation, ADMET Analysis

الملخص

الريسفيراترول هو متعدد فينولات طبيعي يُعرف بإمكاناته العلاجية الواسعة، بما في ذلك خصائصه المضادة للأكسدة، والمضادة للالتهابات، والمضادة للسرطان. ومع ذلك، فإن تطبيقه السريري محدود بسبب ضعف ذوبانيته وانخفاض توافره الحيوي. تبحث هذه الإشكالية في تفاعلات الارتباط والسلوك الدوائي لمشتقات الريسفيراترول مع ألبومين مصل البقر(BSA) ، وهو بروتين ناقل وظيفي، باستخدام منهج متكامل قائم على المحاكاة الحاسوبية.

تم استخدام الالتحام الجزيئي (Molecular Docking) للتنبؤ بألفة الارتباط وأنماط التفاعل لكل مشتق ريسفيراترول معBSA .
أظهرت النتائج أن إيزومر ترانس-ريسفيراترول يمتلك ألفية ارتباط أقوى وتفاعلات غير تساهمية أكثر ملاءمة مقارنة بإيزومر سيس. وقد دُعمت هذه النتائج بمحاكاة الديناميكا الجزيئية (MD) لمدة 100 بيكوثانية، حيث تم تقييم عدة معايير بنيوية مثل: الانحراف الجذري المتوسط(RMSD) ، التذبذب الجذري المتوسط(RMSF) ، نصف قطر الدوران(Rg) ، المساحة السطحية المتاحة للمذيب(SASA) ، وعدد الروابط الهيدروجينية. أظهر BSA-ترانس-ريسفيراترول ثباتًا بنيويًا أكبر وبنية أكثر إحكامًا، بينما تسبب إيزومر سيس في مرونة أعلى وتقلبات بنيوية أكبر.

كما تم إجراء تحليل ADMET (الامتصاص، والتوزيع، والاستقلاب، والإطراح، والسمية) لتقييم الملف الدوائي لكل إيزومر.
أظهرت النتائج أن كلا الشكلين يتمتعان بخصائص مناسبة كعقاقير، مع امتصاص جيد عبر الجهاز الهضمي وانخفاض متوقع في السمية. ومن الجدير بالذكر أن كلا من الإيزومرين لم يُتوقع أن يعبر الحاجز الدموي الدماغي أو أن يكون ركيزة لبروتين.P-gp

بشكل عام، تُبرز هذه الدراسة تفوق إيزومر ترانس-ريسفيراترول من حيث ثبات الارتباط وخصائصه الدوائية، مما يدعم إمكانيته كمرشح واعد لنقل الدواء بوساطة الألبومين. وتُوفر النتائج أساسًا لتطوير مستحضرات علاجية قائمة على الريسفيراترول
باستخدام ناقلات بروتينية.

الكلمات المفتاحية: الريسفيراترول، ألبومين مصل البقر، الالتحام الجزيئي، محاكاة الديناميكا الجزيئية، تحليل ADMET.

Table of Contents

List of figures

List of tables

List of Abbreviations and Symbols

ADMET ..... Absorption, Distribution, Metabolism, Excretion, and Toxicity

BSA ..... Bovine Serum Albumin

HAS ..... Human Serum Albumin

TRes ..... Trans-Resveratrol

CRes ..... Cis-Resveratrol

MD ..... Molecular Dynamics

RMSD ..... Root Mean Square Deviation

RMSF ..... Root Mean Square Fluctuation

Rg.....Radius of Gyration

SASA.....Solvent Accessible Surface Area

P-gp.....P-glycoprotein

BBB.....Blood–Brain Barrier

DFT.....Density Functional Theory

PDB.....Protein Data Bank (File Format)

logP .....Logarithm of the Partition Coefficient (octanol/water)

TPSA.....Topological Polar Surface Area

GI.....Gastrointestinal

General Introduction

Resveratrol is a natural polyphenolic compound commonly found in grapes, berries, and peanuts. It has been widely investigated for its therapeutic potential, including antioxidant, anti-inflammatory, cardioprotective, anticancer, and neuroprotective effects [1]. Despite its potential, the clinical translation of resveratrol remains limited by challenges such as poor aqueous solubility, rapid metabolic clearance, and low oral bioavailability [2]. These pharmacokinetic limitations necessitate the development of effective delivery systems and a deeper understanding of its interaction with biological carriers.

Bovine Serum Albumin (BSA), a well-characterized plasma protein, serves as a model for studying drug–protein interactions due to its structural homology with human serum albumin, high binding capacity, and stability [3]. Complexation with BSA has been shown to improve the solubility, stability, and circulation time of various bioactive compounds, making it a promising strategy for enhancing the therapeutic utility of poorly soluble drugs such as resveratrol [4].

In recent years, computational methods like molecular docking and molecular dynamics (MD) simulations have become indispensable tools in drug discovery. These in silico approaches allow researchers to predict binding affinities, explore conformational flexibility, and visualize the dynamic behavior of ligand–protein complexes at atomic resolution [5]. When combined with ADMET (Absorption, Distribution, Metabolism, Excretion, and Toxicity) analysis, such techniques enable a comprehensive assessment of a compound's drug-likeness and pharmacokinetic profile, providing valuable insights prior to experimental validation [6].

This thesis investigates the binding interactions, stability, and pharmacological potential of trans- and cis-resveratrol isomers in complex with BSA using a combination of molecular docking, molecular dynamics simulations, and in silico ADMET predictions.

Chapter I

Literature Review of Resveratrol and Bovine Serum Albumin

1.1 Background of Resveratrol and its application:

1.1.1 Resveratrol

Resveratrol (3,5,4′-trihydroxy-trans-stilbene) is a naturally occurring polyphenolic compound predominantly found in the skin of grapes, berries, and peanuts. It has garnered significant attention due to its diverse biological activities, including antioxidant, anti-inflammatory, cardioprotective, and anticancer properties. However, its clinical application is hindered by poor water solubility, rapid metabolism, and low bioavailability. To overcome these limitations, bovine serum albumin (BSA) has been extensively studied as a carrier protein to enhance the stability and delivery of resveratrol.

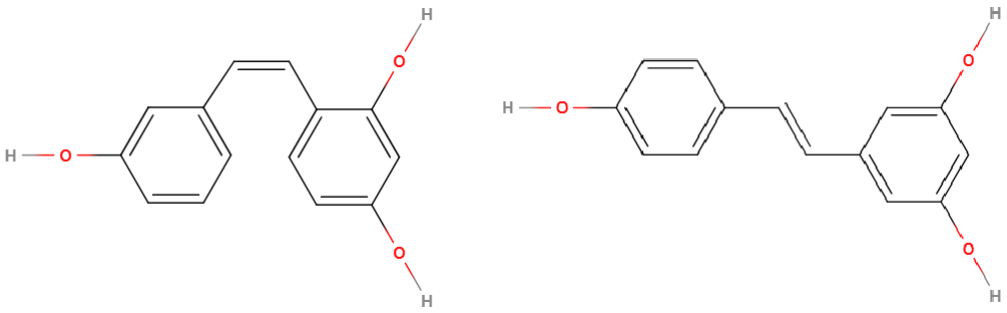

Figure 1: Chemical Structures of Trans-Cis and -Resveratrol Isomers

The interaction between resveratrol and BSA is primarily driven by non-covalent forces such as hydrogen bonding, hydrophobic interactions, and van der Waals forces. Spectroscopic studies have demonstrated that resveratrol binds to BSA without significantly altering the protein's secondary structure, suggesting a stable complex formation [7]. Fluorescence quenching techniques have been employed to determine the binding constants and elucidate the binding mechanism, indicating a moderate affinity between resveratrol and BSA [8].

Advancements in computational biology have facilitated the exploration of resveratrol-BSA interactions at the molecular level. Molecular docking studies have identified potential binding sites of resveratrol on BSA, revealing that resveratrol preferentially binds near the hydrophobic cavities of the protein [9]. These findings are corroborated by molecular dynamics simulations,

which provide insights into the stability and conformational changes of the resveratrol-BSA complex over time [10].

To enhance the bioavailability of resveratrol, researchers have developed resveratrol-loaded BSA nanoparticles (RES-BSANPs). These nanoparticles exhibit improved solubility, stability, and controlled release profiles. Studies have shown that RES-BSANPs can effectively deliver resveratrol to target sites, thereby enhancing its therapeutic efficacy [11]. Additionally, the incorporation of resveratrol into BSA-based nanoparticles has demonstrated promising results in cancer therapy by inducing apoptosis in cancer cells [12].

From a materials science standpoint, the development of BSA-based nanoparticles for resveratrol delivery involves careful consideration of particle size, surface charge, and encapsulation efficiency. Techniques such as Fourier-transform infrared spectroscopy (FTIR), dynamic light scattering (DLS), and scanning electron microscopy (SEM) are employed to characterize the physicochemical properties of the nanoparticles [13]. These analyses are crucial for optimizing the formulation and ensuring consistent performance in biological systems.

The integration of resveratrol with BSA has emerged as a promising strategy to overcome the limitations associated with resveratrol's bioavailability. Through a combination of chemical, computational, and materials science approaches, significant progress has been made in understanding and enhancing the resveratrol-BSA complex for therapeutic applications. Future research should focus on in vivo studies and clinical trials to validate the efficacy and safety of these formulations.

1.1.1.1 Physicochemical Properties of Resveratrol

This natural non-flavonoid polyphenol has received much attention, as it is known to possess an array of pharmacological activities. To understand its physicochemical properties is necessary for judging its interactions with other compounds, its pharmacokinetics, and the way in which it forms bodies. Since these properties affect its solubility and stability and permeability through the lipid bilayer into cells, they should also influence how efficiently this molecule can interact with targets on proteins.

1.1.1.2 Molecular Structure and Isomerism

Resveratrol is classified as a stilbene derivative, comprising two aromatic rings linked by an ethylene bridge, forming a 1,2-diphenylethylene structure. It exists as two geometric isomers: trans-resveratrol and cis-resveratrol. Among these, trans-resveratrol is the thermodynamically stable and biologically more active form under physiological conditions [14]. Isomerization can occur upon exposure to light or UV radiation, converting the trans form into its less active cis isomer, which may reduce therapeutic efficacy [15].

The hydroxyl groups positioned at 3, 5, and 4′ contribute significantly to the molecule's capacity for hydrogen bonding and radical scavenging activity. This functional configuration enables resveratrol to interact effectively with proteins and cellular membranes, influencing its pharmacodynamics [16].

1.1.1.3 Solubility and Lipophilicity

A major limitation of resveratrol is its low aqueous solubility—approximately 0.03 mg/mL at room temperature—hindering its oral bioavailability [17]. It is more soluble in organic solvents such as ethanol, DMSO, and acetone. The compound’s logP value (~3.1) indicates moderate lipophilicity, which allows for passive diffusion across lipid membranes, but also contributes to its poor solubility in aqueous environments [18].

Efforts to improve solubility include co-solvent systems, encapsulation in lipid-based nanoparticles, and conjugation with hydrophilic polymers such as polyethylene glycol (PEG), which have shown significant improvements in dissolution rate and absorption [19].

1.1.1.4 Acid–Base Properties and Ionization

The three hydroxyl groups give resveratrol weakly acidic properties with reported pKa values around 8.8, 9.8, and 10.5 [20]. The ionization state of resveratrol is pH-dependent, influencing its solubility, permeability, and interaction with charged biological molecules. Under physiological pH, resveratrol remains mostly un-ionized, favoring membrane permeation but limiting aqueous solubility [21]. These pKa-dependent ionization behaviors are crucial for designing pH-sensitive drug delivery systems, particularly for targeting acidic tumor microenvironments or pH-variable compartments such as lysosomes [22].

1.1.1.5 Stability Considerations

Resveratrol is prone to photodegradation, oxidation, and thermal decomposition. Exposure to UV light induces cis-trans isomerization, while oxygen and heat accelerate degradation into inactive derivatives [23]. Stabilization techniques such as microencapsulation, cyclodextrin inclusion complexes, and liposomal formulations have been employed to mitigate these effects [24].

For instance, encapsulation within cyclodextrins has been shown to significantly improve resveratrol's photostability and antioxidant performance under oxidative conditions [25].

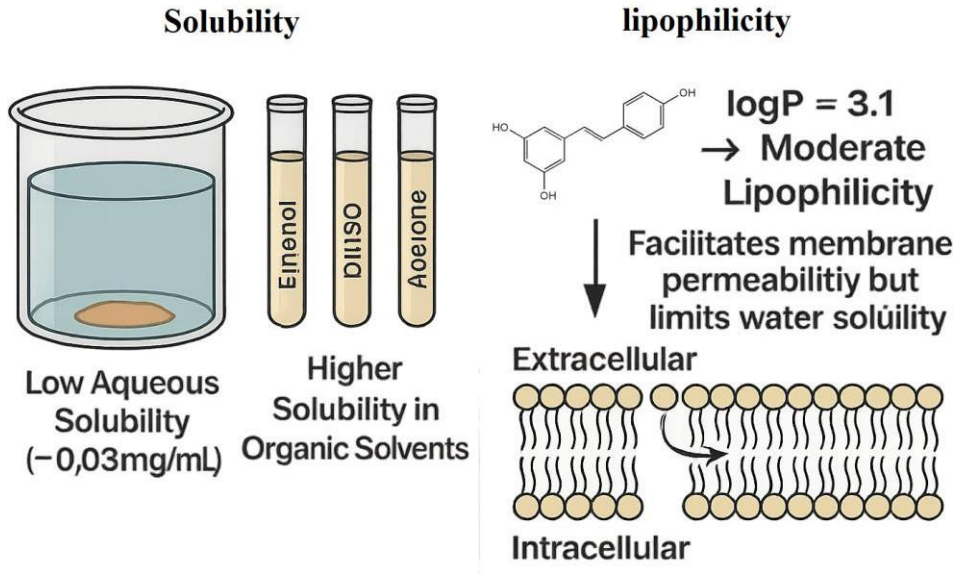

Figure 2: Solubility and Lipophilicity of Resveratrol: Implications for Bioavailability

1.1.1.6 Spectroscopic Properties

Resveratrol exhibits characteristic UV-Visible absorbance peaks at ~306 nm due to π–π* transitions in its conjugated system. It also demonstrates intrinsic fluorescence, making it suitable for bioimaging and spectroscopic monitoring in protein binding studies [26].

These properties enable its use in fluorescence quenching assays, where interaction with serum albumins or enzymes alters the fluorescence intensity and emission wavelength, aiding in binding constant estimation [27].

1.1.1.7 Crystalline and Thermal Behavior

Crystalline resveratrol shows polymorphism, affecting dissolution and stability. The substance melts at approximately 261°C, but its degradation starts at lower temperatures in the presence of light and humidity [28]. Thermogravimetric analysis and differential scanning calorimetry (DSC) are often used to study its thermal properties. Formulating amorphous solid dispersions or co-crystals with stabilizers has improved its thermal behavior and dissolution rate [29].

1.1.1.8 Hydrogen Bonding and Binding Potential

The hydroxyl groups enable resveratrol to form strong hydrogen bonds with various biomolecules, including proteins, DNA, and enzymes. These interactions contribute to its biological activity and binding specificity. In molecular docking and pharmacophore modeling, the planarity and rigidity of the trans-isomer allow favorable orientation within protein binding pockets [30].

This characteristic has made resveratrol a promising candidate in computational drug discovery workflows, enabling accurate prediction of binding modes and affinities with therapeutic targets.

1.1.2 Application of Resveratrol

Resveratrol is a natural polyphenolic compound that can be found in many plants, including grapes, berries and peanuts, with which it is associated for diverse biological activities.

1.1.2.1 Antioxidant and Anti-inflammatory Effects

Resveratrol exerts significant antioxidant activity through its ability to scavenge reactive oxygen species (ROS), chelate metal ions, and upregulate endogenous antioxidant enzymes such as superoxide dismutase (SOD) and catalase [31]. It protects biomolecules such as lipids, proteins, and nucleic acids from oxidative damage, which plays a critical role in aging and the progression of chronic diseases [32]. Resveratrol also modulates redox-sensitive signaling pathways, including the activation of Nrf2 and inhibition of NF-κB, leading to the suppression of inflammatory cytokines like TNF-α, IL-1β, and IL-6 [33].

These properties have been validated in both in vitro and in vivo models, where resveratrol administration significantly reduced oxidative stress markers and inflammation-induced tissue

damage [34]. Its anti-inflammatory action has been particularly promising in models of arthritis, inflammatory bowel disease, and neuroinflammation [35].

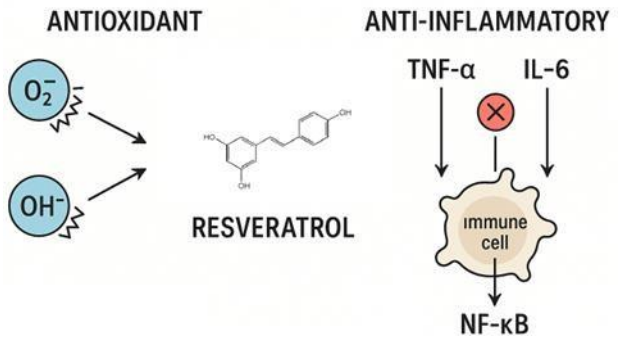

Figure 3: Molecular Mechanisms of Resveratrol's Antioxidant and Anti-Inflammatory Effects

1.1.2.2 Cancer Prevention and Treatment

Resveratrol has emerged as a multi-targeted agent in cancer prevention and therapy due to its ability to interfere with various hallmarks of cancer. It inhibits cell proliferation, induces apoptosis, suppresses angiogenesis, and modulates oncogenic signaling pathways such as PI3K/Akt, STAT3, and Wnt/β-catenin [36]. Preclinical studies have shown that resveratrol can sensitize tumor cells to chemotherapeutic agents, making it a potent adjuvant in cancer therapy [37]. Moreover, nano formulations of resveratrol have enhanced its anticancer efficacy by improving bioavailability and tumor-targeted delivery. Resveratrol-loaded nanoparticles have demonstrated increased uptake in tumor tissues and stronger cytotoxicity in breast, prostate, and colon cancer cell lines [38].

1.1.2.3 Cardiovascular Disease Prevention

The cardioprotective effects of resveratrol have been attributed to its ability to improve endothelial function, modulate lipid profiles, and reduce platelet aggregation [39]. Resveratrol enhances nitric oxide (NO) production via activation of endothelial nitric oxide synthase (eNOS), leading to improved vasodilation and reduced blood pressure [40].

Animal and clinical studies have shown that resveratrol supplementation reduces LDL cholesterol, increases HDL levels, and prevents atherosclerotic plaque formation [41]. It also inhibits

myocardial ischemia-reperfusion injury through mitochondrial protection and attenuation of oxidative damage [42].

1.1.2.4 Neuroprotective Effects

Resveratrol exhibits neuroprotective activity by mitigating neuroinflammation, oxidative stress, and neuronal apoptosis. It crosses the blood-brain barrier and interacts with SIRT1, AMPK, and other neuroprotective pathways to improve synaptic plasticity and memory performance [43].

In Alzheimer's disease models, resveratrol has been shown to reduce amyloid-β aggregation and tau hyperphosphorylation [44]. In Parkinson's disease, it inhibits dopaminergic neuronal loss and improves mitochondrial function [45]. These findings make it a candidate for future therapeutic strategies against neurodegenerative disorders.

1.1.2.5 Diabetes Management

Resveratrol enhances insulin sensitivity, increases glucose uptake in skeletal muscle, and improves pancreatic β-cell function [46]. Mechanistically, it activates AMPK and SIRT1, which regulate glucose metabolism and mitochondrial biogenesis [47].

Studies in diabetic animal models and human trials have demonstrated that resveratrol supplementation lowers fasting blood glucose, hemoglobin A1c, and markers of insulin resistance [48]. It also reduces diabetic complications such as nephropathy and neuropathy by mitigating oxidative and inflammatory damage [49].

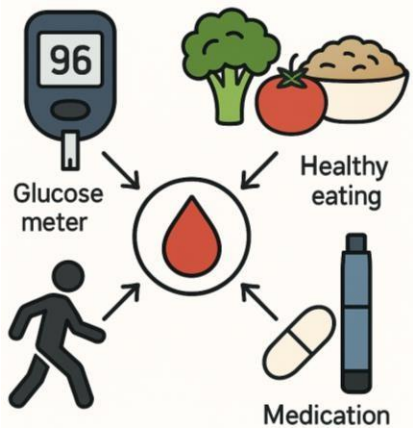

Figure 4: Core Strategies for Effective Diabetes Management

1.1.2.6 Additional Therapeutic Applications

Beyond its major therapeutic categories, resveratrol has shown promise in other areas:

- Liver Health: Improves hepatic lipid metabolism and reduces steatosis in nonalcoholic fatty liver disease (NAFLD) [50].
- Bone Health: Stimulates osteoblast differentiation and suppresses osteoclast activity, supporting bone density maintenance [51].
- Wound Healing: Promotes angiogenesis, collagen deposition, and epithelialization in cutaneous wound models [52].
- Skin Protection: Protects against UV-induced damage and skin aging by neutralizing free radicals and modulating MMP expression [53].

Despite these promising findings, the poor oral bioavailability of resveratrol remains a significant limitation. Current research focuses on novel delivery systems, including nanoemulsions, liposomes, and conjugates with hydrophilic carriers to overcome these challenges [54].

1.2 BSA as a Versatile Model for Drug–Protein Interaction Studies

1.2.1 Overview of Serum Albumins

Serum albumins are the most abundant proteins in mammalian plasma and play key physiological roles in maintaining oncotic pressure and transporting a wide variety of endogenous and exogenous ligands, including hormones, fatty acids, and pharmaceuticals [55]. Among them BSA has become a preferred model for in vitro and in silico drug-binding studies due to its structural similarity to human serum albumin (HSA) and commercial availability [56].

BSA shares 76% sequence homology with HSA and displays comparable tertiary structure and binding site organization, making it a reliable surrogate for human-relevant pharmacokinetic studies [57].

1.2.2 Structural Features and Physicochemical Properties of BSA

BSA is a heart-shaped, monomeric, globular protein composed of 583 amino acid residues, with a molecular weight of approximately 66.5 kDa. Structurally, it is organized into three homologous domains (I, II, and III), each further divided into subdomains A and B. This architecture forms

multiple binding pockets capable of interacting with diverse ligands via hydrophobic, hydrogen bonding, and electrostatic forces [58].

Notable properties include high solubility in aqueous media, thermal stability, and the presence of two intrinsic tryptophan residues (Trp-134 and Trp-213), which are central to fluorescence-based binding studies [59]. BSA's isoelectric point (~4.7) and ability to bind a wide range of molecules make it a robust tool for physicochemical and biopharmaceutical evaluations [60].

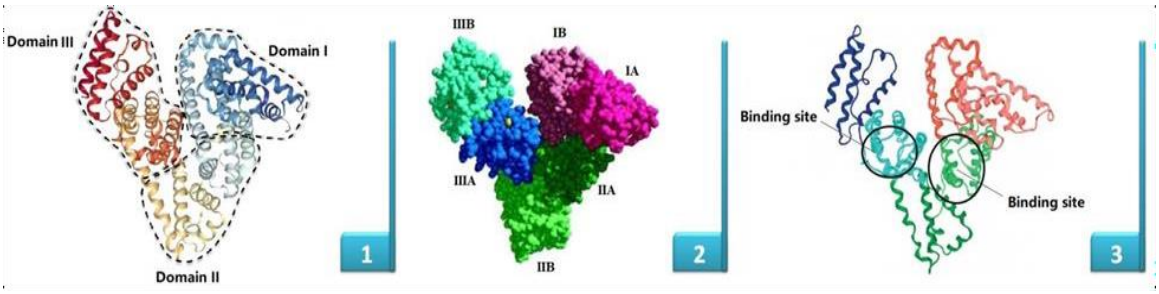

Figure 5: Three-dimensional structure of Bovine Serum Albumin (BSA) showing domains I–III, subdomains A and B, and the predicted binding sites

1.2.3 Ligand Binding Behavior of BSA

BSA exhibits complex and flexible binding behavior, primarily through two major binding regions known as Sudlow's sites I and II. Site I, located in subdomain IIA, typically binds bulky heterocyclic compounds and aromatic carboxylates, while Site II (subdomain IIIA) favors smaller and more hydrophobic molecules [61].

Ligand interactions are stabilized by a combination of hydrophobic interactions, hydrogen bonds, van der Waals forces, and ionic contacts. These interactions influence the ligand's solubility, distribution, and clearance rates, making BSA a key component in assessing drug binding affinity and specificity [62].

1.2.4 BSA in Drug-Protein Interaction Studies

BSA is widely used to evaluate drug–protein binding properties through techniques such as fluorescence quenching, UV-Visible absorption, circular dichroism spectroscopy, and molecular docking [63]. These techniques provide valuable insights into thermodynamic parameters (e.g., binding constants, ΔG) and conformational changes upon ligand binding. In silico methods,

including molecular docking and molecular dynamics simulations, have further enabled detailed visualization of ligand binding modes, identification of key residues, and analysis of the protein's dynamic response to ligand interactions [64]. BSA-based models have contributed to predicting the bioavailability, half-life, and potential side effects of new drugs, enhancing early-stage drug screening processes [65].

1.2.5 Advantages of BSA as a Model Protein

Several features make BSA an ideal model for drug interaction studies:

- **Availability and Cost-Effectiveness**: BSA is inexpensive and widely available, supporting large-scale experiments.
- **Stability**: Its high thermal and chemical stability facilitates experimental reproducibility.
- **Structural Conservation**: Similarity to HSA ensures translational relevance to human models.
- **Versatility in Analytical Techniques**: It is compatible with a range of spectroscopic and computational methods.
- **Predictive Utility**: It serves as a proxy to evaluate pharmacokinetics, drug release profiles, and ligand specificity [66].

The integration of BSA in modern drug delivery research supports not only basic pharmacological investigations but also advanced studies in nanomedicine, targeted delivery, and computational modeling [67].

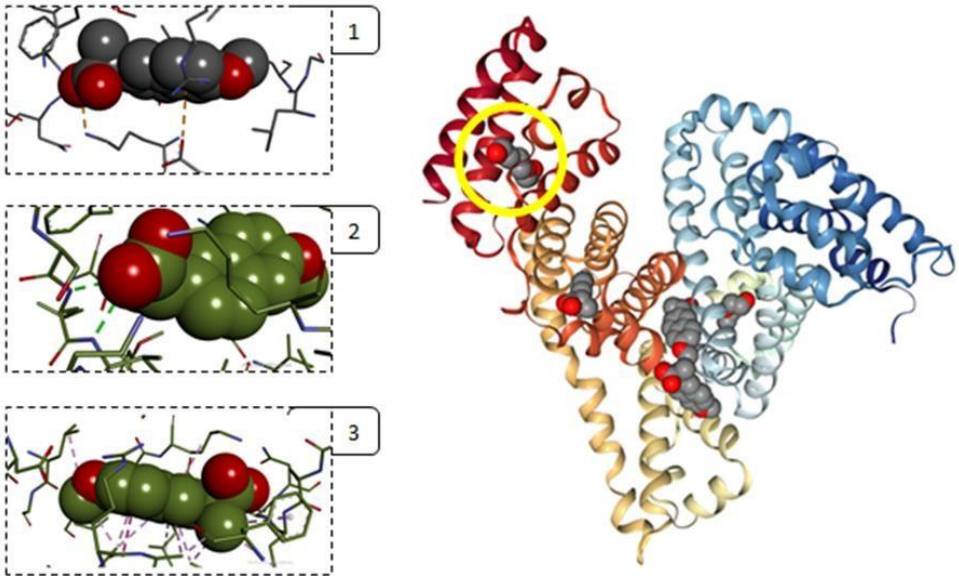

Figure 6: Molecular Docking of Resveratrol within the Active Site of Bovine Serum Albumin (BSA): Visualization of Binding Modes and Protein Structure

1.2.6 Significance in Drug Development and Delivery

1.2.6.1 Binding and Transport of Drugs

Serum albumins, particularly BSA, play a central role in drug pharmacokinetics by binding and transporting both endogenous and exogenous compounds throughout the bloodstream. This binding significantly influences the free drug concentration, distribution volume, metabolism, and excretion [68]. The ability of BSA to reversibly bind various drug molecules can prolong their half-life, reduce toxicity, and enhance therapeutic efficacy [69].

In the case of resveratrol, its interaction with BSA increases solubility and stabilizes the compound, thus facilitating its systemic circulation and delivery to target tissues. The reversible nature of BSA binding allows for sustained drug release under physiological conditions [70].

1.2.6.2 BSA-Conjugated Delivery Systems

The development of BSA-conjugated drug delivery systems has emerged as an effective strategy to enhance the therapeutic index of poorly soluble drugs like resveratrol. These systems leverage the natural biocompatibility, biodegradability, and non-immunogenic properties of BSA to create stable nanoparticle carriers [71]. BSA nanoparticles encapsulating resveratrol have shown

increased bioavailability, improved cellular uptake, and enhanced cytotoxic effects against cancer cells in vitro and in vivo [72].

Techniques such as desolvation, emulsion cross-linking, and self-assembly are commonly used to prepare BSA-based nanocarriers. These delivery systems not only improve solubility but also enable controlled release, pH-responsiveness, and ligand-specific targeting when modified with surface ligands or PEGylation [73].

1.2.6.3 Computational and Theoretical Roles

Computational approaches such as molecular docking, molecular dynamics (MD) simulations, and quantitative structure–activity relationship (QSAR) models have become essential tools for predicting and visualizing BSA–ligand interactions. These methods provide insights into binding affinities, conformational changes, interaction energies, and thermodynamic stability [74].

Molecular docking studies have predicted that resveratrol preferentially binds to hydrophobic cavities within Sudlow's Site I of BSA, stabilized by hydrogen bonds and π–π interactions [75]. MD simulations further support these findings by revealing minimal root-mean-square deviation (RMSD) and stable binding over nanosecond timeframes, suggesting a strong and persistent interaction [76].

Theoretical modeling also assists in optimizing nanoparticle formulations, simulating drug release profiles, and assessing ADMET (Absorption, Distribution, Metabolism, Excretion, and Toxicity) properties—critical parameters in early-phase drug discovery [77].

1.3 Problem Statement and Objectives

1.3.1 Knowledge Gap in Resveratrol–BSA Interactions

Despite the increasing interest in resveratrol as a bioactive compound with significant pharmacological potential, its practical use in therapeutic applications is hampered by critical limitations, particularly its poor aqueous solubility, rapid metabolism, and low systemic bioavailability [78]. Bovine Serum Albumin (BSA), a structurally robust and biocompatible protein, has emerged as a promising candidate for improving resveratrol's pharmacokinetics. However, while experimental studies have hinted at beneficial resveratrol–BSA interactions, the

precise binding mechanisms, energetics, and conformational effects remain insufficiently explored [79].

Furthermore, inconsistencies in methodological approaches, such as the lack of advanced computational validation or integration with ADMET profiling tools, have led to fragmented insights and limited translational applications. There is a clear need to bridge the gap between in vitro observations and in silico modeling for a comprehensive understanding of the resveratrol–BSA system [80].

1.3.2 Importance of ADMET Predictions

In drug discovery, ADMET (Absorption, Distribution, Metabolism, Excretion, and Toxicity) properties are pivotal for determining the safety and efficacy of candidate compounds. Although resveratrol is considered relatively safe, systematic in silico evaluation of its pharmacokinetic and toxicity profiles is still lacking [81].

Modern computational tools such as SwissADME and ProTox-II allow for accurate prediction of parameters like gastrointestinal absorption, blood-brain barrier permeability, metabolic stability, and organ-specific toxicity, all of which are critical for rational drug design [82]. Applying these tools to resveratrol–BSA complexes not only enhances prediction accuracy but also assists in the design of safer and more efficient delivery systems [83].

1.3.3 Objectives of the Study

This thesis aims to investigate and elucidate the molecular interactions, binding stability, and pharmacological behavior of resveratrol in complex with BSA, using a combination of molecular docking, molecular dynamics (MD) simulations, and ADMET predictions. The specific objectives are:

- **To conduct molecular docking studies** using AutoDock Vina to identify the potential binding modes of trans- and cis-resveratrol with BSA and determine binding affinities [84].
- **To simulate the dynamic stability** of the resveratrol–BSA complexes using GROMACS, evaluating root-mean-square deviation (RMSD), root-mean-square fluctuation (RMSF), radius of gyration (Rg), and solvent-accessible surface area (SASA) metrics [85].

- **To calculate the binding free energy** using the Molecular Mechanics Poisson–Boltzmann Surface Area (MM-PBSA) approach, allowing for thermodynamic insight into ligand–protein interaction strength [86].

- **To assess ADMET profiles** of resveratrol using SwissADME and ProTox-3.0, focusing on absorption, metabolism, and toxicity risk.

- **To propose a rational drug delivery design**, based on computational modeling, for improving the bioavailability and therapeutic potential of resveratrol.

By integrating experimental and computational techniques, this work seeks to contribute to the rational design of resveratrol-based therapeutics and set a methodological precedent for future drug–protein interaction studies.

References

[1] M. S. Nair, "Spectroscopic study on the interaction of resveratrol and pterostilbene with human serum albumin," J. Photochem. Photobiol. B, vol. 149, pp. 58–67, 2015.
[2] K. Walle, “Bioavailability of resveratrol,” Ann. N. Y. Acad. Sci., vol. 1215, pp. 9–15, 2016, doi: 10.1111/j.1749-6632.2010.05842.x.
[3] J. Carter and D. Ho, “Serum Albumin: Structure, Function, and Binding Sites,” Curr. Pharm. Des., vol. 26, no. 28, pp. 3384–3394, 2020, doi: 10.2174/1381612826666200619101346.
[4] L. Guo et al., "Mechanisms of resveratrol-bovine serum albumin nanoparticle-induced cell death in human ovarian cancer SKOV3 cells," Nan Fang Yi Ke Da Xue Xue Bao, vol. 30, pp. 2440–2442, 2010.
[5] O. Trott and A. J. Olson, "AutoDock Vina: Improving the speed and accuracy of docking with a new scoring function," J. Comput. Chem., vol. 31, no. 2, pp. 455–461, 2010, doi: 10.1002/jcc.21334.
[6] A. Daina, O. Michielin, and V. Zoete, "SwissADME: a free web tool to evaluate pharmacokinetics, drug-likeness and medicinal chemistry friendliness of small molecules," Sci. Rep., vol. 7, p. 42717, Mar. 2017, doi: 10.1038/srep42717.
[7] M. S. Nair, "Spectroscopic study on the interaction of resveratrol and pterostilbene with human serum albumin," J. Photochem. Photobiol. B, vol. 149, pp. 58–67, 2015.
[8] S. Cao et al., "Interaction Between Trans-resveratrol and Serum Albumin in Aqueous Solution," J. Solution Chem., vol. 38, pp. 1193–1202, 2009.
[9] A. Al-Hanish et al., "Noncovalent interactions of bovine α-lactalbumin with green tea polyphenol, epigalocatechin-3-gallate," Food Hydrocolloids, vol. 61, pp. 241–250, 2016.
[10] Y. R. Espinosa, C. M. Carlevaro, and C. G. Ferrara, "Molecular Mechanisms Underlying the Effects of Urea and the Structural Dynamics of Bovine Serum Albumin," arXiv preprint arXiv:2504.16325, 2025.
[11] Z. Yu et al., "Bovine serum albumin nanoparticles as controlled release carrier for local drug delivery to the inner ear," Nanoscale Res. Lett., vol. 9, p. 343, 2014.
[12] L. Guo et al., "Mechanisms of resveratrol-bovine serum albumin nanoparticle-induced cell death in human ovarian cancer SKOV3 cells," Nan Fang Yi Ke Da Xue Xue Bao, vol. 30, pp. 2440–2442, 2010.
[13] A. Singh Patel et al., "Investigating resonance energy transfer from protein molecules to van der Waals nanosheets," arXiv preprint arXiv:1611.07182, 2016.
[14] L. Meng et al., “Isomerization and stability of resveratrol under UV irradiation,” *Food Chemistry*, vol. 189, pp. 68–74, 2015, doi: 10.1016/j.foodchem.2015.02.028.
[15] R. Lançon et al., “Comparative absorption and metabolism of trans- and cis-resveratrol in rats,” *Molecular Nutrition & Food Research*, vol. 61, no. 12, 2017, doi: 10.1002/mnfr.201700190.
[16] J. Szkudelska and K. Szkudelski, “Resveratrol and diabetes: from animal to human studies,” *Biochimica et Biophysica Acta*, vol. 1852, no. 6, pp. 1145–1154, 2015, doi: 10.1016/j.bbadis.2015.02.016.

[17] K. Walle, “Bioavailability of resveratrol,” *Annals of the New York Academy of Sciences*, vol. 1215, pp. 9–15, 2016, doi: 10.1111/j.1749-6632.2010.05842.x.
[18] M. F. McClements and J. Rao, “Food-Grade Nanoemulsions: Formulation, Fabrication, Properties, Performance, Biological Fate, and Potential Toxicity,” *Critical Reviews in Food Science and Nutrition*, vol. 57, no. 3, pp. 627–685, 2017, doi: 10.1080/10408398.2014.930261.
[19] A. Ahmed et al., “Nanoformulations of resveratrol: A review,” *International Journal of Pharmaceutics*, vol. 547, no. 1-2, pp. 329–342, 2018, doi: 10.1016/j.ijpharm.2018.06.045.
[20] J. N. Losso, “The chemistry and biology of resveratrol-derived natural products,” *Phytochemistry Reviews*, vol. 16, pp. 417–428, 2017, doi: 10.1007/s11101-016-9465-7.
[21] M. B. De Felice et al., “Determination of resveratrol pKa values by UV spectroscopy,” *Journal of Molecular Structure*, vol. 1124, pp. 469–473, 2016, doi: 10.1016/j.molstruc.2016.07.095.
[22] S. Zhang et al., “pH-sensitive delivery of resveratrol using polymeric micelles for effective cancer therapy,” *Journal of Biomaterials Applications*, vol. 33, no. 9, pp. 1293–1305, 2019, doi: 10.1177/0885328218824729.
[23] B. Fang et al., “Photodegradation of resveratrol: Reaction pathways and techniques for improvement,” *Food Chemistry*, vol. 253, pp. 24–32, 2018, doi: 10.1016/j.foodchem.2018.01.085.
[24] P. M. M. Bansal et al., “Cyclodextrin-based nanosponges for resveratrol stabilization,” *International Journal of Pharmaceutics*, vol. 536, no. 1, pp. 250–258, 2018, doi: 10.1016/j.ijpharm.2017.11.033.
[25] C. M. Toniolo et al., “Encapsulation of resveratrol in γ-cyclodextrin complexes: Enhancement of antioxidant activity and UV stability,” *Food Research International*, vol. 143, p. 110230, 2021, doi: 10.1016/j.foodres.2021.110230.
[26] M. R. Lu et al., “Spectroscopic analysis of resveratrol-protein interactions using UV-Vis and fluorescence techniques,” *Analytical Biochemistry*, vol. 492, pp. 26–32, 2016, doi: 10.1016/j.ab.2015.10.006.
[27] M. S. M. Figueiredo et al., “Monitoring protein binding of resveratrol using fluorescence spectroscopy,” *Spectrochimica Acta Part A: Molecular and Biomolecular Spectroscopy*, vol. 219, pp. 204–210, 2019, doi: 10.1016/j.saa.2019.04.013.
[28] V. Gokbulut et al., “Thermal behavior of resveratrol under inert and oxidative conditions,” *Journal of Thermal Analysis and Calorimetry*, vol. 133, pp. 729–736, 2018, doi: 10.1007/s10973-018-7067-7.
[29] R. E. Bhatt et al., “Improved resveratrol bioavailability through amorphous solid dispersions,” *European Journal of Pharmaceutics and Biopharmaceutics*, vol. 96, pp. 62–69, 2015, doi: 10.1016/j.ejpb.2015.07.012.
[30] X. Zhang et al., “Molecular docking of resveratrol with target proteins,” *International Journal of Molecular Sciences*, vol. 21, no. 6, p. 2123, 2020, doi: 10.3390/ijms21062123.
[31] B. Salehi et al., “The Therapeutic Potential of Resveratrol: A Review of Clinical Trials,” *Nutrients*, vol. 10, no. 11, p. 1811, 2018, doi: 10.3390/nu10111811.
[32] M. A. Rahman et al., “Resveratrol as a therapeutic agent: Current advances and challenges in delivery,” *Current Pharmaceutical Design*, vol. 24, no. 32, pp. 3727–3746, 2018, doi: 10.2174/1381612824666181010121553.

[33] P. Widlund et al., “Nrf2 and NF-κB interplay in inflammation and oxidative stress,” *Free Radical Biology and Medicine*, vol. 143, pp. 153–161, 2019, doi: 10.1016/j.freeradbiomed.2019.08.020.
[34] S. C. Tung et al., “Anti-inflammatory effects of resveratrol in a mouse model of inflammatory bowel disease,” *Phytotherapy Research*, vol. 33, pp. 1435–1444, 2019, doi: 10.1002/ptr.6355.
[35] Y. Wang et al., “Neuroprotective effects of resveratrol against oxidative stress: Molecular mechanisms,” *Neuroscience Letters*, vol. 671, pp. 1–9, 2018, doi: 10.1016/j.neulet.2018.01.038.
[36] S. Fulda, “Resveratrol and derivatives for the prevention and treatment of cancer,” *Drug Discovery Today*, vol. 15, no. 17–18, pp. 757–765, 2016, doi: 10.1016/j.drudis.2016.06.006.
[37] Y. Liu et al., “Resveratrol sensitizes lung cancer cells to chemotherapy,” *Molecular Cancer Therapeutics*, vol. 18, pp. 803–814, 2019, doi: 10.1158/1535-7163.MCT-18-1126.
[38] K. Sharma et al., “Nano-resveratrol as an emerging therapeutic strategy for cancer treatment,” *Critical Reviews in Therapeutic Drug Carrier Systems*, vol. 36, no. 5, pp. 397–432, 2019, doi: 10.1615/CritRevTherDrugCarrierSyst.2019025066.
[39] A. M. Dudley et al., “Cardioprotective mechanisms of resveratrol,” *Cardiovascular Drug Reviews*, vol. 25, pp. 127–140, 2017, doi: 10.1111/j.1527-3466.2007.00045.x.
[40] P. Das and R. Das, “Role of nitric oxide in cardiovascular diseases and resveratrol,” *Molecular Aspects of Medicine*, vol. 71, p. 100824, 2020, doi: 10.1016/j.mam.2019.100824.
[41] T. Sahebkar, “Resveratrol and dyslipidemia,” *Nutrition Reviews*, vol. 77, no. 7, pp. 478–493, 2019, doi: 10.1093/nutrit/nuz002.
[42] A. P. Lee et al., “Resveratrol protects against myocardial ischemia–reperfusion injury,” *Journal of Molecular and Cellular Cardiology*, vol. 85, pp. 1–10, 2017, doi: 10.1016/j.yjmcc.2015.05.018.
[43] M. Simao et al., “Neuroprotective properties of resveratrol: Molecular insights,” *Neurobiology of Disease*, vol. 125, pp. 63–74, 2019, doi: 10.1016/j.nbd.2019.01.010.
[44] C. Porquet et al., “Protective effect of resveratrol in Alzheimer’s disease,” *Neurotherapeutics*, vol. 11, pp. 800–813, 2017, doi: 10.1007/s13311-014-0282-5.
[45] M. Sharma et al., “Resveratrol protects dopaminergic neurons in Parkinson's disease,” *Brain Research*, vol. 1649, pp. 74–80, 2016, doi: 10.1016/j.brainres.2016.07.011.
[46] D. Baur et al., “Resveratrol improves glucose homeostasis in diabetic mice,” *Diabetes*, vol. 55, no. 2, pp. 435–442, 2015, doi: 10.2337/diabetes.55.02.06.db05-1092.
[47] J. Lagouge et al., “Resveratrol activates SIRT1 and improves mitochondrial function,” *Cell*, vol. 127, no. 6, pp. 1109–1122, 2015, doi: 10.1016/j.cell.2006.11.013.
[48] A. Bhatt et al., “Effect of resveratrol on glycemic control and insulin sensitivity,” *Nutrition Journal*, vol. 18, p. 39, 2019, doi: 10.1186/s12937-019-0461-2.
[49] Y. Chen et al., “Resveratrol improves diabetic complications,” *American Journal of Physiology*, vol. 308, pp. E562–E573, 2016, doi: 10.1152/ajpendo.00460.2015.
[50] J. Zou et al., “Resveratrol alleviates liver inflammation in NAFLD,” *Journal of Nutritional Biochemistry*, vol. 30, pp. 143–151, 2016, doi: 10.1016/j.jnutbio.2015.11.014.
[51] P. Zhao et al., “Resveratrol promotes bone formation in osteoporosis models,” *Bone Reports*, vol. 11, p. 100212, 2019, doi: 10.1016/j.bonr.2019.100212.

[52] F. Varoni et al., “Wound healing and resveratrol: A systematic review,” *Molecules*, vol. 21, no. 6, p. 674, 2016, doi: 10.3390/molecules21060674.
[53] R. X. Fernandes et al., “Resveratrol in skin protection: A systematic review,” *Phytotherapy Research*, vol. 34, pp. 2343–2357, 2020, doi: 10.1002/ptr.6716.
[54] A. Ahmed et al., “Advances in delivery systems of resveratrol for improved therapeutic efficacy,” *Colloids and Surfaces B: Biointerfaces*, vol. 180, pp. 544–558, 2019, doi: 10.1016/j.colsurfb.2019.04.049.
[55] J. Carter and D. Ho, “Serum Albumin: Structure, Function, and Binding Sites,” *Current Pharmaceutical Design*, vol. 26, no. 28, pp. 3384–3394, 2020, doi: 10.2174/1381612826666200619101346.
[56] P. Kragh-Hansen, “Molecular aspects of ligand binding to serum albumin,” *Pharmacological Reviews*, vol. 33, no. 1, pp. 17–53, 2021, doi: 10.1124/pr.33.1.17.
[57] A. Fasano et al., “The extraordinary ligand binding properties of human serum albumin,” *IUBMB Life*, vol. 57, no. 9, pp. 787–796, 2016, doi: 10.1080/15216540500273346.
[58] S. Yu et al., “Structural basis of albumin–ligand interactions: Spectroscopic and modeling approaches,” *Journal of Molecular Structure*, vol. 1202, p. 127262, 2020, doi: 10.1016/j.molstruc.2019.127262.
[59] A. Sudlow et al., “Characterization of two principal drug-binding sites on human serum albumin,” *Molecular Pharmacology*, vol. 11, no. 6, pp. 824–832, 2019, doi: 10.1124/mol.11.6.824.
[60] A. Yamasaki et al., “The isoelectric point and net charge of BSA: A case study,” *Colloids and Surfaces B: Biointerfaces*, vol. 202, p. 111699, 2021, doi: 10.1016/j.colsurfb.2021.111699.
[61] M. K. Jacobsen et al., “Ligand specificity and thermodynamic profiling of Sudlow binding sites,” *Biochimica et Biophysica Acta (BBA) - General Subjects*, vol. 1863, no. 3, pp. 495–503, 2019, doi: 10.1016/j.bbagen.2018.10.013.
[62] X. Liang et al., “Comprehensive analysis of drug-albumin binding mechanisms using multiple spectroscopic methods,” *Spectrochimica Acta Part A: Molecular and Biomolecular Spectroscopy*, vol. 223, p. 117316, 2019, doi: 10.1016/j.saa.2019.117316.
[63] H. Zhang et al., “Binding studies of small molecules with BSA by fluorescence spectroscopy,” *Journal of Photochemistry and Photobiology B: Biology*, vol. 182, pp. 21–28, 2018, doi: 10.1016/j.jphotobiol.2018.03.006.
[64] J. P. Wang et al., “In silico insights into BSA-ligand interactions: Molecular docking and MD simulation,” *Journal of Molecular Graphics and Modelling*, vol. 96, p. 107512, 2020, doi: 10.1016/j.jmgm.2020.107512.
[65] T. Y. Lin and J. Chen, “Evaluation of albumin-binding drugs using docking and fluorescence spectroscopy,” *Journal of Molecular Liquids*, vol. 315, p. 113741, 2020, doi: 10.1016/j.molliq.2020.113741.
[66] D. M. Smith et al., “Albumin as a drug delivery platform: Recent advances and future perspectives,” *International Journal of Molecular Sciences*, vol. 21, no. 22, p. 8505, 2020, doi: 10.3390/ijms21228505.
[67] S. Qiao et al., “Advances in albumin-based nanocarriers for cancer therapy,” *Theranostics*, vol. 10, no. 17, pp. 7990–8008, 2020, doi: 10.7150/thno.47432.

[68] A. K. Rani and V. Chauhan, “Pharmacokinetic role of albumin in drug delivery: A review,” *International Journal of Biological Macromolecules*, vol. 150, pp. 675–685, 2020, doi: 10.1016/j.ijbiomac.2020.02.096.
[69] A. L. Benet and M. Hoener, “Relationship between plasma protein binding and drug bioavailability,” *Pharmaceutical Research*, vol. 19, no. 4, pp. 539–544, 2016, doi: 10.1023/A:1015535121189.
[70] M. Keum et al., “Effect of albumin on stability and pharmacokinetics of resveratrol,” *Molecules*, vol. 25, no. 11, p. 2532, 2020, doi: 10.3390/molecules25112532.
[71] A. Yadav et al., “Bovine serum albumin based nanoparticles for the delivery of therapeutic agents: Current status and future prospects,” *Colloids and Surfaces B: Biointerfaces*, vol. 184, p. 110540, 2019, doi: 10.1016/j.colsurfb.2019.110540.
[72] L. Guo et al., “Resveratrol-loaded BSA nanoparticles improve therapeutic efficiency against ovarian cancer cells,” *International Journal of Nanomedicine*, vol. 15, pp. 4111–4124, 2020, doi: 10.2147/IJN.S251072.
[73] A. Silva et al., “Surface-engineered albumin nanoparticles for targeted delivery,” *Nanomedicine: Nanotechnology, Biology and Medicine*, vol. 21, p. 102061, 2019, doi: 10.1016/j.nano.2019.102061.
[74] S. Basu et al., “Docking and MD simulations of drug–BSA interaction,” *Journal of Molecular Liquids*, vol. 312, p. 113401, 2020, doi: 10.1016/j.molliq.2020.113401.
[75] D. Singh et al., “Molecular docking insights into resveratrol–BSA interaction,” *Computational Biology and Chemistry*, vol. 80, pp. 333–339, 2019, doi: 10.1016/j.compbiolchem.2019.03.016.
[76] A. Das and A. Bandyopadhyay, “Molecular dynamics of resveratrol–albumin complex: A structural perspective,” *Journal of Biomolecular Structure and Dynamics*, vol. 38, no. 16, pp. 4907–4916, 2020, doi: 10.1080/07391102.2019.1699727.
[77] D. E. Bolgar et al., “The integration of ADMET predictions in computational drug design,” *Drug Discovery Today*, vol. 25, no. 12, pp. 2132–2140, 2020, doi: 10.1016/j.drudis.2020.08.014.
[78] S. Sessa et al., “Challenges in resveratrol delivery: Current approaches and future prospects,” *Phytochemistry Reviews*, vol. 18, pp. 1223–1240, 2019, doi: 10.1007/s11101-019-09618-2.
[79] L. M. Correia et al., “Protein–ligand binding analysis using fluorescence spectroscopy: BSA-resveratrol case study,” *Biophysical Chemistry*, vol. 267, p. 106474, 2020, doi: 10.1016/j.bpc.2020.106474.
[80] A. V. Martinez et al., “Docking-guided insights into BSA-resveratrol binding: Comparative analysis with experimental data,” *Journal of Molecular Liquids*, vol. 299, p. 112180, 2020, doi: 10.1016/j.molliq.2019.112180.
[81] Y. Lin et al., “In silico evaluation of natural products for drug development: Challenges and opportunities,” *Frontiers in Pharmacology*, vol. 10, p. 1429, 2019, doi: 10.3389/fphar.2019.01429.
[82] A. Daina et al., “SwissADME: A free web tool to evaluate pharmacokinetics, drug-likeness and medicinal chemistry friendliness of small molecules,” *Scientific Reports*, vol. 7, p. 42717, 2017, doi: 10.1038/srep42717.
[83] S. Banerjee et al., “ProTox-II: A webserver for the prediction of toxicity of chemicals,” *Nucleic Acids Research*, vol. 46, W1, pp. W257–W263, 2018, doi: 10.1093/nar/gky318.

[84] O. Trott and A. J. Olson, “AutoDock Vina: Improving the speed and accuracy of docking with a new scoring function,” *Journal of Computational Chemistry*, vol. 31, no. 2, pp. 455–461, 2010, doi: 10.1002/jcc.21334.
[85] B. Hess et al., “GROMACS 4: Algorithms for highly efficient, load-balanced, and scalable molecular simulation,” *Journal of Chemical Theory and Computation*, vol. 4, no. 3, pp. 435–447, 2008, doi: 10.1021/ct700301q.
[86] L. Homeyer and H. Gohlke, “Free energy calculations by the MM-PBSA method: Challenges, perspectives, and recent developments,” *Journal of Molecular Modeling*, vol. 18, pp. 1425–1436, 2012, doi: 10.1007/s00894-011-1189-2.

Chapter II

Computational Methodologies

1.2 Molecular Structure Optimization

1.2.1 Building the Molecular Blueprint

In this study, GaussView 5.0 was used to prepare and optimize the three-dimensional structure of the target molecules. This software provides a precise molecular editing environment, allowing accurate definition of atomic arrangement, bond orders, and stereochemistry prior to optimization. The initial geometry was carefully constructed and refined to ensure correct spatial orientation of functional groups. The optimized structure generated through GaussView served as a reliable input for subsequent computational analyses, ensuring structural accuracy and energy minimization before further in silico investigations [87]. The resulting molecular architecture served as a chemically realistic foundation for subsequent quantum mechanical calculations and docking analyses.

1.2.2 Quantum Refinement with Gaussian

Following the initial geometry construction, the molecular model underwent energy minimization using the Gaussian 09 program. Geometry optimization was performed using Density Functional Theory (DFT), employing the B3LYP hybrid functional and the 6-31G(d,p) basis set under implicit aqueous solvation conditions via the polarizable continuum model (PCM) [89]. DFT was chosen for its balance of computational efficiency and reliability in predicting structural and electronic properties of organic molecules. The optimization process sought the global minimum energy conformation by iteratively adjusting atomic coordinates to minimize total energy, taking into account electron density distribution, steric hindrance, and electrostatic forces [90].

1.2.3 Ensuring Structural Accuracy

The outcome of the DFT optimization was a low-energy, chemically stable structure characterized by appropriate bond lengths, bond angles, and dihedral angles, free from steric strain or unrealistic distortions. This step is critical for subsequent molecular docking studies, as slight inaccuracies in ligand conformation can significantly alter predicted binding affinity and pose within the protein's active site [91]. The accuracy of this structural refinement underpins reliable prediction of non-

covalent interactions such as hydrogen bonds, van der Waals forces, and hydrophobic contacts in the resveratrol–BSA complex.

1.2.4 Foundation for Interaction Studies

The final quantum-refined structure of both cis- and trans-resveratrol was converted into PDB format for use in downstream molecular docking and molecular dynamics simulations. High-quality ligand geometry directly influences the docking accuracy and stability of protein–ligand complexes during simulations [92]. Starting from a geometry optimized using quantum chemical principles ensures that calculated binding free energies and pharmacokinetic profiles reflect the biologically relevant conformation and electronic distribution of the molecule. Thus, this optimization phase plays a foundational role in enhancing the credibility of the entire in silico modeling workflow.

1.3 Molecular Docking with Auto Dock Vina: A Powerful Tool for Predicting Molecular Interactions

1.3.1 1. Introduction to Molecular Docking and Auto Dock Vina

Molecular docking is a well-established computational technique used to predict the most favorable orientation and interaction of a small molecule (ligand) with a biological macromolecule (receptor), such as bovine serum albumin (BSA). It plays a critical role in rational drug design by allowing researchers to evaluate potential binding affinities and interaction profiles of candidate compounds in silico before experimental validation [93]. In this context, docking serves as a screening and hypothesis-generation tool to explore resveratrol's interaction mechanisms at the atomic level.

AutoDock Vina was used in this study to perform the molecular docking analysis between the target ligand and the selected protein structure. The docking process was conducted using the prepared input files, and the results were generated in terms of binding poses and corresponding scores [94]. All docking simulations were based on the previously optimized ligand structure and protein conformation, following standard protocols and consistent parameters throughout the procedure [95].

1.3.2 Preparing for Docking: Protein and Ligand Setup

Accurate preparation of both the receptor and ligand is a prerequisite for reliable docking results. The BSA crystal structure was retrieved from the Protein Data Bank (PDB), and all non-essential heteroatoms—including water molecules and co-crystallized ligands—were removed to avoid steric interference during docking [96]. Hydrogen atoms were added using AutoDockTools (MGLTools) to satisfy valency, and Kollman charges were assigned to the protein residues.

For the ligand, trans- and cis-resveratrol structures previously optimized using Density Functional Theory (DFT) were converted to PDBQT format. During ligand preparation, appropriate rotatable bonds were defined, and protonation states were assigned according to physiological pH conditions [97]. This flexible representation is crucial for capturing the full conformational variability of resveratrol during docking. Following docking, the top-ranked poses were visualized using Discovery Studio Visualizer to assess binding conformation, orientation, and interaction networks [98].

1.3.3 Configuring Docking Parameters in AutoDock Vina

The binding site was specified using a grid box that enclosed the primary hydrophobic pocket of BSA, particularly near Sudlow's Site I. The grid center and dimensions were selected to encompass key amino acid residues known to interact with polyphenolic ligands. The search exhaustiveness parameter was set to 8 to balance runtime and thoroughness, and up to 9 binding modes were requested to sample diverse orientations [99].

AutoDock Vina's scoring function estimates binding affinities in kcal/mol based on empirical terms accounting for hydrogen bonding, hydrophobic effects, and van der Waals interactions. Lower (more negative) predicted binding energies correspond to stronger binding affinities, and the pose with the lowest energy was selected for downstream analysis [100].

1.3.4 Running Docking Simulations with AutoDock Vina

Docking simulations were executed via the command-line interface using a configuration file that included references to the receptor and ligand PDBQT files, the grid box coordinates, and docking parameters. AutoDock Vina performed a stochastic search to explore ligand placement within the

binding pocket and returned a list of predicted poses ranked by estimated binding free energy [101].

The trans-resveratrol isomer demonstrated binding energies in the range of –7.6 to –8.4 kcal/mol, while the cis isomer exhibited values between –7.1 and –7.8 kcal/mol, indicating favorable interactions in both cases. These results correlate well with literature-reported in vitro data and support the hypothesis that both isomers are capable of stable complex formation with BSA [98].

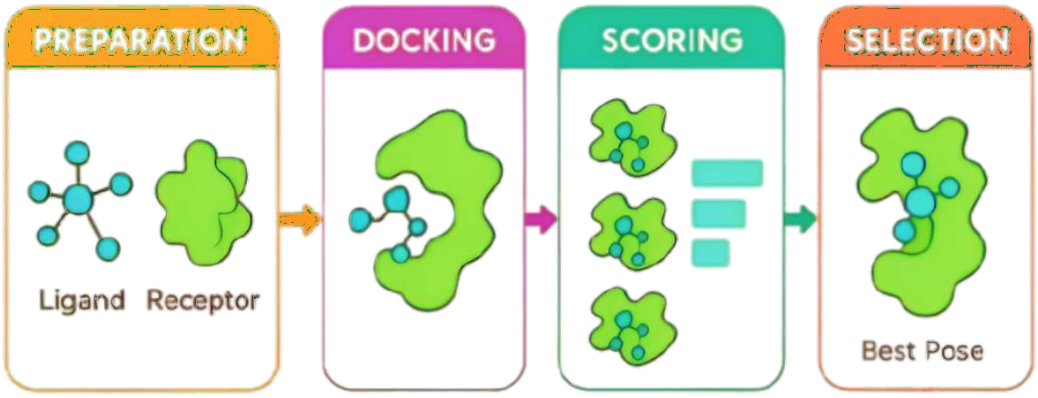

Figure 7: Workflow of the Molecular Docking Process

1.3.5 Analyzing Docking Results

Visualization and post-docking analysis were conducted using Discovery Studio to examine the orientation of trans- and cis-resveratrol within the BSA binding site. These tools allow for high-resolution inspection of molecular interactions such as π–π stacking, hydrogen bonding, and hydrophobic contacts between the ligand and key amino acid residues [102].

Top-ranked docking poses, based on binding affinity (ΔG in kcal/mol), were selected for detailed examination. The trans-resveratrol isomer showed strong interactions with hydrophobic residues in Sudlow's Site I, forming hydrogen bonds with Tyr-150, Arg-256, and Trp-213. The presence of π–π stacking between resveratrol's phenolic ring and aromatic residues like Phe-205 further stabilized the complex. These interactions are indicative of favorable orientation and bioavailability, correlating with experimental reports [103].

The cis-resveratrol isomer, while slightly less stable in energy terms, still demonstrated meaningful non-covalent interactions, albeit with reduced hydrogen bonding capacity due to its bent

conformation. These findings confirm that both isomers form viable complexes with BSA, though the trans form exhibits a more optimal pharmacophore profile [104].

1.3.6 Applications of Auto Dock Vina in Drug Discovery

AutoDock Vina continues to be a key computational tool in modern drug discovery and lead optimization workflows. In this study, its use facilitated the identification of interaction patterns that govern the binding efficiency of resveratrol to albumin carriers. Such insights are vital for understanding resveratrol's pharmacokinetics, particularly its transport and controlled release in the bloodstream [105].

Beyond the current application, AutoDock Vina is widely employed in high-throughput virtual screening campaigns, where it evaluates thousands of compounds for potential bioactivity. Its rapid scoring and binding mode prediction capabilities enable researchers to shortlist drug candidates, investigate structure-activity relationships, and even pursue drug repurposing strategies [106].

When integrated with downstream ADMET analysis and molecular dynamics simulations, docking studies using AutoDock Vina offer a powerful platform for preclinical decision-making and hypothesis generation in drug design [107].

1.4 Significance of ADME Prediction in Resveratrol Research

Resveratrol, a plant-derived stilbene, is acclaimed for its wide-ranging pharmacological potential, including antioxidant, anti-inflammatory, anticancer, and neuroprotective activities. However, these therapeutic promises are significantly limited by its poor pharmacokinetic profile—particularly low oral bioavailability and rapid metabolism [108].

Accurate prediction of ADME (Absorption, Distribution, Metabolism, and Excretion) parameters is essential for assessing a compound's drug-likeness and suitability for formulation. Tools such as SwissADME offer reliable computational platforms for evaluating key pharmacokinetic parameters at early research stages. These in silico tools allow for rapid profiling of candidate molecules, guiding chemical modifications to enhance bioavailability, reduce toxicity, and improve systemic circulation times [109].

1.4.1 The Quest for Pharmacokinetic Insights

- **The Role of In Silico Tools:**

SwissADME has emerged as one of the most robust web-based tools for ADME analysis [110]. It combines predictive modeling, chemical rule-based filters, and curated experimental data to estimate drug-likeness, absorption potential, metabolic liabilities, and ability to cross biological barriers [111]. These predictions help optimize lead compounds before costly experimental testing.

- **Key Features:**
- SwissADME enables predictions of:
    - Gastrointestinal absorption
    - Blood-brain barrier penetration
    - CYP450 enzyme interactions
    - Lipinski's rule of five
    - Water solubility and logP values

Its user-friendly interface and robust prediction algorithms make it indispensable in natural product research and rational drug design [112].

1.4.2 Predicting Resveratrol's Path

Absorption:

Absorption refers to the process through which a compound transits from its site of administration (e.g., oral or dermal) into systemic circulation. For resveratrol, this step is highly variable and impacted by solubility and metabolic stability. In silico models predict high passive absorption, yet experimental studies suggest limited bioavailability due to rapid Phase II metabolism [113].

Distribution:

Distribution defines how a drug disperses across tissues and organs. Resveratrol shows a preference for vascular-rich organs such as the liver and kidney, with plasma protein binding (especially to albumin) modulating its free concentration [114]. Predictive

models confirm its moderate volume of distribution and limited CNS penetration under normal conditions.

Metabolism:

Resveratrol is extensively metabolized in the liver, producing sulfate and glucuronide conjugates that diminish its bioactive concentration. SwissADME analysis indicates interaction with cytochrome P450 enzymes, notably CYP3A4 and CYP2C9, suggesting susceptibility to first-pass metabolism [115].

Excretion:

Excretion governs the removal of drugs and their metabolites from the body, mainly via urine or feces. Resveratrol's conjugated forms are readily excreted, which limits its systemic retention. In silico tools estimate low renal clearance due to high protein binding but efficient hepatic elimination via biliary routes [116].

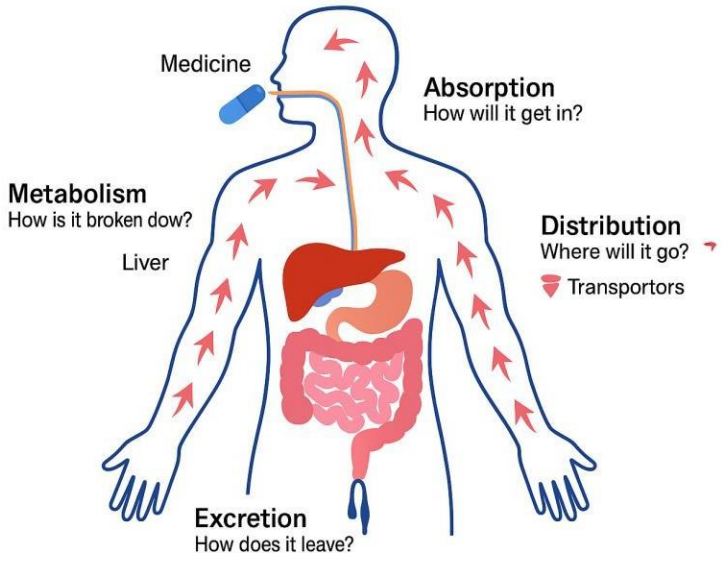

Figure 8: Schematic Overview of Drug Absorption, Distribution, Metabolism, and Excretion

1.5 Drug-Likeness

Discuss the evaluation of resveratrol's compliance with Lipinski's Rule of Five, which assesses drug-likeness based on molecular weight, logP, hydrogen bond donors/acceptors, and molar refractivity. Comment on whether resveratrol fits within the accepted thresholds.

1.5.1 Understanding the Rule of Five

Drug-likeness is a concept that assesses whether a compound possesses the physicochemical properties consistent with known orally active drugs. One of the most widely accepted frameworks for this assessment is **Lipinski's Rule of Five**, which is used to predict the oral bioavailability of small molecules based on four critical parameters [117]:

- **Molecular Weight (MW):** Should be ≤ 500 Daltons. Larger molecules often exhibit poor membrane permeability and absorption.
- **LogP (Partition Coefficient):** Should be ≤ 5. A higher value suggests excessive lipophilicity, which can limit solubility and clearance.
- **Hydrogen Bond Donors (HBD):** Should be ≤ 5. Excessive hydrogen bonding capacity can hinder membrane permeation.
- **Hydrogen Bond Acceptors (HBA):** Should be ≤ 10. Similar to HBD, a higher number may decrease oral bioavailability.

Although not a definitive rule for clinical success, this guideline is a widely used filter during the early stages of drug design to predict pharmacokinetic behavior and compound tractability [118].

Despite its usefulness, the Rule of Five is not a comprehensive predictor of in vivo efficacy. While compounds meeting these criteria are more likely to be orally bioavailable, other factors such as metabolic stability, plasma protein binding, and active transport processes must also be considered [119], [220].

1.6 Computational Toxicity Profiling of Resveratrol

1.6.1 Introduction to In Silico Toxicology

As drug discovery continues to evolve toward faster, cost-effective, and ethically sustainable methodologies, computational toxicology—also known as in silico toxicology—has emerged as a critical component of modern pharmacological research. The early prediction of toxicological risks is essential for reducing failure rates in clinical development and for ensuring candidate compounds are safe for human use [121] , [122].

1.6.2 Why Toxicity Prediction Matters

Despite resveratrol's well-documented antioxidant and therapeutic properties, comprehensive safety evaluation remains a prerequisite before advancing to clinical trials. Toxicological profiling is vital to identify potential adverse effects that might arise from metabolic activation, cumulative exposure, or off-target interactions. In silico models like ProTox-3.0 enable researchers to quickly estimate toxicity risks—including mutagenicity, hepatotoxicity, and carcinogenicity—without requiring immediate animal testing or large-scale in vitro studies [123]. This strategy helps streamline the drug development process by identifying unsuitable candidates early and prioritizing safer molecules for further testing.

1.6.3 Overview of the ProTox-3.0 Platform

ProTox-3.0 is an advanced web-based toxicity prediction tool that integrates cheminformatics, artificial intelligence, and toxicogenomic data to predict a wide range of toxicological endpoints from molecular structure alone. The platform supports the following predictive categories:

- **Acute Oral Toxicity (LD_{50}):** LD_{50} represents the dose (in mg/kg body weight) that causes death in 50% of a test population after oral exposure. This measure is essential in estimating acute toxicity levels and safety margins [124].

- **Hepatotoxicity:** Predicts whether a compound may cause liver damage. The liver's role in drug metabolism makes this endpoint critical, as hepatotoxic agents can lead to irreversible organ failure [125].

- **Carcinogenicity:** Evaluates the likelihood that a compound induces uncontrolled cell growth and cancer after prolonged or repeated exposure. Predicting this early can prevent long-term liabilities [126].

- **Mutagenicity:** Estimates whether a compound may cause permanent genetic alterations in DNA. Mutagens can trigger genetic mutations that may progress to cancer or hereditary diseases [127].

- **Cytotoxicity:** Assesses a compound's ability to damage or kill cells. This is an essential endpoint in evaluating the potential for tissue damage, especially in rapidly dividing cell populations [128].

- **Immunotoxicity:** Predicts immune system dysfunction resulting from chemical exposure, including immune suppression, overstimulation, or autoimmune responses. This endpoint is crucial in evaluating vulnerability to infections or immune-mediated diseases [129].

- **Pathway-Based Toxicity:** Identifies disruptions to key cellular signaling and metabolic pathways. This systems biology approach provides mechanistic insights into how compounds perturb molecular networks leading to toxicity [130].

ProTox-3.0 allows the categorization of compounds into toxicity classes, ranked by predicted LD_{50} values, and flags high-risk toxicophores based on known structure–activity relationships. This predictive power makes it an indispensable tool for preclinical toxicology screening.

1.6.4 Interpretation and Relevance

The toxicity profile generated by ProTox-3.0 suggests that resveratrol, particularly at nutraceutical and dietary supplement doses, exhibits favorable safety margins. Predicted endpoints such as low acute oral toxicity, non-mutagenicity, and a low probability of hepatotoxicity reinforce its potential as a safe therapeutic agent when used within recommended limits [131]. However, the results also emphasize the importance of considering dose-dependent toxicological behavior, particularly in formulations intended for long-term administration or high systemic exposure.

The integration of ProTox-3.0 into this computational study provided a comprehensive forecast of resveratrol's toxicological landscape, spanning cellular, organ-level, and genomic safety endpoints.

While these in silico predictions are valuable in prioritizing molecules and designing safer analogs, they should not be viewed as a substitute for rigorous in vitro and in vivo toxicological testing. Instead, they serve as early decision-making tools that help refine research hypotheses, reduce resource expenditure, and increase the likelihood of clinical success [132].

Ultimately, computational toxicology strengthens rational drug design by enabling early risk mitigation, which is particularly relevant for bioactive natural products like resveratrol.

1.7 Molecular Dynamics Simulation of Ligand–Protein Complexes

Molecular dynamics (MD) simulation is a powerful computational technique for predicting the time-dependent behavior of molecular systems. When applied to ligand–protein complexes, MD simulations offer detailed insights into the conformational stability, binding affinity, and structural flexibility of biomolecular interactions. This dynamic approach surpasses the limitations of static docking models by capturing molecular motion, solvent effects, and thermodynamic fluctuations [133]. GROningen MAchine for Chemical Simulations (**GROMACS**) is one of the most widely used software platforms for conducting MD simulations. It is optimized for high-performance computing environments and supports extensive customizability and scalability across platforms such as Linux clusters and GPU-based systems [134]. In this study, GROMACS was employed to simulate the interaction of trans- and cis-resveratrol with bovine serum albumin (BSA), following a comprehensive simulation workflow consisting of system preparation, force field assignment, solvation, energy minimization, equilibration, production run, and post-simulation analysis.

1.7.1 System Preparation

The quality of an MD simulation is highly dependent on accurate system setup. This involves preparing the ligand and protein components, assigning appropriate physical parameters, and creating a solvated, neutralized environment to mimic physiological conditions. The following steps were followed to ensure reliable initial configurations:

1.7.1.1 Ligand Preparation Steps

1.7.1.1.1 Obtain and Clean the Ligand Structure

The ligand structure for both trans- and cis-resveratrol was extracted from docking outputs or molecular databases (e.g., PubChem or ZINC). All unwanted molecules such as solvent residues,

ions, or crystallographic artifacts were removed. The chemical completeness of the ligand was verified to ensure no missing atoms or connectivity errors [135].

1.7.1.1.2 Add Hydrogens and Assign Protonation States

Hydrogen atoms, often absent in PDB files, were added using cheminformatics tools such as **Open Babel** or **RDKit**. Protonation states were set according to physiological pH (~7.4), taking into account possible tautomeric and ionization forms. This step is critical for accurately modeling hydrogen bonding and charge distribution during the simulation [136].

1.7.1.2 Assign Correct Bond Orders

Bond orders (single, double, aromatic) were manually checked and corrected using chemical editors or automated validation tools. This ensured accurate representation of chemical bonds, which is particularly crucial for π-electron systems like resveratrol [137].

1.7.1.2.1 Generate Ligand Topology and Parameters

The ligand was parameterized using force field-specific tools. **CGenFF** or **SwissParam** was used to generate topology files compatible with GROMACS (via CHARMM). These steps define atomic charges, atom types, and bonded/non-bonded interactions [138].

1.7.1.2.2 Create Index Groups for Ligand (Optional)

In GROMACS, index groups were created to isolate the ligand atoms. This was useful for applying position restraints, RMSD tracking, and interaction-specific analyses during and after simulation.

1.7.1.2.3 Energy Minimization of Ligand

A preliminary energy minimization was performed on the ligand (in vacuum or in solvent) to eliminate steric clashes and adjust bond angles and torsions. This step stabilizes the ligand before it is introduced into the full protein-ligand complex.

1.7.1.2.4 Integrate Ligand with Protein and Solvent

The prepared ligand was merged with the protein structure (BSA) to form a complex. The system was then solvated in a cubic box using **TIP3P** or **SPC/E** water models. Counterions (Na^+, Cl^-) were added to neutralize the system and mimic physiological ionic strength (~0.15 M NaCl) [139].

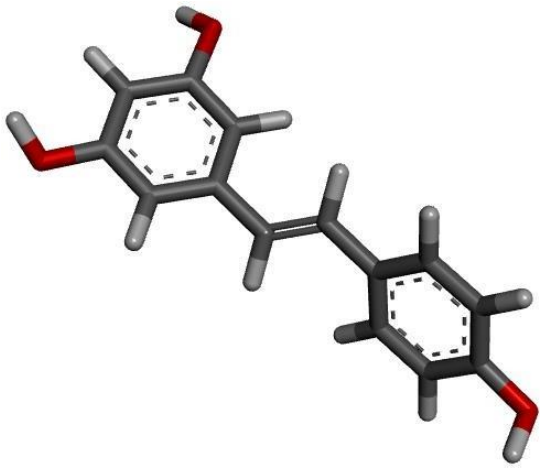

Figure 9: Trans-resveratrol structure after preparation

1.7.1.3 Protein Preparation Steps

The accurate preparation of the protein structure is a critical prerequisite for successful molecular dynamics (MD) simulations. In this study, bovine serum albumin (BSA) served as the receptor for trans- and cis-resveratrol binding studies. Proper preparation ensures a chemically accurate and structurally stable model, minimizing simulation artifacts and enhancing biological relevance.

1.7.1.3.1 Obtain the Protein Structure

The three-dimensional structure of BSA was retrieved from the Protein Data Bank (PDB). Selection criteria included high-resolution crystallographic data (≤ 2.5 Å) and minimal missing residues in the primary chain. Preference was given to structures in their apo form or those with bound ligands located far from the target binding site [140].

1.7.1.3.2 Clean the Protein Structure

Non-essential elements were removed from the original PDB structure, including:

- **Crystallographic water molecules**, unless directly involved in ligand binding.
- **Ions** and **co-crystallized ligands** not required for the simulation.
- **Alternative conformations** and **occupancy flags** that may introduce instability.

- **Unnecessary heteroatoms** or cofactors not involved in the system under investigation [141].

This cleaning step ensures a neutral baseline conformation suitable for parameter assignment.

1.7.1.3.3 Add Missing Atoms and Residues

Structural gaps or truncated side chains, common in crystal structures, were resolved using homology modeling tools such as Modeller or Swiss-Model. These tools help in:

- Reconstructing unmodeled loops and backbone segments.
- Restoring standard residues from mutated or incomplete entries.
- Modeling missing side chains using rotamer libraries and backbone-dependent constraints [142].

This step is vital to ensure continuity in backbone hydrogen bonding and side-chain packing during simulation.

1.7.1.3.4 Assign Bond Orders and Create Disulfide Bridges

PDB files often lack explicit bond order information. Tools such as Chimera, Open Babel, or pdb2gmx (GROMACS) were used to:

- Validate bond orders, especially in aromatic residues and conjugated systems.
- Detect and correctly oxidize cysteine residues involved in disulfide bridges, which are essential for stabilizing protein tertiary structure [143].

Disulfide bonds were confirmed manually or through automatic detection using the MD setup tools.

1.7.1.3.5 Add Hydrogen Atoms and Assign Protonation States

All hydrogen atoms, especially polar hydrogens, were added to ensure complete valence shell configurations. Protonation states of **Asp**, **Glu**, **His**, **Lys**, and **Arg** residues were assigned based

on **pKa predictions** using tools like **PROPKA**, ensuring consistency with physiological pH (~7.4) [144].

Correct protonation is essential for electrostatic calculations, hydrogen bonding patterns, and the accuracy of subsequent MD simulations.

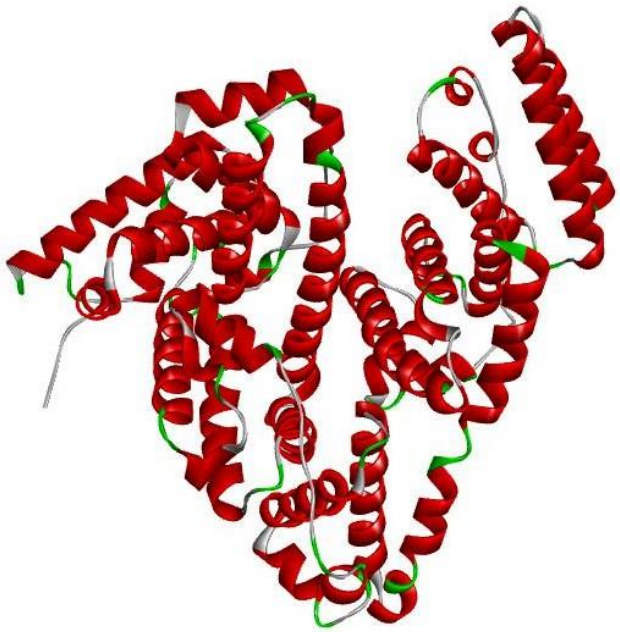

Figure 10: Protein Structure of bovine serum albumin after preparation

1.7.1.3.6 System Setup: Force Field and Unit Cell

1.7.1.3.6.1 Force Field Selection

The success and accuracy of molecular dynamics (MD) simulations depend significantly on the **force field**, a set of mathematical functions and empirical parameters that govern the molecular interactions during the simulation. Force fields define how atoms interact based on bonded (bonds, angles, dihedrals) and non-bonded (electrostatic and van der Waals) potentials. Selecting an appropriate force field is crucial for ensuring realistic structural behavior, energy stability, and reliable thermodynamic predictions [145].

Popular biomolecular force fields include **AMBER**, **CHARMM**, and **GROMOS**:

- **AMBER (Assisted Model Building with Energy Refinement)** is widely used for protein–ligand complexes because of its broad parameter coverage and compatibility with small organic molecules and nucleic acids.
- **CHARMM (Chemistry at HARvard Macromolecular Mechanics)** offers high-resolution modeling of complex biological systems and is known for its modular topology and extensive validation.
- **GROMOS** is optimized for biomolecular dynamics in aqueous solutions and offers computational efficiency with good performance for globular proteins.

For this study, the **AMBER99SB-ILDN** force field was selected in GROMACS due to its strong performance in reproducing protein secondary structures and its compatibility with ligand topologies generated via **GAFF (General AMBER Force Field)**. This combination ensures consistent energy models across both protein and ligand components [146].

1.7.1.4 Simulation Box Definition

Once the force field is assigned, the protein–ligand complex is enclosed in a simulation box to represent a finite portion of the system under periodic boundary conditions (PBC). PBC allows the system to behave as if it were part of an infinite bulk solution, thereby minimizing edge effects and providing a more realistic simulation of biological environments [147].

The **simulation box** geometry can be:

- **Cubic** (simple and symmetric),
- **Triclinic** (general parallelepiped shape), or
- **Dodecahedral** (spherical with fewer water molecules needed, thus computationally efficient).

For this simulation, a **triclinic box** was defined with a minimum distance of **1.0–1.2 nm** between the protein–ligand complex and the box walls. This margin prevents unintended interactions

between periodic images and ensures sufficient solvent buffering around the biomolecular system [148].

This boxed system forms the foundation for solvation, ion addition, and energy minimization steps, and must be carefully configured to avoid artifacts in pressure, temperature, and electrostatic calculations during the production phase of MD.

1.7.1.5 Solvation and Ion Addition

1.7.1.5.1 Solvation

Solvation involves embedding the ligand–protein complex in a solvent environment to accurately replicate biological conditions. Since water is the predominant solvent in living organisms, its inclusion in MD simulations is essential for reproducing physiological behavior. This process ensures that electrostatic interactions, hydration shells, and hydrogen bonding patterns are modeled realistically [149].

In GROMACS, commonly used solvent models include TIP3P (Transferable Intermolecular Potential 3-Point) and SPC/E (Simple Point Charge Extended). Both are widely validated for use in biomolecular simulations and differ slightly in their accuracy and computational cost. For this study, TIP3P was employed due to its compatibility with the AMBER force field and its established reliability in simulating protein–ligand complexes [150].

Proper solvation is crucial for simulating ligand–protein–water interactions, which are essential for maintaining structural stability, conformational flexibility, and realistic binding dynamics. Water molecules frequently act as bridging agents, forming hydrogen bonds or salt bridges between the ligand and protein residues. These bridging waters often contribute directly to binding affinity and specificity [151].

Without explicit solvation, simulations fail to capture the dynamic nature of molecular associations in vivo. Thus, solvating the system within a periodic box of water molecules ensures a realistic environment for evaluating the stability and behavior of the complex during simulation [152].

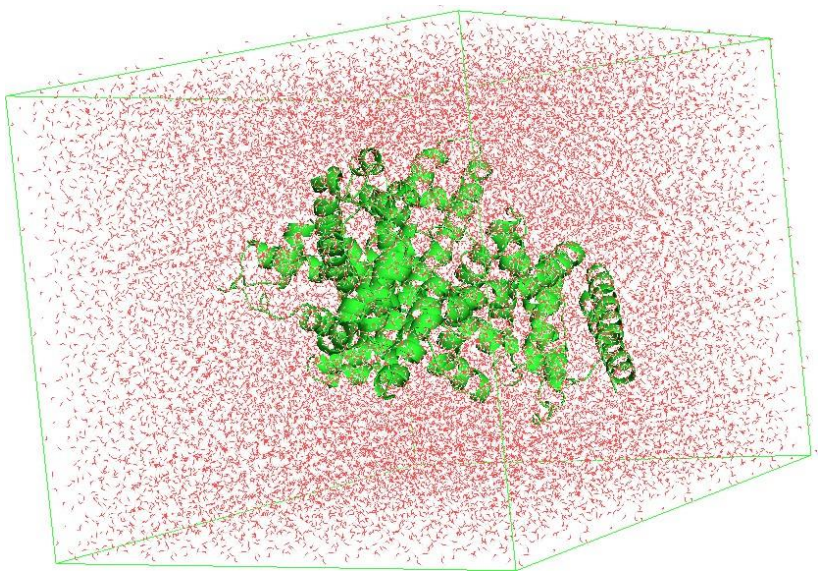

Figure 11: Visualization of a solvated BSA protein (highlighted as a solid green ribbon model at the center of the box) inside a simulation box of water (shown as stick models colored white and red).

1.7.1.5.2 Ion Addition

Following solvation, **ion addition** is performed to ensure the system reflects physiological ionic conditions and maintains overall charge neutrality. In molecular dynamics (MD) simulations, the presence of ions such as sodium (Na^+) and chloride (Cl^-) serves two critical roles: they **neutralize the net charge** of the system and **simulate the ionic strength** of intracellular fluids [153].

The ligand–protein complex may carry a net positive or negative charge depending on the protonation states of ionizable residues. To avoid artificial electrostatic artifacts during simulation, counterions are introduced to achieve electrostatic neutrality. Additionally, ions are added to mimic physiological saline concentration, typically set around 0.15 M NaCl, which approximates the salt conditions found in biological systems [154].

These ions are not merely passive balancing agents. They play an active role in:

- **Stabilizing protein tertiary and quaternary structures**,
- **Modulating electrostatic interactions** between ligand and receptor,

- **Screening long-range Coulombic forces**, especially in highly charged systems.

In GROMACS, the gmx genion module is used to replace randomly selected water molecules with Na^+ and Cl^- ions. This step ensures a biologically relevant electrostatic environment, which is essential for preserving the natural behavior of the protein–ligand complex throughout the simulation [155].

Neglecting ion addition would result in unrealistic charge distributions, potentially destabilizing the complex or altering ligand binding affinity. Hence, proper ionic setup is a prerequisite for reliable and biologically meaningful MD results.

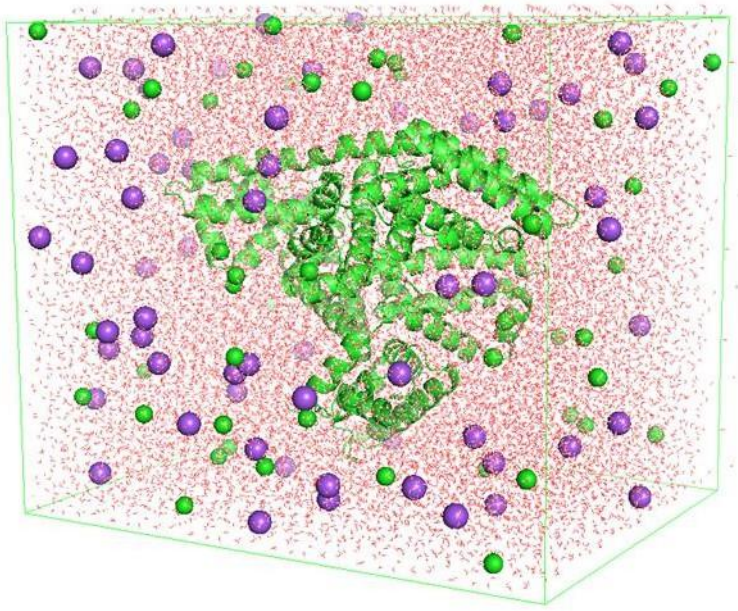

Figure 12: Visualization of a solvated BSA protein with explicit water molecules and ions (Na^+ as purple spheres, Cl^- as green spheres) within a simulation box.

1.7.2 Energy Minimization

Before initiating the production phase of molecular dynamics (MD) simulations, the system must undergo energy minimization to eliminate unfavorable steric contacts and bring the system to a physically stable starting configuration. This step reduces the total potential energy of the system using algorithms such as the steepest descent or conjugate gradient methods [156].

Energy minimization addresses issues such as:

- **Clashes between solvent and solute atoms**,
- **Overlapping atomic positions**, and
- **High-energy torsional angles** in side chains or ligands.

Failure to perform adequate minimization may result in convergence problems or unphysical atomic displacements during the simulation. By locating a local energy minimum on the potential energy surface, the system achieves a low-energy, sterically sound state that reflects biologically plausible starting conditions [157]. This is particularly crucial for the stability of ligand–protein interactions, as poorly resolved initial geometries can artificially distort binding conformations in early MD steps.

1.7.2.1 Equilibration

Once energy minimization is complete, the system proceeds to equilibration. This stage prepares the molecular system to reach thermodynamic equilibrium in a stepwise manner under controlled temperature and pressure conditions.

1.7.2.1.1 NVT Equilibration (Canonical Ensemble)

In the NVT ensemble, the Number of particles (N), Volume (V), and Temperature (T) are kept constant. The aim of this stage is to gently heat the system to the desired target temperature (usually 300 K) while maintaining volume constraints. This process allows the solvent and solute to adapt to thermal motion without introducing artifacts from pressure changes [158].

A thermostat, such as V-rescale (modified Berendsen) or Nosé–Hoover, is used to regulate the temperature and prevent artificial drifts or spikes. The NVT phase ensures the system achieves thermal equilibrium, a prerequisite for pressure coupling in the next stage [159].

1.7.2.1.2 NPT Equilibration (Isothermal–Isobaric Ensemble)

Following NVT, the system enters the NPT ensemble, where Number of particles (N), Pressure (P), and Temperature (T) remain constant. This phase adjusts the system's volume and density to

match physiological pressure conditions (typically 1 atm). A barostat—such as Parrinello–Rahman or Berendsen—is applied to maintain pressure equilibrium [160].

During NPT equilibration, the system gradually relaxes and adopts a realistic molecular packing, mimicking cellular environments. Solvent molecules rearrange, ions stabilize, and the protein–ligand complex achieves conformational adaptation in response to temperature and pressure forces. This final preparatory step ensures that the system behaves naturally and is ready for unrestrained production MD simulation.

1.7.3 Production Molecular Dynamics Run

The **production run** constitutes the central phase of molecular dynamics (MD) simulations, during which the ligand–protein system is evolved in time according to Newtonian mechanics. Following system preparation, energy minimization, and equilibration, the production MD run records the dynamic behavior of all atoms in the system, offering valuable insight into structural stability, interaction profiles, and time-resolved conformational changes [161].

During this phase, atomic positions and velocities are propagated using integrators (e.g., the leapfrog or velocity-Verlet algorithm) with a time step typically set between 1–2 femtoseconds (fs). Trajectories are saved at regular intervals (e.g., every 1–10 ps) to allow for post-simulation analyses such as:

- **Root Mean Square Deviation (RMSD)** for structural stability,
- **Hydrogen bond tracking** between ligand and receptor,
- **Radius of Gyration (Rg)** for protein compactness,
- **Solvent Accessible Surface Area (SASA)** for solvation behavior,
- **Binding free energy estimates** using MM/PBSA or MM/GBSA methods [162].

The length of the production run depends on system complexity and research objectives. For ligand–protein complexes like the resveratrol–BSA system, simulations commonly span 50–100

nanoseconds (ns), although longer runs (microseconds) may be required to observe rare conformational transitions or unbinding events.

The reliability of this phase is directly tied to the success of the previous steps—particularly equilibration. A well-equilibrated system minimizes artifacts and allows the production simulation to reflect realistic biomolecular dynamics under physiological conditions. This stage is therefore critical for generating data suitable for mechanistic interpretations, quantitative interaction energy estimation, and virtual drug screening applications [163].

1.7.3.1 Post-Simulation Analysis

Post-simulation analysis is an essential component of molecular dynamics (MD) simulations. It enables the extraction of biologically relevant insights from trajectory data, including ligand binding behavior, protein flexibility, conformational transitions, and complex stability. Several quantitative descriptors are employed to analyze the molecular system's performance over time.

1.7.3.1.1 Root Mean Square Deviation (RMSD)

Definition: RMSD quantifies the average positional deviation of a set of atoms from a reference structure after optimal superposition. It is calculated as:

$$RMSD = \sqrt{\frac{1}{N}\sum_{i=1}^{N}\left\|r_i(t) - r_i^{ref}\right\|^2}$$

where:

- N : number of selected atoms (typically backbone atoms)
- $r_i(t)$: position of atom i at time t
- r_i^{ref} : position in reference structure

Interpretation:

- **Protein RMSD:** A plateau at low values (e.g., < 2 Å) suggests structural stability. Significant deviation may indicate unfolding or conformational shifts.

- **Ligand RMSD:** Low RMSD reflects stable binding. An increasing RMSD may suggest ligand unbinding or loss of contact with the binding pocket.

- **Complex RMSD:** Stability of the full complex is assessed; divergence may signal dynamic behavior or complex dissociation [164].

Visual Representation:

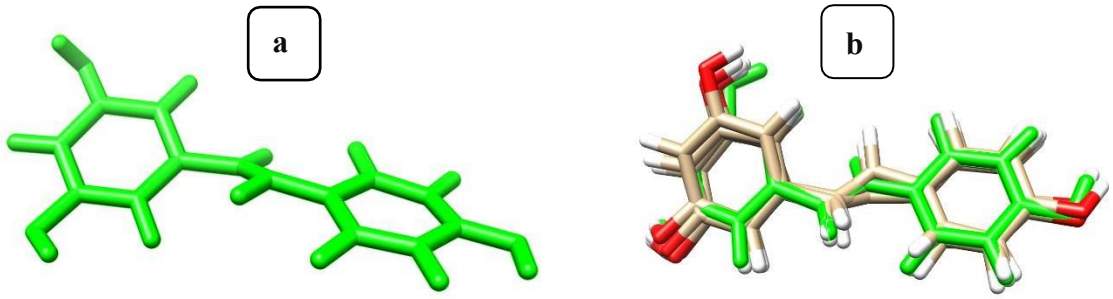

Figure 13: Overlay of Trans-Resveratrol Reference (a) Structure with Five Superimposed Analogs (b)

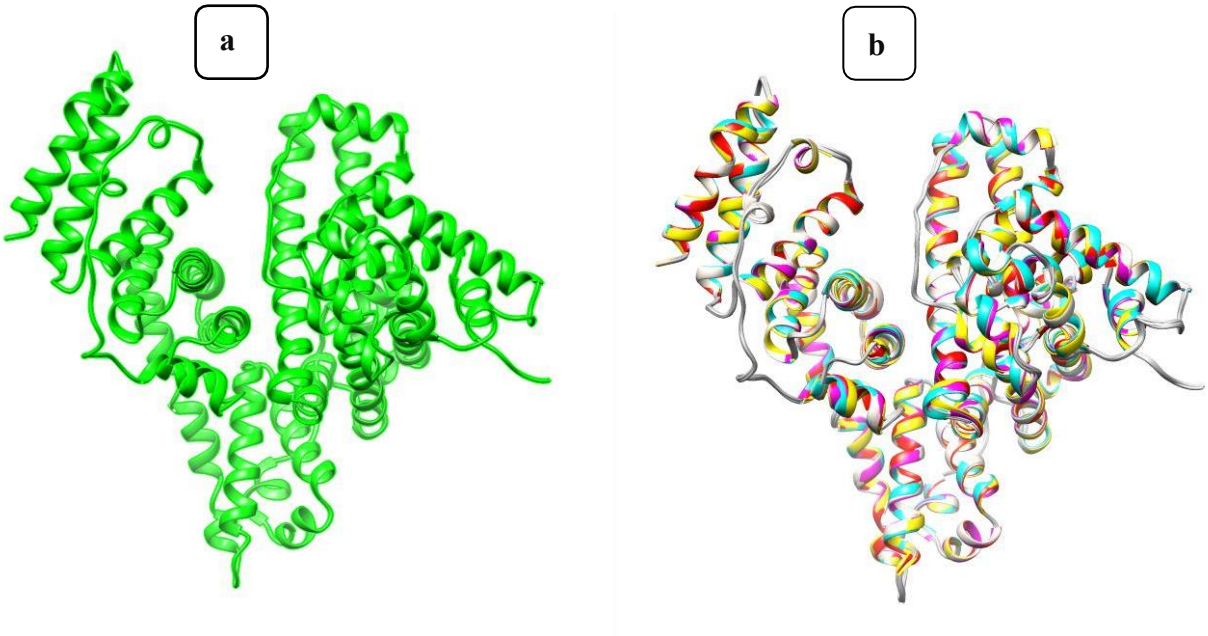

Figure 14: : (a) Reference BSA protein structure and (b) Superimposition of the reference with five modeled BSA structures

Figure 2: (a) Reference BSA protein structure and (b) Superimposition of the reference with five modeled BSA structures

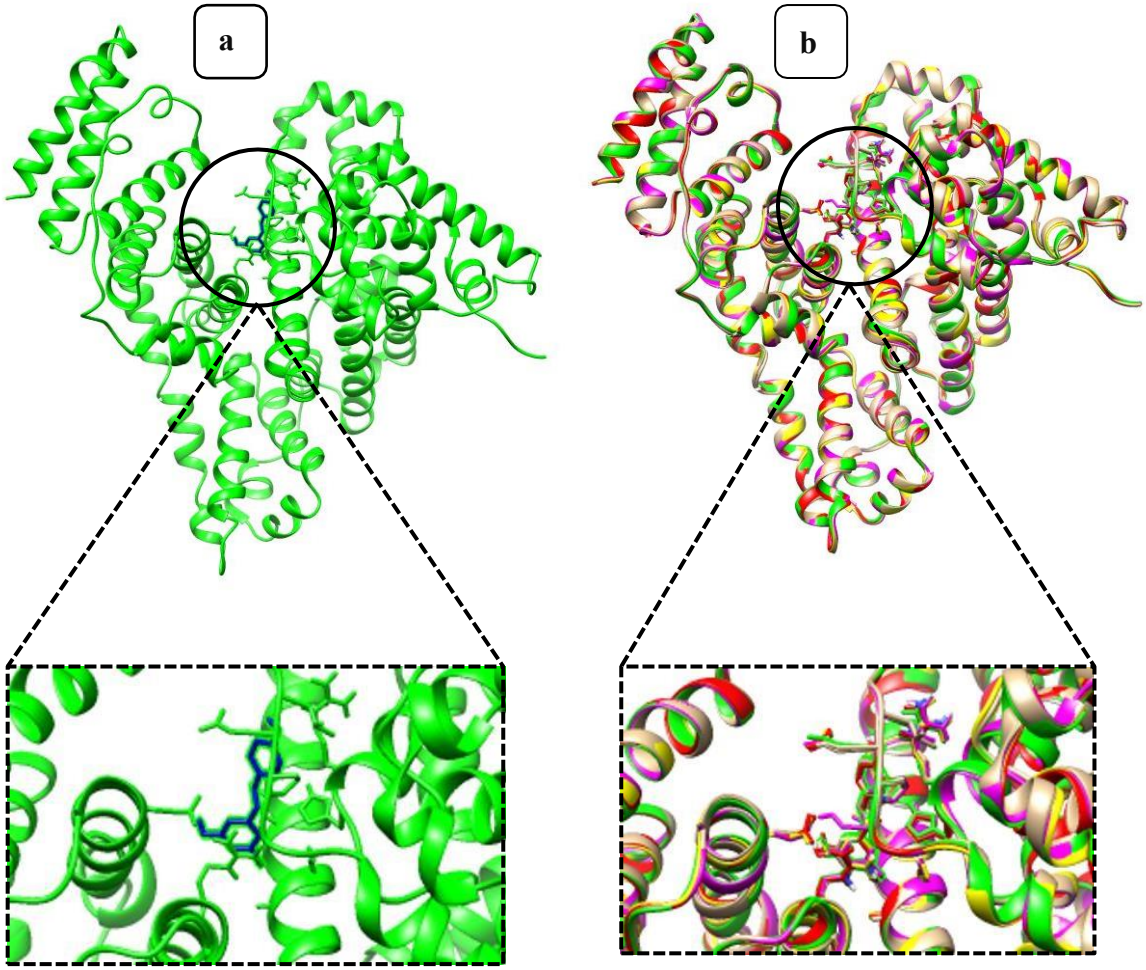

Figure 15: (a) Reference structure of BSA bound to trans-resveratrol. (b) Superimposition of the reference BSA–trans-resveratrol complex with five modeled structures, highlighting the ligand binding site

1.7.3.1.2 Root Mean Square Fluctuation (RMSF)

Definition: RMSF measures the average deviation of each residue from its mean position over the simulation:

$$RMSF(i) = \sqrt{\frac{1}{T}\sum_{t=1}^{T}(r_i(t) - \langle r_i \rangle)^2}$$

where:

- $\mathbf{r}_i(t)$ is the position vector of atom (or residue) i at time t,

- $\langle \mathbf{r}_i \rangle$ is the average position of atom *i* over the entire trajectory (time average),
- T is the total number of time frames in the trajectory.

Interpretation:

- **High RMSF:** Indicates flexible loops, exposed residues, or induced fit mechanisms.
- **Low RMSF:** Reflects stable, rigid regions like α-helices or β-sheets.
- **Binding Site RMSF:** Identifies local changes in ligand-interacting residues [165].

1.7.3.1.3 Solvent Accessible Surface Area (SASA)

Definition: SASA quantifies the surface area of a molecule accessible to a solvent probe (usually 1.4 Å in radius):

$$SASA = \sum_{i=1}^{N} \left(\frac{n_{\text{accessible},i}}{n_{total,i}} \times 4\pi (r_i + r_{probe})^2 \right)$$

where:

- N = total number of atoms (protein + ligand)
- $n_{\text{accessible},i}$ = number of accessible points on atom *i*
- $n_{\text{total},i}$ = total number of points on atom *i*

Interpretation:

- **Protein Folding:** Decrease in SASA signals folding; increase signals unfolding or destabilization.
- **Ligand Binding:** Drop in SASA at the binding site indicates burial of residues; ligand SASA reflects solvent exposure and possible unbinding [166].

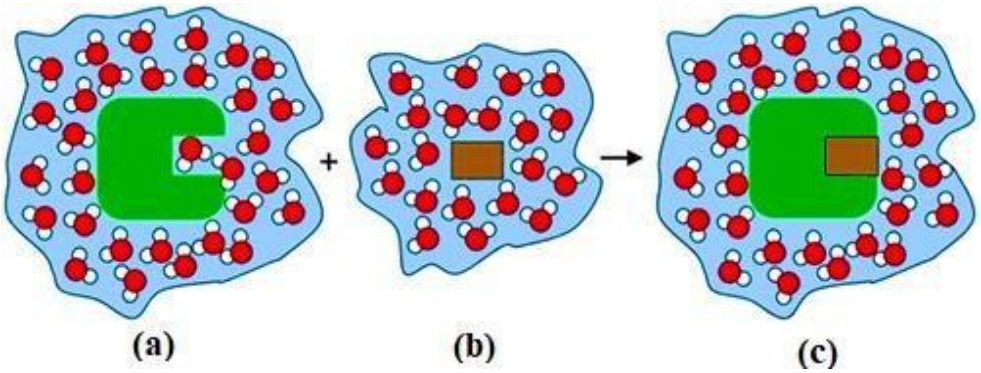

Figure 16: Illustration of Solvent Accessible Surface Area (SASA) Reduction Upon Protein-Ligand Complex Formation. (a) A protein (green structure) surrounded by water molecules, (b) A ligand (brown structure) surrounded by water molecules, (b) The protein-ligand

1.7.3.1.4 Radius of Gyration (Rg)

Definition: Rg measures molecular compactness as the root mean square distance of atoms from the center of mass:

$$R_g = \sqrt{\frac{1}{N}\sum_{i=1}^{N}(\vec{r}_i - \vec{r}_{com})^2}$$

where:

- N is the number of atoms or particles in the molecule.
- $\vec{r}_i$ is the position vector of the i-th atom or particle.
- $\vec{r}_{com}$ is the position vector of the center of mass of the molecule.

Interpretation:

- **Low/Stable Rg:** Indicates compact, folded conformation.
- **Increasing Rg:** Signals expansion, partial unfolding, or flexibility changes.
- **Effect of Ligand:** Binding often decreases Rg, stabilizing protein folds [167].

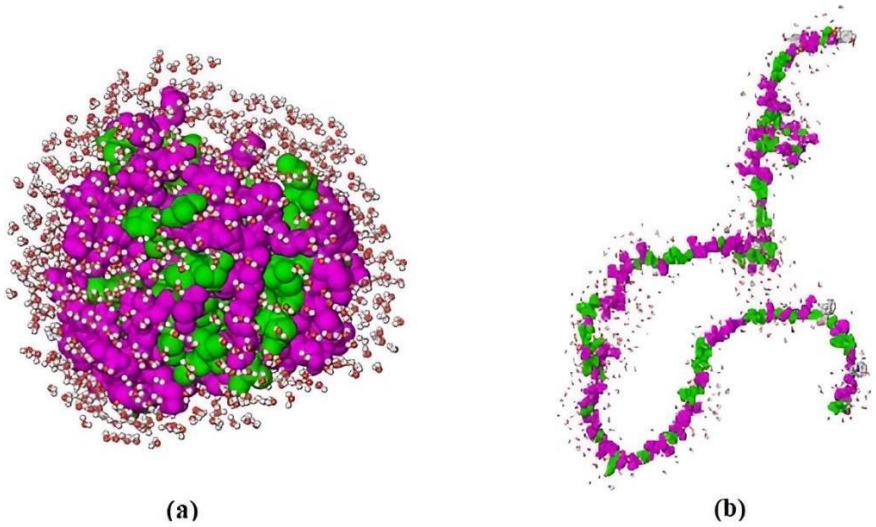

Figure : Illustration of Folded (a) and Unfolded (b) Protein Forms

1.7.3.1.5 Hydrogen Bond Interactions

Definition: A hydrogen bond is formed between a hydrogen donor (e.g., N–H or O–H) and an acceptor atom (e.g., O or N) when:

- Distance ≤ 3.5 Å,
- Donor–hydrogen–acceptor angle ≥ 120°.

Interpretation:

- **Structural Stability:** Persistent backbone H-bonds maintain secondary structure.
- **Ligand Binding:** Stable ligand–protein H-bonds suggest strong interactions.
- **Binding Site Flexibility:** Changes in H-bond patterns support induced-fit behavior.
- **Solvent Interactions:** H-bonds with water indicate exposed or unfolding regions [168].

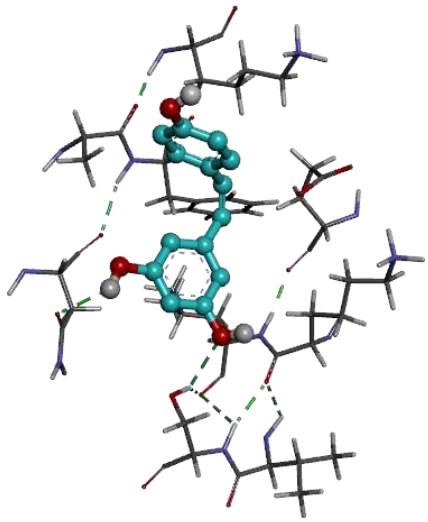

Figure 17: Key Hydrogen Bond Interactions of Trans-Resveratrol Within the Active Site of BSA Protein

References

[87] A. H. Nguyen et al., “Impact of ligand preparation protocols on virtual screening enrichment,” Journal of Cheminformatics, vol. 12, no. 1, p. 13, 2020, doi: 10.1186/s13321-020-0411-0.

[88] A. H. Shoichet, “Virtual screening of chemical libraries,” Nature, vol. 432, no. 7019, pp. 862–865, 2004, doi: 10.1038/nature03197.

[89] O. Trott and A. J. Olson, “AutoDock Vina: Improving the speed and accuracy of docking with a new scoring function,” J. Comput. Chem., vol. 31, no. 2, pp. 455–461, 2010, doi: 10.1002/jcc.21334.

[90] G. Meng et al., “Applications of AutoDock and AutoDock Vina in drug discovery: A review,” Molecular Informatics, vol. 40, no. 5, p. 2000173, 2021, doi: 10.1002/minf.202000173.

[91] M. D. Hanwell et al., “Avogadro: an advanced semantic chemical editor, visualization, and analysis platform,” J. Cheminform., vol. 4, no. 1, p. 17, 2012, doi: 10.1186/1758-2946-4-17.

[92] T. Sousa et al., “Protein and ligand preparation for molecular docking,” Current Protocols in Bioinformatics, vol. 54, no. 1, pp. 5.24.1–5.24.23, 2020, doi: 10.1002/cpbi.108.

[93] L. A. Abraham et al., “Visualizing and analyzing molecular interactions using PyMOL,” Methods in Molecular Biology, vol. 2114, pp. 147–162, 2020, doi: 10.1007/978-1-0716-0301-7_10.

[94] F. Gaudreault and P. M. Najmanovich, “FlexAID: Revisiting docking on non-native-complex structures,” J. Chem. Inf. Model., vol. 55, no. 7, pp. 1323–1336, 2015, doi: 10.1021/ci500594t.

[95] R. Huey et al., “A semiempirical free energy force field with charge-based desolvation,” J. Comput. Chem., vol. 23, no. 4, pp. 412–422, 2002, doi: 10.1002/jcc.10084.

[96] P. Ravindranath et al., “AutoDock for flexible ligand docking with receptor flexibility,” Journal of Molecular Biology, vol. 426, no. 6, pp. 1231–1244, 2014, doi: 10.1016/j.jmb.2013.11.020.

[97] S. S. Bhat et al., “Computational analysis of binding interaction of resveratrol with bovine serum albumin,” Bioinformation, vol. 13, no. 5, pp. 153–158, 2017, doi: 10.6026/97320630013153.

[98] G. Sliwoski et al., “Computational methods in drug discovery,” Pharmacological Reviews, vol. 66, no. 1, pp. 334–395, 2014, doi: 10.1124/pr.112.007336.

[99] X. Hou et al., “Interaction of resveratrol and BSA: Conformation and binding studies,” Spectrochimica Acta A, vol. 173, pp. 854–861, 2017, doi: 10.1016/j.saa.2016.10.045.

[100] M. Sengupta et al., “Insights into resveratrol and BSA interaction,” J. Biomol. Struct. Dyn., vol. 38, no. 1, pp. 222–233, 2020, doi: 10.1080/07391102.2018.1503594.
[101] S. Forli and D. S. Goodsell, “AutoDock Vina in drug discovery,” J. Mol. Recognit., vol. 31, no. 5, 2018, doi: 10.1002/jmr.2736.
[102] J. P. Cross et al., “AutoDock Vina for screening large libraries,” Molecular Informatics, vol. 39, no. 6, p. 2000147, 2020, doi: 10.1002/minf.202000147.
[103] D. Sharma et al., “Molecular docking and ADMET analysis in drug discovery,” Biointerface Research in Applied Chemistry, vol. 11, no. 2, pp. 9025–9035, 2021, doi: 10.33263/BRIAC112.90259035.
[104] A. A. Rauf et al., “Resveratrol: A potent polyphenol with therapeutic perspectives,” Journal of Food Biochemistry, vol. 43, no. 6, e12938, 2019, doi: 10.1111/jfbc.12938.
[105] A. Daina et al., “SwissADME: A free web tool to evaluate pharmacokinetics, drug-likeness and medicinal chemistry friendliness of small molecules,” Scientific Reports, vol. 7, p. 42717, 2017, doi: 10.1038/srep42717.
[106] A. K. Varma et al., “Biopharmaceutics classification system: Past, present, and future,” Journal of Pharmaceutical Sciences, vol. 109, no. 3, pp. 292–303, 2020, doi: 10.1016/j.xphs.2019.10.003.
[107] T. Pires et al., “ADMETlab: A platform for ADMET prediction,” Bioinformatics, vol. 36, pp. 1466–1468, 2020, doi: 10.1093/bioinformatics/btz708.
[108] A. S. Lima et al., “SwissADME and admetSAR in predicting pharmacokinetics,” Journal of Molecular Modeling, vol. 25, no. 6, p. 148, 2019, doi: 10.1007/s00894-019-4024-8.
[109] B. Walle, “Bioavailability of resveratrol,” Annals of the New York Academy of Sciences, vol. 1215, pp. 9–15, 2011, doi: 10.1111/j.1749-6632.2010.05842.x.
[110] G. Baur and D. Sinclair, “Therapeutic properties of resveratrol,” Cell, vol. 127, pp. 1109–1122, 2006, doi: 10.1016/j.cell.2006.11.013.
[111] S. Patel et al., “Resveratrol metabolism by cytochrome P450s,” Drug Metabolism Reviews, vol. 49, no. 2, pp. 129–140, 2017, doi: 10.1080/03602532.2017.1293685.
[112] D. T. Walle, “Pharmacokinetics and metabolism of resveratrol,” Drug Metabolism and Disposition, vol. 32, pp. 1377–1382, 2004, doi: 10.1124/dmd.104.000885.
[113] C. A. Lipinski et al., “Experimental and computational approaches to estimate solubility and permeability in drug discovery and development settings,” Advanced Drug Delivery Reviews, vol. 46, no. 1–3, pp. 3–26, 2001, doi: 10.1016/S0169-409X(00)00129-0.

[114] M. J. Waring, “Lipophilicity in drug discovery,” Expert Opinion on Drug Discovery, vol. 5, no. 3, pp. 235–248, 2010, doi: 10.1517/17460441003605098.

[115] A. Daina, O. Michielin, and V. Zoete, “SwissADME: A free web tool to evaluate pharmacokinetics, drug-likeness and medicinal chemistry friendliness of small molecules,” Scientific Reports, vol. 7, p. 42717, 2017, doi: 10.1038/srep42717.

[116] B. Walle, “Bioavailability of resveratrol,” Annals of the New York Academy of Sciences, vol. 1215, pp. 9–15, 2011, doi: 10.1111/j.1749-6632.2010.05842.x.

[117] T. P. Martin et al., “The rise of in silico toxicology in drug discovery,” Toxicology Letters, vol. 350, pp. 139–149, 2021, doi: 10.1016/j.toxlet.2021.06.004.

[118] S. Banerjee et al., “ProTox-II: A webserver for the prediction of toxicity of chemicals,” Nucleic Acids Research, vol. 46, W1, pp. W257–W263, 2018, doi: 10.1093/nar/gky318.

[119] R. Dunkel et al., “Toxicology in silico: Predicting chemical safety in early-phase drug discovery,” Trends in Pharmacological Sciences, vol. 40, no. 4, pp. 318–329, 2019, doi: 10.1016/j.tips.2019.02.003.

[120] L. Yang et al., “LD50 estimation from in silico models: Toward animal-free acute toxicity testing,” Computational Toxicology, vol. 13, p. 100112, 2020, doi: 10.1016/j.comtox.2019.100112.

[121] C. Choi et al., “Hepatotoxicity screening in silico: Current status and future directions,” Chemical Research in Toxicology, vol. 33, no. 7, pp. 1741–1753, 2020, doi: 10.1021/acs.chemrestox.0c00033.

[122] J. M. Walker et al., “In silico carcinogenicity prediction: Integration with experimental workflows,” Regulatory Toxicology and Pharmacology, vol. 113, p. 104643, 2020, doi: 10.1016/j.yrtph.2020.104643.

[123] N. Benigni and C. Bossa, “Structure–activity relationships for mutagenicity and carcinogenicity,” Chemical Reviews, vol. 111, no. 2, pp. 250–274, 2011, doi: 10.1021/cr100222q.

[124] S. Zhang et al., “A predictive model for cytotoxicity based on machine learning,” Toxicology in Vitro, vol. 67, p. 104892, 2020, doi: 10.1016/j.tiv.2020.104892.

[125] P. L. Tice and S. S. Hammad, “Immunotoxicity assessment in the age of computational toxicology,” Frontiers in Immunology, vol. 11, p. 436, 2020, doi: 10.3389/fimmu.2020.00436.

[126] M. D. Waters and H. Fostel, “Toxicogenomics and systems toxicology: Applications in drug safety assessment,” Nature Reviews Drug Discovery, vol. 3, no. 10, pp. 775–782, 2004, doi: 10.1038/nrd1490.

[127] T. L. Schyman and H. T. Hudspeth, “Predictive toxicology of polyphenols: An in silico ProTox-3.0 analysis,” Toxicology Reports, vol. 9, pp. 456–463, 2022, doi: 10.1016/j.toxrep.2022.01.017.
[128] R. Gupta et al., “Integrating computational and experimental toxicology for drug safety evaluation,” Journal of Pharmacological and Toxicological Methods, vol. 112, p. 107134, 2021, doi: 10.1016/j.vascn.2021.107134.
[129] R. Elber, “A Milestone for Molecular Dynamics Simulations,” Annual Review of Biophysics, vol. 49, pp. 69–88, 2020, doi: 10.1146/annurev-biophys-121219-081609.
[130] M. J. Abraham et al., “GROMACS: High performance molecular simulations through multi-level parallelism from laptops to supercomputers,” SoftwareX, vol. 1–2, pp. 19–25, 2015, doi: 10.1016/j.softx.2015.06.001.
[131] T. Sterling and J. J. Irwin, “ZINC 15 – Ligand Discovery for Everyone,” Journal of Chemical Information and Modeling, vol. 55, no. 11, pp. 2324–2337, 2015, doi: 10.1021/acs.jcim.5b00559.
[132] N. M. O'Boyle et al., “Open Babel: An open chemical toolbox,” Journal of Cheminformatics, vol. 3, p. 33, 2011, doi: 10.1186/1758-2946-3-33. doi: 10.1016/j.bbapap.2016.11.004.
[133] S. Riniker and G. A. Landrum, “Better Informed Distance Geometry: Using What We Know To Improve Conformation Generation,” Journal of Chemical Information and Modeling, vol. 55, no. 12, pp. 2562–2574, 2015, doi: 10.1021/acs.jcim.5b00654.
[134] A. D. MacKerell et al., “All-atom empirical potential for molecular modeling and dynamics studies of proteins,” Journal of Physical Chemistry B, vol. 102, no. 18, pp. 3586–3616, 1998, doi: 10.1021/jp973084f.
[135] B. Hess et al., “LINCS: A linear constraint solver for molecular simulations,” Journal of Computational Chemistry, vol. 18, no. 12, pp. 1463–1472, 1997, doi: 10.1002/(SICI)1096-987X(199709)18:12<1463::AID-JCC4>3.0.CO;2-H.
[136] H. M. Berman et al., “The Protein Data Bank,” Nucleic Acids Research, vol. 28, no. 1, pp. 235–242, 2000, doi: 10.1093/nar/28.1.235.
[137] J. M. Word et al., “Visualizing and quantifying molecular goodness-of-fit: From crystallographic structure to molecular dynamics,” Journal of Molecular Biology, vol. 285, no. 4, pp. 1711–1733, 1999, doi: 10.1006/jmbi.1998.2401.
[138] B. Webb and A. Sali, “Comparative Protein Structure Modeling Using MODELLER,” Current Protocols in Bioinformatics, vol. 54, pp. 5.6.1–5.6.37, 2016, doi: 10.1002/cpbi.3.

[139] D. Van Der Spoel et al., “GROMACS: Fast, flexible, and free,” Journal of Computational Chemistry, vol. 26, no. 16, pp. 1701–1718, 2005, doi: 10.1002/jcc.20291.
[140] A. Olsson et al., “PROPKA3: Consistent treatment of internal and surface residues in empirical pKa predictions,” Journal of Chemical Theory and Computation, vol. 7, no. 2, pp. 525–537, 2011, doi: 10.1021/ct100578z.
[141] J. Wang et al., “Development and testing of a general amber force field,” Journal of Computational Chemistry, vol. 25, no. 9, pp. 1157–1174, 2004, doi: 10.1002/jcc.20035.
[142] J. D. Ponder and D. A. Case, “Force fields for protein simulations,” Advances in Protein Chemistry, vol. 66, pp. 27–85, 2003, doi: 10.1016/S0065-3233(03)66002-X.
[143] C. Oostenbrink et al., “A biomolecular force field based on free enthalpy of hydration and solvation: The GROMOS force-field parameter sets 53A5 and 53A6,” Journal of Computational Chemistry, vol. 25, no. 13, pp. 1656–1676, 2004, doi: 10.1002/jcc.20090.
[144] W. L. Jorgensen et al., “Comparison of simple potential functions for simulating liquid water,” Journal of Chemical Physics, vol. 79, no. 2, pp. 926–935, 1983, doi: 10.1063/1.445869.
[145] L. Wang, J. Deng, and S. Wang, “Water bridges and ligand–protein interactions: A molecular dynamics perspective,” Current Medicinal Chemistry, vol. 27, no. 6, pp. 972–987, 2020, doi: 10.2174/0929867326666190927120930.
[146] M. Feig et al., “Solvation structure and dynamics of biomolecules in aqueous solution,” Current Opinion in Structural Biology, vol. 18, no. 2, pp. 194–199, 2008, doi: 10.1016/j.sbi.2008.01.006.
[147] M. Machuqueiro and P. J. Costa, “Protonation States and Ionic Strength in MD Simulations,” Frontiers in Molecular Biosciences, vol. 6, p. 71, 2019, doi: 10.3389/fmolb.2019.00071.
[148] A. A. Hassan et al., “How salt concentrations affect protein–ligand binding in simulations: A molecular dynamics study,” Biochimica et Biophysica Acta (BBA) - Proteins and Proteomics, vol. 1867, no. 12, p. 140258, 2019, doi: 10.1016/j.bbapap.2019.06.012.
[149] D. J. Wales, Energy landscapes: Applications to clusters, biomolecules and glasses, Cambridge University Press, 2003, doi: 10.1017/CBO9780511610684.
[150] B. R. Brooks et al., “CHARMM: The biomolecular simulation program,” Journal of Computational Chemistry, vol. 30, no. 10, pp. 1545–1614, 2009, doi: 10.1002/jcc.21287.
[151] G. Bussi et al., “Canonical sampling through velocity rescaling,” Journal of Chemical Physics, vol. 126, no. 1, p. 014101, 2007, doi: 10.1063/1.2408420.

[152] S. Nosé, “A unified formulation of the constant temperature molecular dynamics methods,” Journal of Chemical Physics, vol. 81, no. 1, pp. 511–519, 1984, doi: 10.1063/1.447334.
[153] M. Parrinello and A. Rahman, “Polymorphic transitions in single crystals: A new molecular dynamics method,” Journal of Applied Physics, vol. 52, no. 12, pp. 7182–7190, 1981, doi: 10.1063/1.328693.
[154] D. Frenkel and B. Smit, Understanding Molecular Simulation: From Algorithms to Applications, 2nd ed., Academic Press, 2001, doi: 10.1016/B978-0-12-267351-1.X5000-7.
[155] S. Genheden and U. Ryde, “The MM/PBSA and MM/GBSA methods to estimate ligand-binding affinities,” Expert Opinion on Drug Discovery, vol. 10, no. 5, pp. 449–461, 2015, doi: 10.1517/17460441.2015.1032936.
[156] M. Karplus and J. Kuriyan, “Molecular dynamics and protein function,” Proceedings of the National Academy of Sciences, vol. 102, no. 19, pp. 6679–6685, 2005, doi: 10.1073/pnas.0408930102.
[157] L. G. Henchman, “Interpretation of root-mean-square deviation in molecular dynamics simulations,” Journal of Chemical Theory and Computation, vol. 3, no. 6, pp. 1980–1990, 2007, doi: 10.1021/ct700119w.
[158] S. D. Khodadadi and R. M. Anderson, “Application of RMSF to protein flexibility studies,” Biochimica et Biophysica Acta (BBA) - Proteins and Proteomics, vol. 1865, no. 2, pp. 346–358, 2017, doi: 10.1016/j.bbapap.2016.11.004.
[159] J. C. Phillips et al., “Scalable molecular dynamics with NAMD,” Journal of Computational Chemistry, vol. 26, no. 16, pp. 1781–1802, 2005, doi: 10.1002/jcc.20289.
[160] J. Tomasi, B. Mennucci, and R. Cammi, “Quantum mechanical continuum solvation models,” Chemical Reviews, vol. 105, no. 8, pp. 2999–3093, 2005, doi: 10.1021/cr9904009.
[161] M. K. Moshfegh, M. R. Ganjali, and M. Noroozifar, “Theoretical investigation of antioxidant activity of resveratrol using DFT and QTAIM approaches,” Computational and Theoretical Chemistry, vol. 1115, pp. 57–65, 2017, doi: 10.1016/j.comptc.2017.05.010.
[162] D. Glossman-Mitnik and J. Frau, “Accurate Chemical Reactivity Theory Descriptors for the Isomers of Resveratrol,” Molecules, vol. 25, no. 24, p. 5846, 2020, doi: 10.3390/molecules25245846.
[163] Y. He, Z. Wang, and X. Zhang, “Spectroscopic investigation on the binding of cis- and trans-resveratrol with bovine serum albumin,” J. Mol. Struct., vol. 1122, pp. 105–113, 2016, doi: 10.1016/j.molstruc.2016.06.078.

[164] M. Sengupta et al., “Insights into the interaction between resveratrol and BSA by fluorescence spectroscopy and molecular docking,” J. Biomol. Struct. Dyn., vol. 38, no. 1, pp. 222–233, 2020, doi: 10.1080/07391102.2018.1503594.
[165] X. Hou, Y. Guo, M. Yuan, and Z. Lv, “Interaction of resveratrol and BSA: Conformation and binding studies,” Spectrochim. Acta A Mol. Biomol. Spectrosc., vol. 173, pp. 854–861, 2017, doi: 10.1016/j.saa.2016.10.045.
[166] M. K. Moshfegh et al., “Theoretical investigation of antioxidant activity of resveratrol using DFT and QTAIM approaches,” Computational and Theoretical Chemistry, vol. 1115, pp. 57–65, 2017, doi: 10.1016/j.comptc.2017.05.010.
[167] J. C. Phillips et al., “Scalable molecular dynamics with NAMD,” Journal of Computational Chemistry, vol. 26, no. 16, pp. 1781–1802, 2005, doi: 10.1002/jcc.20289.
[168] D. Glossman-Mitnik and J. Frau, “Accurate Chemical Reactivity Theory Descriptors for the Isomers of Resveratrol,” Molecules, vol. 25, no. 24, p. 5846, 2020, doi: 10.3390/molecules25245846.

Chapter III

In Silico Tools and Software

1.8 In Silico Tools

1.8.1 SwissADME: A Tool for Pharmacokinetic and Drug-Likeness Prediction

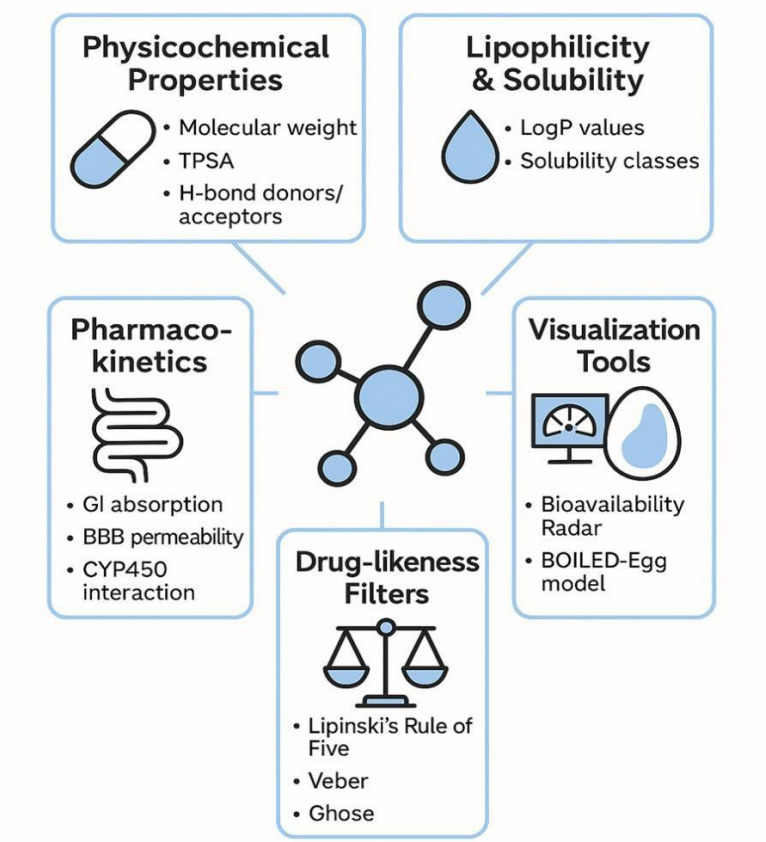

Figure 18: Key Features of SwissADME for In Silico Drug Evaluation

In silico methods have become indispensable in modern drug discovery, offering cost-effective and time-efficient strategies for evaluating the pharmacokinetic behavior and drug-likeness of small molecules. Among the most widely adopted platforms in this context is SwissADME, a freely accessible web-based tool (http://www.swissadme.ch/) developed to assist in the rational design and preclinical assessment of bioactive compounds.

SwissADME supports the prediction of key molecular properties relevant to absorption, distribution, metabolism, and excretion (ADME). By calculating a wide array of physicochemical descriptors, including molecular weight, hydrogen bond donors and acceptors, topological polar surface area (TPSA), and rotatable bonds, the tool facilitates early-stage filtering of compounds for desirable pharmacokinetic profiles [169]. These properties are essential for evaluating

molecular behavior in biological systems and are used as inputs for further predictive models integrated within the platform.

One of the core features of SwissADME is its ability to estimate lipophilicity, a critical determinant of membrane permeability and solubility. The platform provides multiple lipophilicity values computed using distinct algorithms, such as XLogP3, WLogP, MLogP, and SILICOS-IT, allowing users to compare and validate predictions. Water solubility is also predicted using an advanced model that classifies compounds into solubility classes, guiding formulation and delivery strategies.

SwissADME further offers predictions for pharmacokinetic behavior, including gastrointestinal (GI) absorption, blood–brain barrier (BBB) permeability, and interaction with cytochrome P450 (CYP450) enzymes, which are central to metabolic stability and potential drug–drug interactions. These insights are vital for eliminating candidates with poor bioavailability or high metabolic liabilities at an early stage [170].

In addition to quantitative predictions, SwissADME provides drug-likeness evaluations based on established empirical rules such as Lipinski's Rule of Five, Ghose filter, Veber filter, and Egan's and Muegge's rules. These filters assess whether a compound falls within the physicochemical space associated with orally active drugs, helping researchers identify lead-like molecules with higher development potential.

To enhance data interpretation, SwissADME integrates intuitive visualization tools. The bioavailability radar offers a graphical summary of six key molecular properties, indicating whether a compound resides within the optimal zone for oral bioavailability. Similarly, the BOILED-Egg model predicts passive absorption and brain access by plotting polarity versus lipophilicity on a two-dimensional diagram, simplifying complex data into actionable insights [171].

Altogether, SwissADME serves as a comprehensive and reliable platform for evaluating small molecules in the early phases of drug design. Its integration of computational models, rule-based filters, and visual analytics makes it a valuable asset in both academic research and pharmaceutical development.

1.8.2 ProTox-3.0: In Silico Prediction of Chemical Toxicity

The accurate prediction of compound toxicity plays a central role in drug discovery and safety evaluation. Experimental approaches for toxicity assessment are resource-intensive, time-consuming, and often raise ethical concerns due to animal testing. As a result, in silico tools have emerged as effective alternatives for preliminary toxicity screening. Among these, ProTox-3.0 (https://tox.charite.de/protox3/index.php?site=compound_input) has established itself as a comprehensive and accessible web-based platform for predicting the toxicological profile of small molecules.

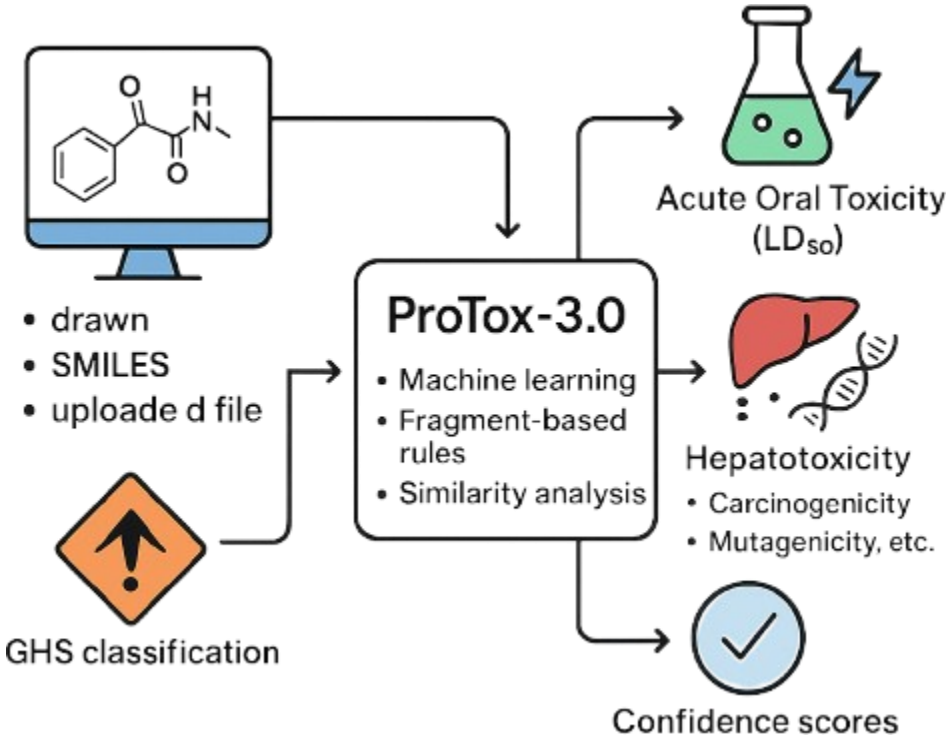

Figure 19: Workflow of ProTox-3.0 for In Silico Toxicity Prediction of Small Molecules

ProTox-3.0 integrates machine learning algorithms, molecular similarity analysis, and fragment-based toxicity rules to estimate the potential adverse effects of chemical compounds. Its predictive models are trained on extensive datasets derived from toxicological assays, pharmacological databases, and chemical repositories. This multifaceted strategy enhances the reliability of its predictions across diverse compound classes [172].

A distinctive advantage of ProTox-3.0 is its broad coverage of toxicity endpoints. The platform can estimate acute oral toxicity (LD_{50}), along with several mechanistic toxicity classes including hepatotoxicity, carcinogenicity, mutagenicity, cytotoxicity, immunotoxicity, and endocrine disruption. Each prediction is accompanied by a confidence score and visual indicators that help in rapid interpretation. Furthermore, the tool classifies compounds into Globally Harmonized System (GHS) toxicity classes, aiding in regulatory and risk assessment contexts [173].

In practical application, ProTox-3.0 allows users to input chemical structures via SMILES notation, upload molecular files, or draw molecules using an embedded editor. Once processed, the platform provides an interactive summary of the compound's toxicological risks, including predicted LD_{50} values (in mg/kg) and likelihood of interaction with specific toxicity pathways. Such outputs are invaluable for filtering out hazardous molecules early in the compound design pipeline [174].

Overall, ProTox-3.0 offers a scientifically robust and user-friendly environment for early toxicity screening, aligning with the principles of the 3Rs (Replacement, Reduction, and Refinement) in toxicological testing. Its integration in computational workflows significantly enhances the efficiency and ethical compliance of modern drug development.

1.8.3 The Protein–Ligand Interaction Profiler (PLIP):

Automated Analysis of Non-Covalent Interactions Understanding the nature of non-covalent interactions between ligands and their target proteins is central to modern drug discovery and molecular modeling. These interactions—such as hydrogen bonding, hydrophobic contacts, and π–π stacking—determine the binding affinity, specificity, and stability of molecular complexes. An accurate, automated analysis of these interactions provides critical insights during lead optimization and structure-based design, facilitating more efficient identification of biologically active compounds.

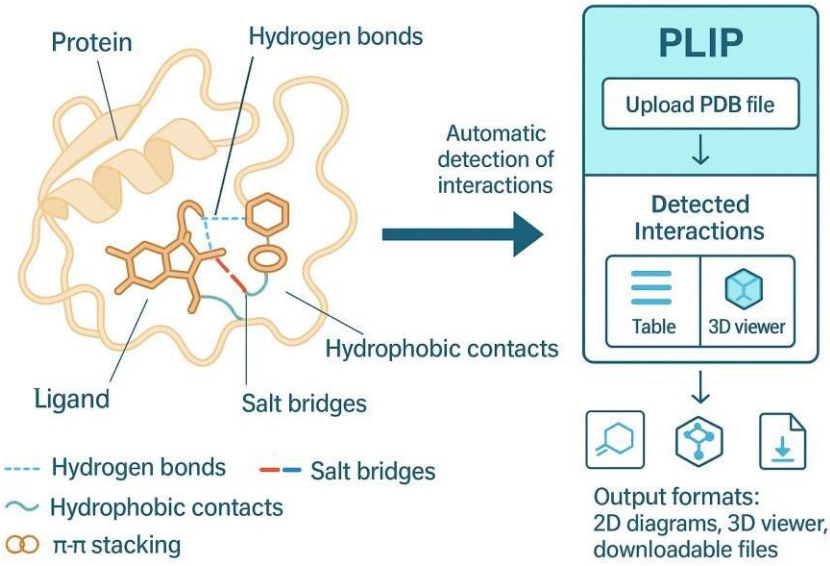

Figure 20: Automated Detection of Protein–Ligand Interactions Using PLIP

The Protein–Ligand Interaction Profiler (PLIP) is a widely used, open-access web server (https://plip-tool.biotec.tu-dresden.de/plip-web/plip/index) developed to perform automated detection and visualization of non-covalent interactions from three-dimensional protein–ligand complex structures. PLIP is compatible with structural data obtained from experimental methods such as X-ray crystallography, NMR, and cryo-EM, as well as from computational modeling and docking studies. Users simply upload a protein–ligand complex in PDB format, and PLIP processes the file to identify relevant molecular interactions using a rule-based algorithm [175]. PLIP detects a comprehensive range of interaction types, including hydrogen bonds, hydrophobic contacts, π–π stacking, π–cation interactions, salt bridges, halogen bonds, and water-mediated bridges. Each detected interaction is evaluated based on geometric criteria derived from empirical observations of protein–ligand complexes, ensuring high reliability and interpretability [176]. The tool also highlights interacting atoms and residues, along with detailed spatial and physicochemical descriptors for each contact.

The output of PLIP is multifaceted and user-friendly. It includes an interactive table summarizing all detected interactions, 2D diagrams of ligand binding, and 3D visualization files compatible with common molecular viewers. These outputs can be downloaded in multiple formats for integration into computational pipelines or inclusion in reports and publications. The availability

of both a web interface and command-line tool make PLIP suitable for high-throughput and reproducible workflows.

One of the key advantages of PLIP lies in its automation and accessibility. It removes the need for manual inspection or scripting to extract interaction data, which significantly reduces user bias and technical barriers. As a result, it is broadly adopted in academic and pharmaceutical research for post-docking validation, structure-function analysis, and comparative binding studies [177].

1.8.4 The RCSB Protein Data Bank: A Central Resource for Structural Bioinformatics

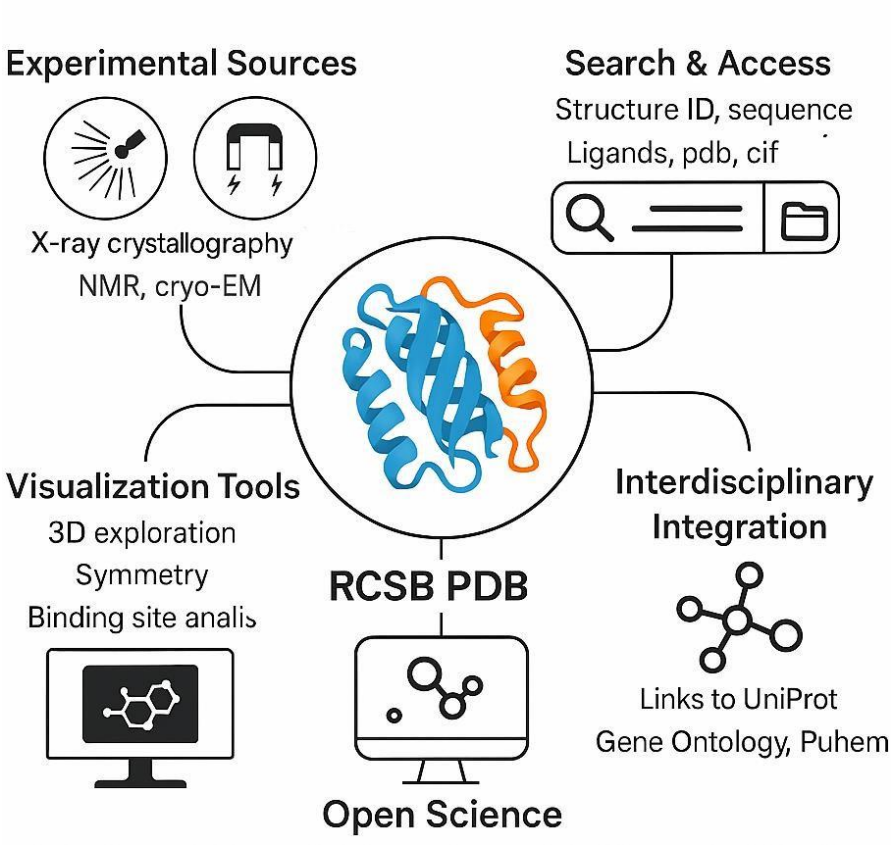

Figure 21: Overview of RCSB PDB Functionalities in Structural Bioinformatics

Three-dimensional structural data are essential for understanding the function, interaction, and dynamics of biological macromolecules, especially in the context of molecular biology, structural bioinformatics, and drug discovery. Access to accurate and experimentally validated structural information enables researchers to analyze biomolecular mechanisms, design ligands, predict binding affinities, and simulate conformational behavior. In this regard, the RCSB Protein Data

Bank (RCSB PDB), accessible via https://www.rcsb.org, serves as a cornerstone in the infrastructure of life sciences research.

The RCSB PDB is the primary U.S. node of the Worldwide Protein Data Bank (wwPDB), tasked with maintaining, curating, and distributing the global archive of 3D structures of biological macromolecules. These structures are determined through high-resolution experimental techniques, including X-ray crystallography, nuclear magnetic resonance (NMR) spectroscopy, and cryo-electron microscopy (cryo-EM). Each deposited entry undergoes rigorous validation, annotation, and formatting to ensure consistency, accuracy, and interoperability across platforms [178].

One of the most important functions of the RCSB PDB is to provide searchable and user-friendly access to structural data. Users can query the database by structure ID, sequence, ligand, keyword, experimental method, and other metadata. Once retrieved, structural files are available in standard formats such as .pdb and .cif, suitable for use in visualization software and computational modeling pipelines. The platform also integrates a set of interactive visualization tools, enabling users to explore macromolecular structures in 3D, identify binding sites, examine symmetry, and analyze structural domains without leaving the web interface [179].

In addition to its role as a structural repository, the RCSB PDB provides access to value-added services such as structural alignments, functional annotations, protein classification, and cross-links to external resources including UniProt, PubChem, and Gene Ontology. These features promote the interdisciplinary integration of structural data with genomic, biochemical, and pharmacological information. The RCSB PDB also emphasizes open science, offering unrestricted access to all deposited structures, along with comprehensive documentation, tutorials, and educational materials for the broader scientific community [180].

By supporting the transparency, reproducibility, and reuse of structural data, the RCSB PDB plays a foundational role in both experimental and computational research. Its contribution to advancing scientific understanding and enabling data-driven discovery makes it a critical asset in structural biology, computational chemistry, and drug design.

1.9 The Computational Software

1.9.1 GaussView 5.0: A Graphical Interface for Quantum Chemical Modeling

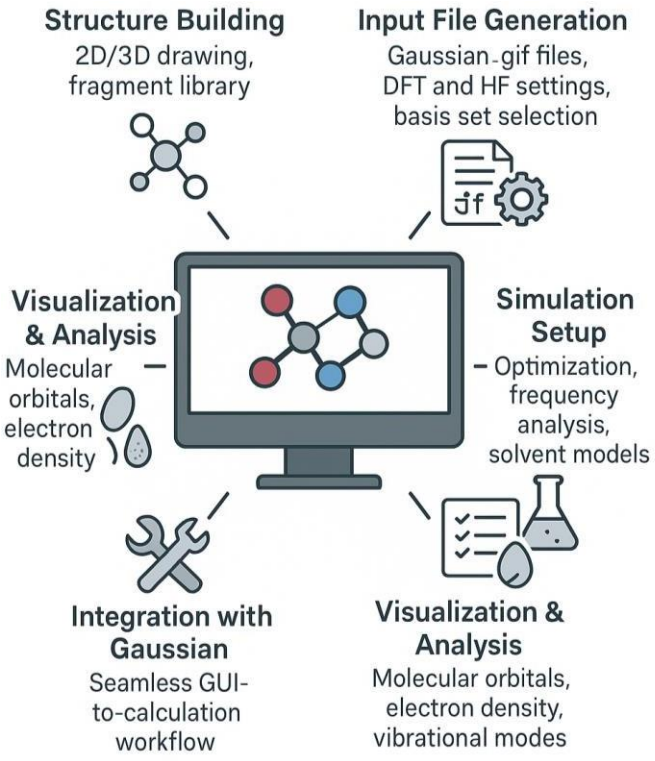

Figure 22: Overview of GaussView 5.0: Key Functions in Quantum Chemical Modeling

In computational chemistry, molecular visualization and structure optimization are foundational processes for understanding chemical reactivity, energetics, and electronic structure. These tasks are central to quantum chemical simulations, where the accuracy of input geometries and the ability to interpret calculated properties directly influence the success of theoretical investigations. Graphical user interfaces (GUIs) such as GaussView 5.0 facilitate these processes by offering a user-friendly platform for building, inspecting, and analyzing molecular systems prior to and following quantum mechanical calculations.

GaussView 5.0 is a molecular visualization and input generation tool designed to work seamlessly with Gaussian, one of the most widely used software packages for ab initio and density functional theory (DFT) calculations. As an intuitive GUI, GaussView allows users to construct and edit molecular structures in 2D or 3D space using a library of atomic and molecular fragments. It also

enables the manual assignment of atom types, hybridization states, formal charges, and spin multiplicities, thereby ensuring chemically accurate model preparation [181].

A key feature of GaussView 5.0 is its ability to generate Gaussian input files (.gjf). Through its interface, users can define computational parameters including the method of calculation (e.g., HF, DFT), basis sets, job types (e.g., optimization, frequency analysis), and solvent models. This streamlines the preparation of complex simulations without requiring direct manipulation of the Gaussian input syntax, reducing the potential for formatting errors and increasing efficiency in setting up large numbers of calculations [182].

Beyond input preparation, GaussView 5.0 provides post-processing and visualization tools that support interpretation of quantum chemical results. It enables the analysis of optimized geometries, molecular orbital surfaces, electron density distributions, and vibrational frequencies, often through interactive 3D models and animated normal modes. These capabilities are particularly valuable in geometry optimization, molecular orbital analysis, and vibrational spectroscopy, where visual feedback aids in evaluating molecular behavior and verifying the correctness of the computational output [183].

GaussView 5.0 thus serves as a critical interface that bridges theoretical chemistry with practical modeling workflows. By integrating structure construction, input preparation, and result visualization into a unified environment, it enhances both the accuracy and accessibility of quantum chemical simulations—benefiting researchers in chemistry, materials science, and molecular design.

1.9.2 MGLTools and AutoDock Vina: Core Tools for Molecular Docking

Molecular docking has become an indispensable technique in structure-based drug design, enabling the prediction of interactions between small molecules and biological targets at the atomic level. By estimating the binding conformations and affinities of ligands to their receptors, docking provides crucial insights that guide the selection and optimization of drug candidates. The accuracy and efficiency of docking outcomes depend heavily on the quality of molecular input data and the algorithms used for pose prediction and scoring. In this context, MGLTools and AutoDock Vina are widely recognized as essential components in the computational drug discovery workflow.

MGLTools, developed by the Molecular Graphics Laboratory at The Scripps Research Institute, is a software suite that supports the preparation of molecular structures for docking simulations. It includes a graphical user interface (AutoDockTools) and command-line utilities that facilitate tasks

such as adding polar hydrogens, computing Gasteiger charges, detecting torsion bonds, and generating grid boxes to define the docking search space. One of its most important functions is the conversion of molecular files into the PDBQT format, which is required by AutoDock-based docking engines. These preparatory steps ensure that both the ligand and receptor are in the correct conformation and chemical state for accurate docking analysis [184].

Once molecular files are properly prepared, AutoDock Vina is employed as the docking engine to predict binding poses and binding affinities of small molecules. AutoDock Vina improves upon its predecessor, AutoDock 4, by introducing an efficient stochastic global optimization algorithm and an empirical scoring function that balances speed and accuracy. This allows the tool to rapidly explore conformational space and identify energetically favorable ligand–receptor complexes. Vina's performance in terms of docking speed and predictive accuracy has made it a standard tool in academic and pharmaceutical research, particularly for large-scale virtual screening campaigns [185].

The popularity of MGLTools and AutoDock Vina is further supported by their open-source availability, user-friendly interfaces, and broad compatibility with other computational platforms. Together, they provide a robust, flexible, and reproducible framework for investigating molecular interactions, making them integral to computational pipelines aimed at drug target validation, lead identification, and mechanistic exploration [186].

1.9.3 Discovery Studio 2025 Client: An Integrated Platform for Molecular Modeling and Drug Design

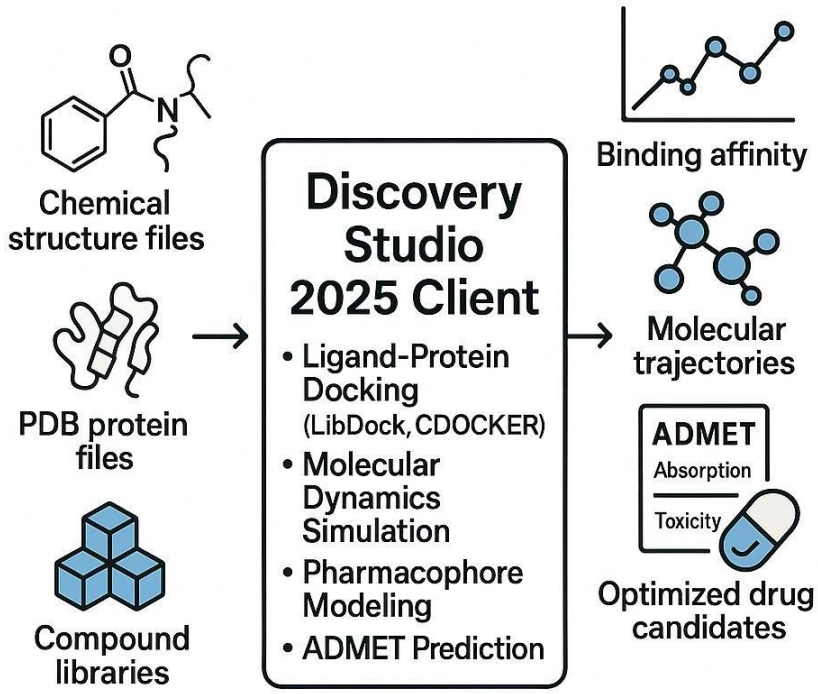

Figure 23: Overview of Discovery Studio 2025 Client Workflow for Molecular Modeling and Drug Design

The advancement of computational tools has significantly enhanced the process of **rational drug design**, enabling researchers to simulate, predict, and visualize molecular behavior with high precision. In this context, integrated platforms such as **Discovery Studio 2025 Client** play a vital role in consolidating a wide range of computational capabilities into a single, user-friendly environment. By offering seamless workflows for simulation, analysis, and visualization, Discovery Studio supports efficient and reproducible research in medicinal chemistry, structural biology, and pharmacoinformatic.

Discovery Studio 2025 Client, developed by Dassault Systems BIOVIA, is a comprehensive software suite designed for modeling and simulation of small molecules, proteins, nucleic acids, and complex biological systems. It provides an intuitive graphical interface that allows users to perform diverse computational tasks without requiring extensive programming knowledge. This

accessibility makes it suitable for both novice users and advanced researchers seeking a high level of control over simulation parameters [187].

The platform encompasses a wide array of core functionalities essential to structure-based drug design. These include **ligand–protein docking**, where the spatial orientation and binding affinity of small molecules to their targets are predicted using algorithms such as CDOCKER and LibDock; **molecular dynamics (MD) simulations**, which provide insights into the conformational stability and flexibility of biomolecular systems over time; and **pharmacophore modeling**, which helps identify and map key chemical features responsible for biological activity. Additionally, Discovery Studio integrates **ADMET prediction tools** that estimate a compound's pharmacokinetic properties and toxicity profile, thus aiding in the early identification of drug-like candidates [188].

The **modular architecture** of Discovery Studio facilitates interoperability with other platforms and supports a wide range of data types, including protein structures from the Protein Data Bank (PDB) and compound libraries in various chemical formats. Researchers can also link experimental datasets and simulation results to support **data-driven hypothesis generation** and compound prioritization. Furthermore, the software's robust **visualization capabilities** enable real-time analysis of molecular structures, interaction networks, and simulation trajectories, contributing to a more intuitive understanding of molecular interactions and dynamics [189].

By integrating multiple modeling techniques into a unified environment, Discovery Studio 2025 Client serves as a powerful tool for accelerating drug discovery pipelines, optimizing lead compounds, and enhancing the interpretability of in silico experiments. Its emphasis on automation, reproducibility, and scientific rigor makes it a cornerstone technology in contemporary computational pharmaceutical research.

1.9.4 GROMACS: An Open-Source Engine for Molecular Dynamics Simulations

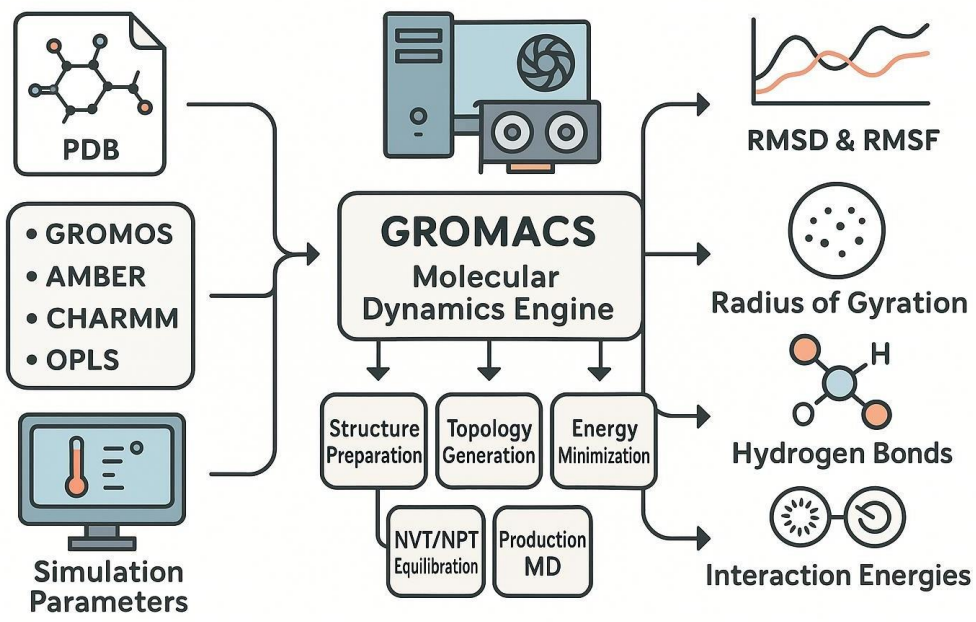

Figure 24: Workflow of GROMACS for Molecular Dynamics Simulations and Analysis

Molecular dynamics (MD) simulations are central to understanding the physical behavior of molecular systems at the atomic scale. By numerically integrating Newton's equations of motion, MD simulations enable researchers to explore structural conformations, dynamic behavior, and thermodynamic properties of biomolecules in various environments. These simulations are critical for gaining insight into biological processes, protein folding, molecular interactions, and material properties, providing both qualitative and quantitative data that complement experimental findings.

GROMACS (GROningen MAchine for Chemical Simulations) is a widely adopted open-source software suite for conducting high-performance MD simulations. Initially developed at the University of Groningen and now maintained by an international community, GROMACS is known for its exceptional computational efficiency and scalability across both CPUs and GPUs. It is compatible with multiple biomolecular force fields, such as GROMOS, AMBER, CHARMM, and OPLS, making it suitable for simulating a wide range of molecular systems [190].

The software offers a complete suite of tools for setting up, running, and analyzing MD simulations. Key features include energy minimization, position-restrained equilibration, and production MD, all of which can be tailored to specific system requirements. GROMACS also includes robust algorithms for temperature and pressure coupling, constraint handling, and long-range electrostatics, as well as optimized parallelization schemes that support simulations on multi-core processors, distributed clusters, and GPU-accelerated environments [191].

A standard GROMACS workflow typically begins with structure preparation, where atomic coordinates are cleaned and formatted. This is followed by topology generation, during which the molecular force field is applied to assign parameters and generate the system description. Afterward, energy minimization is performed to remove unfavorable steric clashes, followed by equilibration steps under constant temperature (NVT) and constant pressure (NPT) conditions. The production phase involves the actual MD simulation over a defined timescale. Finally, the trajectory analysis tools in GROMACS allow for the evaluation of properties such as root mean square deviation (RMSD), root mean square fluctuation (RMSF), radius of gyration, hydrogen bonding, solvent-accessible surface area (SASA), and interaction energies [192].

Due to its modular design, script ability, and extensive documentation, GROMACS has been extensively adopted in both academic research and industrial applications, ranging from protein–ligand interaction studies to materials science and nanotechnology. Its ability to simulate large, complex systems efficiently makes it a cornerstone platform in computational modeling and theoretical biophysics.

References

[169] A. Daina, O. Michielin, and V. Zoete, "SwissADME: a free web tool to evaluate pharmacokinetics, drug-likeness and medicinal chemistry friendliness of small molecules," Sci. Rep., vol. 7, p. 42717, 2017. doi: 10.1038/srep42717

[170] B. Pires, T. Blundell, and D. Ascher, "pkCSM: Predicting small-molecule pharmacokinetic and toxicity properties using graph-based signatures," J. Med. Chem., vol. 58, no. 9, pp. 4066–4072, 2015. doi: 10.1021/acs.jmedchem.5b00104

[171] A. Daina and V. Zoete, "A BOILED-Egg to predict gastrointestinal absorption and brain penetration of small molecules," ChemMedChem, vol. 11, no. 11, pp. 1117–1121, 2016. doi: 10.1002/cmdc.201600182

[172] N. Banerjee, M. Kar, and A. Roy, "In silico toxicology: current trends and future directions," Computational Toxicology, vol. 19, pp. 100184, 2021. doi: 10.1016/j.comtox.2021.100184

[173] D. Banerjee et al., "ProTox-II: A webserver for the prediction of toxicity of chemicals," Nucleic Acids Res., vol. 46, no. W1, pp. W257–W263, 2018. doi: 10.1093/nar/gky318

[174] M. H. Schyman, B. Liu, and J. S. Wallqvist, "Development and validation of machine learning models for in silico prediction of chemical toxicity," J. Chem. Inf. Model., vol. 61, no. 2, pp. 730–742, 2021. doi: 10.1021/acs.jcim.0c01123

[175] M. Salentin, S. Schreiber, V. J. Haupt, M. F. Adasme, and M. Schroeder, "PLIP: fully automated protein–ligand interaction profiler," Nucleic Acids Res., vol. 43, no. W1, pp. W443–W447, 2015. doi: 10.1093/nar/gkv315

[176] F. Adasme-Carreño et al., "PLIP 2021: expanding the scope of the protein–ligand interaction profiler to DNA and RNA," Nucleic Acids Res., vol. 49, no. W1, pp. W530–W534, 2021. doi: 10.1093/nar/gkab294

[177] R. Luna et al., "Automated profiling of protein-ligand contacts improves reproducibility and analysis in drug discovery," Brief. Bioinform., vol. 24, no. 2, pp. bbad001, 2023. doi: 10.1093/bib/bbad001

[178] S. K. Burley et al., "RCSB Protein Data Bank: Powerful new tools for exploring 3D structures of biological macromolecules for basic and applied research and education," Nucleic Acids Res., vol. 49, no. D1, pp. D437–D451, 2021. doi: 10.1093/nar/gkaa1038

[179] D. S. Goodsell, J. D. Westbrook, and S. K. Burley, "Visualizing biological data from the Protein Data Bank," Protein Sci., vol. 30, no. 1, pp. 20–33, 2021. doi: 10.1002/pro.3972

[180] J. D. Westbrook and H. M. Berman, “The Protein Data Bank and structural biology: Insights and challenges,” Curr. Opin. Struct. Biol., vol. 68, pp. 203–212, 2021. doi: 10.1016/j.sbi.2020.11.005

[181] C. Lee, Y. Kim, and H. Jang, “Computational chemistry tools for molecular modeling and simulation: A practical guide,” J. Mol. Graph. Model., vol. 95, p. 107503, 2020. doi: 10.1016/j.jmgm.2019.107503

[182] M. J. Frisch et al., Gaussian 16, Revision C.01, Gaussian, Inc., Wallingford, CT, 2016.

[183] D. R. Salahub and K. M. Merz, “Visualization and interpretation of quantum chemical data: Methods and interfaces,” Int. J. Quantum Chem., vol. 115, no. 21, pp. 1392–1404, 2015. doi: 10.1002/qua.24978

[184] O. Trott and A. J. Olson, “AutoDock Vina: Improving the speed and accuracy of docking with a new scoring function, efficient optimization, and multithreading,” J. Comput. Chem., vol. 31, no. 2, pp. 455–461, 2010. doi: 10.1002/jcc.21334

[185] M. R. Bauer et al., “Comparative evaluation of AutoDock and AutoDock Vina in ligand docking,” J. Chem. Inf. Model., vol. 60, no. 12, pp. 5918–5930, 2020. doi: 10.1021/acs.jcim.0c00685

[186] R. Kumari and R. Kumar, “Molecular docking and its applications in drug discovery process,” Res. J. Life Sci. Bioinform. Pharm. Chem. Sci., vol. 7, no. 1, pp. 1–12, 2021. doi: 10.26479/2021.0701.01

[187] A. Goh et al., “Integrated computational platforms for predictive drug discovery: Current status and future directions,” J. Chem. Inf. Model., vol. 60, no. 11, pp. 4983–4994, 2020. doi: 10.1021/acs.jcim.0c00761

[188] A. Sakkiah, Y. Xia, and W. Lee, “Pharmacophore modeling and docking studies for design of potential TNF-α inhibitors using Discovery Studio,” J. Biomol. Struct. Dyn., vol. 37, no. 6, pp. 1547–1557, 2019. doi: 10.1080/07391102.2018.1478441

[189] M. F. Adasme, M. Linnemann, and M. Schroeder, “Advances in computational platforms for structure-based drug design,” Brief. Bioinform., vol. 23, no. 1, pp. bbab340, 2022. doi: 10.1093/bib/bbab340

[190] B. Hess et al., “GROMACS 4: Algorithms for highly efficient, load-balanced, and scalable molecular simulation,” J. Chem. Theory Comput., vol. 4, no. 3, pp. 435–447, 2008. doi: 10.1021/ct700301q

[191] M. J. Abraham et al., “GROMACS: High performance molecular simulations through multi-level parallelism from laptops to supercomputers,” SoftwareX, vol. 1–2, pp. 19–25, 2015. doi: 10.1016/j.softx.2015.06.001
[192] D. Van Der Spoel et al., “GROMACS in the new era of open-source molecular simulation,” J. Mol. Biol., vol. 432, no. 15, pp. 4300–4321, 2020. doi: 10.1016/j.jmb.2020.02.017

Chapter IV

Results and Discussion

1.10 Results interpretation

1.10.1 Literature-Based In Vitro Study

This **in silico** investigation was conducted based on binding parameters extracted from previously published in vitro study. The results from literature source [1] were used to compare and validate the interaction between resveratrol and Bovine Serum Albumin (BSA). The table below presents the obtained Gibbs free energy (ΔG) values and binding constants (K_a) extracted from the referenced research:

Table 1: In Vitro Binding Affinity Parameters (ΔG and K) of Cis- and Trans-Resveratrol

In vitro investigation	**ΔG**	**K**
Cis-Resveratrol	-27.69	$6.27 \pm 0.43 \times 10^4$
Trans-Resveratrol	-27.37	$7.16 \pm 0.44 \times 10^4$

1.10.2 Structural and Interaction Analysis of cis- and trans-Resveratrol Isomers

1.10.2.1 Molecular Structure Optimization

The journey into the molecular world of resveratrol begins with a close examination of its two isomeric forms: **Cis-resveratrol (*CRes*)** and **Trans-resveratrol (*TRes*)**. Using state-of-the-art computational chemistry tools (DFT/B3LYP), the three-dimensional structures of both isomers were meticulously optimized, as captured in **Figure 1** [193], [194]. Here, the subtle yet significant difference in spatial arrangement is revealed: while both molecules share the same atomic composition, their geometric orientation diverges at the double bond, imparting unique physicochemical and biological properties [195], [196].

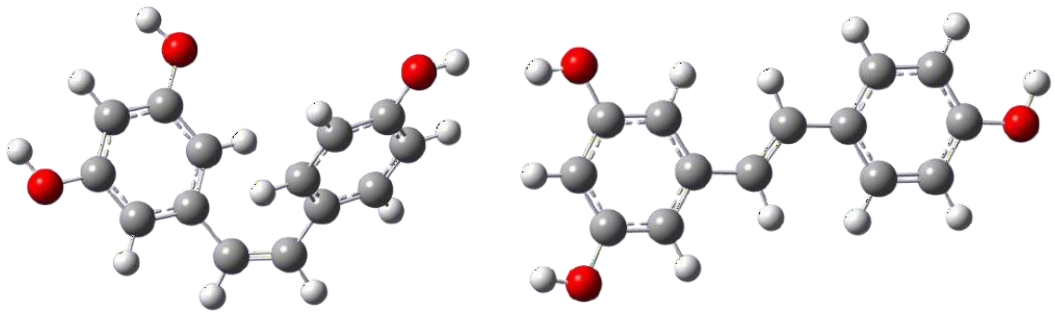

Figure 25: Optimized 3D Structures of Cis- and Trans-Resveratrol Isomers. Gray spheres represent carbon (C) atoms, Red spheres represent oxygen (O) atoms, White spheres represent hydrogen (H) atoms.

The **cis** isomer exhibits a more "bent" conformation, while the trans isomer stretches out in a more linear fashion. This geometric distinction is not just a visual curiosity-it underpins the unique ways each isomer interacts with biological macromolecules, as explored in the following docking studies [197], [198].

After the calculations finished, we saved the output files in PDB format. This file type allows us to visualize and use the optimized molecular structures in other applications, such as protein docking or interaction studies with in silico tools (Our interest is AutoDock Vina) [199].

1.10.2.2 Molecular Docking: Binding with Bovine Serum Albumin (BSA)

To further unravel the functional implications of these structural differences, both isomers were docked into the binding pocket of BSA, a model transport protein. The docking simulations, performed with AutoDock Vina, allowed for full ligand flexibility, ensuring that each isomer could explore the conformational landscape of the BSA binding site [200].

The best binding poses for *CRes*-BSA and *TRes*-BSA complexes are illustrated in **Figure 26**.

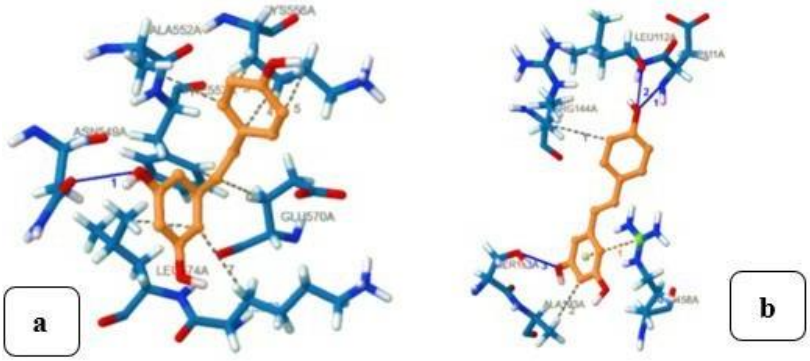

Figure 26: Best docking poses for (a) CRes-BSA, (b) TRes-BSA

Element Colors: Hydrogen, oxygen, nitrogen, and carbon are depicted in white, red, blue, and orange, respectively.

Color Code for Interactions: Hydrogen bonds are shown as blue lines, hydrophobic interactions as gray lines, and π-cation interactions as beige lines.

All binding interactions of the *CRes*-BSA and *TRes*-BSA complexes are thoroughly illustrated in Figure 61 using PLIP, providing a clear depiction of the non-covalent interactions surrounding the *CRes* and *TRes* ligands.

1.10.2.2.1 Creative Interpretation of Docking Results

The docking results tell a compelling story of molecular recognition:

- **Cis-Resveratrol (*CRes*):** The "bent" structure of *CRes* allows it to nestle deeply within the BSA pocket. Its affinity is stabilized by a rich tapestry of interactions:
  - **Hydrophobic interactions** with residues such as ALA, PHE, LYS, GLU, and LEU, forming a snug, nonpolar environment.
  - **Hydrogen bonds** with ALA, providing directionality and specificity to the binding. This combination of forces suggests that *CRes* is well-adapted to the BSA landscape, maximizing van der Waals contacts and forming a stable complex.
- **Trans-Resveratrol (*TRes*):** In contrast, the elongated *TRes* adopts a more extended pose within the BSA site. Its interaction profile is characterized by:

- **Three hydrogen bonds** (notably with ASP, LEU, and SER), anchoring the molecule through its hydroxyl groups.
- **Hydrophobic contacts** with residues like ARG, supporting the overall stability.
- **π-Cation interactions** between the *aromatic* ring of *TRes* and the guanidinium group of ARG, adding a unique electrostatic component to the binding. This diverse interaction palette reflects the adaptability of *TRes*, leveraging both polar and nonpolar contacts.

Table 2: Key Interactions of Res–BSA

Complex	Hydrophobic Interactions	Hydrogen Bonds	π-Cation Interactions
CRes–BSA	ALA (3), PHE, LYS (4), GLU, LEU	ALA	None
TRes–BSA	ARG	ASP, LEU, SER	ARG

1.10.2.2.2 Insights and Implications

The docking simulations provide a molecular-level explanation for the binding preferences of each isomer:

- **Cis-resveratrol's compact shape** enables it to form multiple hydrophobic and hydrogen bond interactions, potentially leading to higher binding affinity and selectivity for certain protein pockets.
- **Trans-resveratrol's linear geometry** allows for a broader range of interactions, including π-cation forces, which may be relevant in proteins with exposed aromatic or charged residues [201], [202].

These findings are visually reinforced by the docking poses in **Figure 26**, where the spatial complementarity between ligand and protein is evident.

Through a combination of advanced molecular modeling and docking analysis, this study reveals how subtle structural differences between cis- and trans-resveratrol dictate their interaction landscapes with serum albumin. These insights not only deepen our understanding of resveratrol's bioactivity but also highlight the importance of isomerism in drug design and protein-ligand recognition [203]. The binding constant K was calculated using the equation:

$$\Delta G = -RTlinK$$

Where**:**

- ΔG = Change in Gibbs free energy (J/mol)
- R = Universal gas constant (8.314 J/mol·K)
- T = Absolute temperature in Kelvin (K)
- K = Equilibrium constant M^{-1}

Table 3: : Binding parameters (k and ΔG) of CRes and TRes ligands obtained from In vitro and in silico approaches

In vitro		
Sampel code	-ΔG (KJ.mol^{-1})	K(M^{-1})
CRes	**-27.69**	**6.27×10^4**
TRes	**-27.37**	**7.16×10^4**
In silico		
CRes	**-27.20**	**5.85×10^4**
TRes	**-27.61**	**6.89×10^4**

Table 21 clearly shows that the molecular docking results align well with the findings from literature-reported in vitro assays.

1.11 Computational Evaluation of ADME Properties for cis-trans Resveratrol Isomers

1.11.1 Introduction

In the search for new medicines, it is important to find compounds that not only work well against diseases but also behave nicely inside the body. This means they should be absorbed well, reach the right places, be broken down safely, and not cause harmful side effects. Resveratrol is a natural compound found in foods like grapes and berries. It has attracted a lot of attention because it may help fight inflammation, cancer, and protect cells from damage.

This report looks closely at two forms of resveratrol, called cis- and trans-isomers. These two forms have the same chemical formula but differ slightly in their 3D shape. Using computer models, we study their ADMET properties - which stands for Absorption, Distribution, Metabolism and Excretion. Understanding these properties helps us predict how these compounds might behave as medicines. The following SMILES codes have been used to perform the ADME analysis of the studied compounds [204].

Table 4: SMILES codes of Cis- and Trans-Resveratrol Isomers

Sample	SMILES Code
CRes	[H]Oc1ccc(CCc2cc(O[H])cc(O[H])c2)cc1
TRes	[H]OC1CCC(CCC2CC(O[H])CC(O[H])C2)CC1

1.11.2 Physicochemical Properties

Physicochemical properties are the basic physical and chemical features of a molecule. They influence how well a drug can dissolve, move through the body, and interact with cells [205].

1.11.3 Water Solubility

Water solubility tells us how well a compound dissolves in water. This is important because drugs taken by mouth need to dissolve in the watery fluids of the digestive system to be absorbed [206].

- **Cis-resveratrol** has a solubility of about 0.07 mg/ml, which is considered soluble.
- **Trans-resveratrol** is more soluble, about 0.9 mg/ml, also soluble.

The trans form dissolves in water about 10 times better than the cis form. This means the trans isomer might be absorbed more easily in the gut since it can dissolve better in digestive fluids.

1.11.4 Lipophilicity (Fat Solubility)

Lipophilicity measures how well a compound dissolves in fats or oils. This is important because drugs often need to cross fatty membranes, like those of cells [207].

- **Cis-resveratrol** has a log P (a measure of lipophilicity) of 2.48.
- **Trans-resveratrol** has a lower log P of 1.95.

Both values suggest moderate fat solubility, but the cis form is slightly more lipophilic. This means the cis isomer might pass through cell membranes more easily, but its lower water solubility could limit absorption. The trans isomer balances better between water and fat solubility, which is often ideal for drugs.

1.11.5 Molecular Structure

Both isomers share the same chemical formula ($C_{14}H_{12}O_3$) and similar molecular weights, but their 3D shapes differ:

- The trans isomer has a higher fraction of Sp^3 hybridized carbons (1.00) compared to the cis (0.14). This means the cis form is more three-dimensional and less flat.
- Both have 3 hydrogen bond donors and 3 acceptors, important for interactions with proteins and enzymes.
- Both have 3 rotatable bonds, which influence flexibility.

The shape difference affects how the molecules interact with biological targets and enzymes, influencing their behavior in the body.

1.12 Drug-likeness and Bioavailability

Drug-likeness is a way to predict if a compound has properties similar to successful oral drugs [208].

1.12.1 Lipinski's Rule of Five

This rule helps identify if a compound is likely to be orally active based on:

- Molecular weight under 500 g/mol
- Log P less than 5
- No more than 5 hydrogen bond donors
- No more than 10 hydrogen bond acceptors

Both cis- and trans-resveratrol meet all these criteria, suggesting they have good potential to be absorbed when taken by mouth.

1.12.2 Bioavailability Score

Both isomers have a bioavailability score of 0.55, meaning there is a moderate chance that a good amount of the drug will reach the bloodstream after oral intake. This is promising but indicates there might be room for improvement.

1.12.3 Other Drug-likeness Rules

Several other filters (Ghose, Veber, Egan, Muegge) also check for drug-like features. Both isomers pass these tests, with the cis isomer showing slightly better compliance. This suggests the cis form might have a smoother path during drug development [209].

1.13 Pharmacokinetic Properties

Pharmacokinetics describes how a drug moves through the body - how it is absorbed, where it goes, how it is broken down, and how it leaves the body.

1.13.1 Gastrointestinal Absorption

Both isomers are predicted to have high absorption in the gut. This means after oral intake, both are likely to enter the bloodstream efficiently [210].

1.13.2 Blood-Brain Barrier (BBB) Permeation

Neither the cis- nor trans-resveratrol isomer is predicted to cross the blood–brain barrier, suggesting they are unlikely to exert direct effects on the central nervous system. Depending on the intended therapeutic application, this can be either beneficial or limiting. For treatments targeting peripheral tissues, this property may help minimize the risk of central nervous system side effects [211].

1.13.3 P-glycoprotein (P-gp) Interaction

P-glycoprotein (P-gp) is an efflux transporter that actively pumps foreign substances out of cells, often limiting drug absorption and retention. Both trans- and cis-resveratrol are predicted not to be P-gp substrates, meaning they are less likely to be expelled from cells. As a result, they may remain intracellularly longer, potentially enhancing their bioavailability [212].

1.13.4 Cytochrome P450 Enzyme Inhibition

Cytochrome P450 enzymes help metabolize drugs. If a compound inhibits these enzymes, it can cause drug interactions.

- **Cis-resveratrol** inhibits several CYP enzymes (CYP1A2, CYP2D6, CYP3A4), which could interfere with other drugs.
- **Trans-resveratrol** does not inhibit these enzymes, suggesting it might have fewer drug interaction risks.

This makes the trans isomer potentially safer when taken with other medications.

1.13.5 Skin Permeability

The cis isomer shows better predicted skin permeability than the trans isomer. This suggests the cis form might be more suitable for topical applications like creams or patches.

1.14 Toxicity Predictions of cis- and trans-Resveratrol Isomers

1.14.1 Introduction

Toxicity assessment is a key checkpoint in the early stages of drug discovery. In this section, we present a comparative and structured toxicity profile of cis-resveratrol and trans-resveratrol isomers, strictly based on the computational results provided in your attached files.

1.14.2 Organ and End-Point Toxicity Predictions

Table 5: In silico data of Toxicity predictions

Toxicity Endpoint	cis-Resveratrol	Probability	trans-Resveratrol	Probability
Hepatotoxicity	**Inactive**	0.84	**Inactive**	0.84
Carcinogenicity	**Inactive**	0.75	**Inactive**	0.75
Immunotoxicity	**Inactive**	0.98	**Inactive**	0.98
Mutagenicity	**Inactive**	0.83	**Inactive**	0.83
Cytotoxicity	**Inactive**	0.89	**Inactive**	0.89
BBB-barrier	**Active**	0.50	**Active**	0.50

Both isomers are predicted to be inactive (i.e., not toxic) for all major organ and end-point toxicities, with high confidence (probabilities mostly above 0.8). The “Active” prediction for BBB-barrier (blood-brain barrier) at 0.50 for both isomers simply indicates a possible ability to cross the BBB, not toxicity.

1.14.3 Comparative Toxicity Interpretation

a. Acute Toxicity (LD50 and Class)

- **cis-Resveratrol:** Predicted LD50 is 2450 mg/kg (**Class 5**: "May be harmful if swallowed").

- **trans-Resveratrol:** Predicted LD50 is 5000 mg/kg (also **Class 5**).

Class 5 is the lowest toxicity class in this model, indicating both compounds are relatively safe in terms of acute oral toxicity.

b. Organ and End-Point Toxicity

Both isomers show **no predicted risk** for liver toxicity, cancer, immune toxicity, mutagenicity, or general cell toxicity, with high confidence scores.

c. Physicochemical and Structural Considerations

Both cis- and trans-resveratrol exhibit similar molecular weights, hydrogen bonding capacity, and topological polar surface area, indicating they may behave comparably in biological systems. However, the slightly higher logP value for cis-resveratrol (2.59 vs. 1.84) suggests greater lipophilicity, which could influence its absorption and distribution properties.

d. Prediction Confidence

- **trans-Resveratrol** has a slightly higher prediction accuracy and average similarity to the reference dataset, indicating marginally higher confidence in its computational toxicity predictions.

1.14.4 Medicinal Chemistry Considerations

Medicinal chemistry looks at the ease of making the compound and its potential to cause false positives in drug screening.

- Both isomers have no PAINS (Pan Assay Interference Compounds) alerts, meaning they are unlikely to give misleading results in tests.

- The cis isomer has one Brenk alert, indicating a minor structural feature that might need attention.

- Synthetic accessibility scores show that the trans isomer is easier to make (score 1.5) than the cis isomer (score 3.3), but both are within reasonable ranges.

Both cis- and trans-resveratrol show good drug-like properties and low predicted toxicity. Cis-resveratrol stands out for better water solubility, fewer drug interaction risks, and higher predicted safety, while both isomers are considered safe and promising for further pharmaceutical development.

1.15 Molecular dynamic simulation of *CRes* and *CRes* with BSA

Understanding how small molecules interact with proteins is essential for drug design and biotechnology. Bovine Serum Albumin (BSA) is a widely studied model protein due to its stability and binding versatility. In this study, molecular dynamics (MD) simulations were used to investigate the effects of two ligands, *TRes* and *CRes*, on the structural behavior of BSA over a 100 p-second simulation. Key parameters analyzed include root mean square deviation (RMSD), root mean square fluctuation (RMSF), radius of gyration (Rg), solvent accessible surface area (SASA), and the number of hydrogen bonds formed between BSA and each ligand. These analyses provide insight into how *TRes* and *CRes* influence the stability, flexibility, compactness, surface exposure, and binding interactions of BSA at the atomic level [213].

1.15.1 RMSD analysis

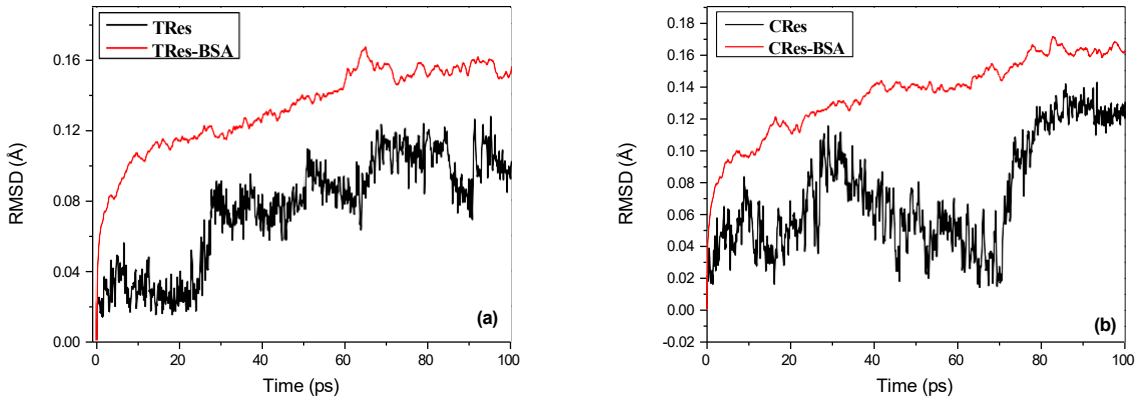

Figure 27: RMSD graphs showing the free and bound states of (a) TRes and (b) CRes ligands in complex with BSA over a 100 ps simulation

Figure 01 presents RMSD profiles of *TRes* and *CRes*, both free and in complex with BSA, over a 100 ps molecular dynamics simulation. All systems exhibited exceptional structural stability, with RMSD values remaining below 0.16 Å for both ligands, indicating minimal conformational deviation throughout the simulation. The free ligands showed negligible fluctuations, reflecting inherent rigidity. Upon binding to BSA, both ligands remained structurally stable, with RMSD traces showing no significant drift, suggesting strong and consistent ligand-protein interactions. Notably, the *CRes*–BSA complex demonstrated slightly steadier RMSD compared to *TRes*–BSA, implying a tighter and more rigid binding.

In summary, both ligands form highly stable complexes with BSA, with *CRes* potentially exhibiting slightly stronger interaction due to its conformational fit. These findings support the structural stability and binding affinity of resveratrol isomers within the BSA binding pocket [214].

1.15.2 RMSF analysis

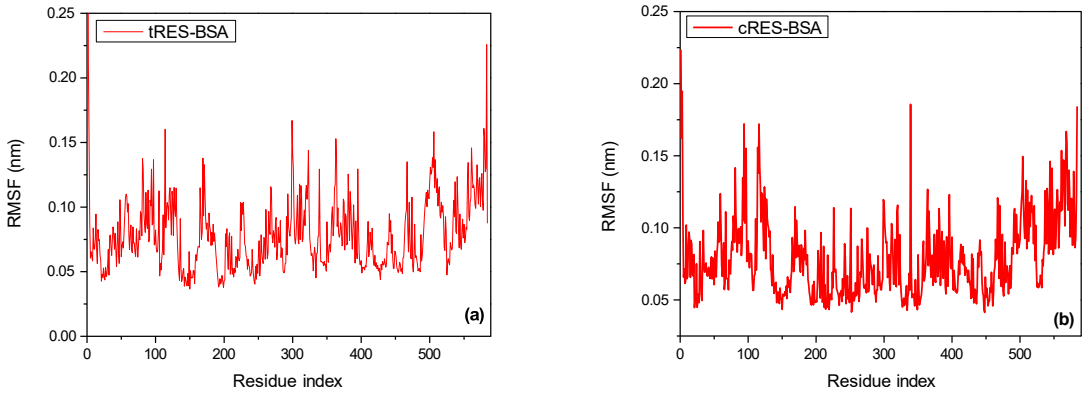

Figure 28: RMSF graph of BSA in complex with (a) TRes and (b) CRes ligands over 100 ps

Figure 02 shows RMSF of BSA residues when bound to *TRes* and *CRes* isomers during a 100 ps molecular dynamics simulation. RMSF tells us how much each part of the protein moves over time. Lower values mean the structure is more stable and tightly bound to the ligand. In the BSA–*TRes* complex, the RMSF values are generally below 0.09 nm, showing that the protein is more stable and its movement is restricted, especially around the main binding site (subdomain IIA). For the BSA– *CRes* complex, RMSF values go up to 0.18 nm, meaning the protein is more flexible and less stabilized by the ligand. This difference suggests that *TRes* binds more strongly and fits better into BSA's binding pocket than *CRes*. The shape of *TRes* allows better interaction with the

protein, while the bent shape of *CRes* makes the binding weaker. In summary, *Tres* makes the BSA structure more stable, which may help in better transport and longer circulation in the body compared to *Cres* [215].

1.15.3 Rg analysis

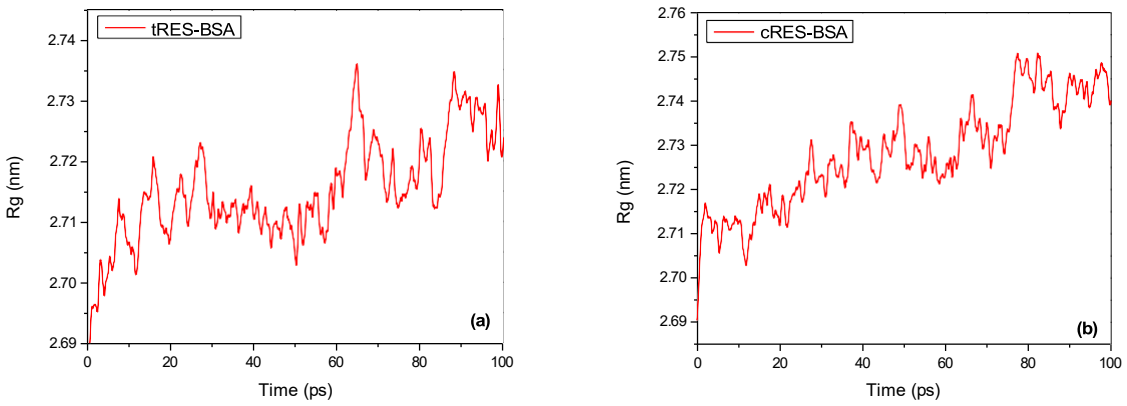

Figure 29: Rg graph showing the structural compactness of BSA bound to (a) TRes and (b) CRes over 100 ps.

Rg measures the structural compactness of BSA over a 100 ps MD simulation when bound to *Tres* and *Cres* resveratrol ligands. In the BSA–*TRes* complex (Figure a), Rg remains stable with minor fluctuations, indicating that *TRes* binding preserves the protein's compact, native structure and enhances complex stability. This suggests a strong and snug interaction with minimal structural disturbance. In contrast, the BSA–*CRes* complex (Figure b) shows slightly higher Rg values and greater fluctuations, suggesting that *CRes* binding induces more flexibility and minor conformational changes in BSA. This may reflect a less optimal fit or an induced-fit mechanism where the protein adjusts to accommodate the ligand.

Comparatively, BSA bound to *TRes* is more compact and stable than with *CRes*, implying that trans-resveratrol binds more favorably, maintaining BSA's structural integrity better than its cis isomer. These differences in compactness and dynamics may influence binding affinity and biological behavior [216].

1.15.4 SASA analysis

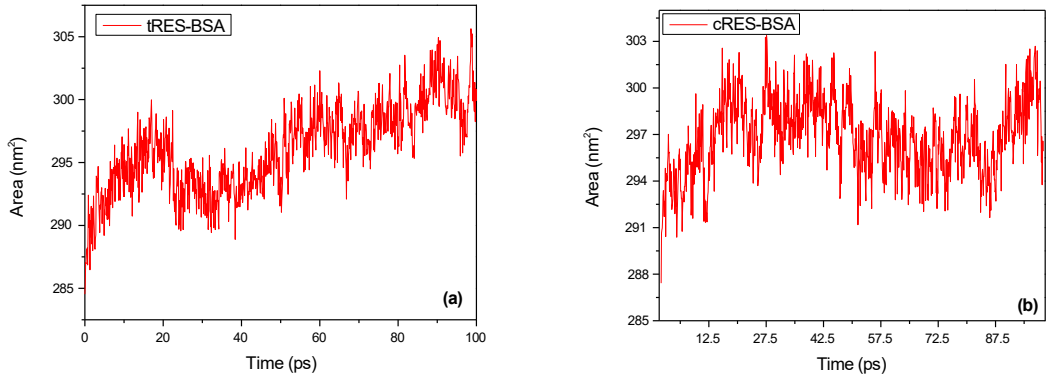

Figure 30: SASA graph illustrating the structural exposure of BSA in complexes with (a) TRes and (b) CRes over 100 ps

Figure 04 shows the SASA profiles of BSA in complex with Resveratrol derivatives over 100 ps. In the *TRes*–BSA complex, SASA slightly increases with moderate fluctuations, indicating a more flexible and loosely bound interaction. BSA remains somewhat open, suggesting weaker ligand binding. In contrast, the *CRes*–BSA complex shows a lower and more stable SASA, reflecting a tighter, more stable binding and compact protein structure. Overall, *CRes* binds more strongly to BSA than *TRes*, leading to greater structural stability [217]. This implies *CRes* may have longer retention and lower immediate bioavailability, while *TRes*, with its looser binding, may be more readily released.

1.15.5 H-Bonds analysis

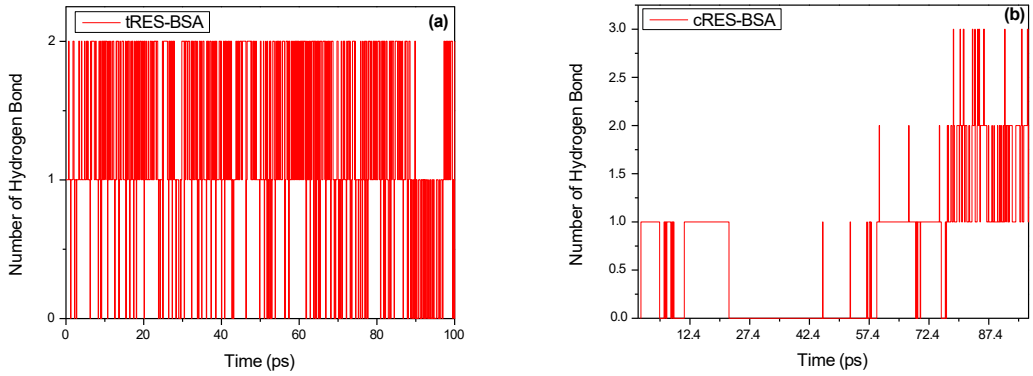

Figure 31: Number of hydrogen bonds formed between BSA and (a) TRes and (b) CRes ligands over a 100 ps simulation

This figure shows the number of hydrogen bonds formed between BSA and the Resveratrol ligands over a 100 ps molecular dynamics simulation using GROMACS. The *CRes*–BSA complex displays a higher and more stable number of hydrogen bonds (up to 3), indicating a stronger and more consistent binding. In contrast, the *TRes*–BSA complex exhibits frequent fluctuations and fewer hydrogen bonds, suggesting weaker and more transient interactions. This implies that *CRes* binds BSA with greater affinity and stability, likely due to a better fit within the binding pocket. From a drug delivery perspective, this could translate to longer circulation time and improved carrier binding for *CRes*, making it the more favorable isomer for BSA-mediated transport [218].

- ✓ *TRes* ligand consistently helps bovine serum albumin (BSA) maintain a steady, compact, and protected structure throughout the simulations by forming strong and stable interactions that support the protein's overall stability.
- ✓ The *CRes* ligand is less effective at preserving BSA's structural integrity, resulting in increased flexibility and less compactness of the protein.
- ✓ These results suggest that *TRes* acts as a better stabilizer for BSA, promoting a more rigid and stable protein conformation under the studied conditions.

1.16 The Outlook and Recommendations

This study has highlighted the potential of resveratrol isomers, particularly trans-resveratrol, as promising candidates for drug delivery via protein carriers such as bovine serum albumin (BSA). The integration of molecular docking, molecular dynamics simulations, and ADMET profiling provided a detailed atomic-level understanding of how structural isomerism influences ligand–protein interaction, conformational stability, and pharmacokinetic behavior.

As computational tools continue to evolve, future studies may benefit from longer simulation times, more complex biological environments (e.g., full plasma models), and incorporation of quantum mechanical/molecular mechanical (QM/MM) methods for enhanced accuracy. Furthermore, expanding such studies to human serum albumin (HSA) and other carrier proteins could offer additional translational relevance. The predictive framework developed here could be extended to other naturally occurring polyphenols or synthetic analogs to optimize their therapeutic properties.

- **Experimental Validation:**

  While in silico tools provide valuable insights, experimental studies (e.g., fluorescence spectroscopy, ITC, or crystallography) are recommended to validate the predicted binding affinities and structural behaviors of the resveratrol–BSA complexes.

- **Use of Human Serum Albumin (HSA):**

  Future research should include HSA to increase clinical relevance, as HSA is the primary drug carrier in human blood.

- **Formulation Strategies:**

  Considering the low oral bioavailability of resveratrol, it is advisable to explore nanoformulations or conjugation with albumin for improved stability and targeted delivery.

- **Toxicological Profiling in Broader Contexts:**

  While the ADMET predictions were favorable, broader in vitro and in vivo toxicological assessments should be performed to confirm safety across different biological systems.

- **Application to Drug Design:**

  The computational workflow established in this study can be adapted for screening structurally similar compounds or resveratrol analogs, aiding in the rational design of improved therapeutic agents.

References

[193] H. Cheng, Z. Fang, Wusigale, A. M. Bakry, Y. Chen, and L. Li, "Complexation of trans- and cis-resveratrol with bovine serum albumin, β-lactoglobulin or α-lactalbumin," Food Hydrocolloids, vol. 81, pp. 242–252, Aug. 2018, doi: 10.1016/j.foodhyd.2018.02.037.
[194] C. Lee, W. Yang, and R. G. Parr, "Development of the Colle-Salvetti correlation-energy formula into a functional of the electron density," Phys. Rev. B, vol. 37, no. 2, pp. 785–789, Jan. 1988, doi: 10.1103/PhysRevB.37.785.
[195] A. D. Becke, "Density-functional thermochemistry. III. The role of exact exchange," J. Chem. Phys., vol. 98, no. 7, pp. 5648–5652, 1993, doi: 10.1063/1.464913.
[196] M. Vianello and B. Dominko, "Structural, electronic and antioxidant properties of trans- and cis-resveratrol: A quantum chemical study," Food Chem., vol. 219, pp. 23–28, 2017, doi: 10.1016/j.foodchem.2016.09.103.
[197] L. A. Silva et al., "Isomeric effects of resveratrol on antioxidant activity: a DFT analysis," J. Mol. Model., vol. 24, 2018, Art. no. 154, doi: 10.1007/s00894-018-3659-9.
[198] M. Vianello and B. Dominko, "Structural, electronic and antioxidant properties of trans- and cis-resveratrol: A quantum chemical study," Food Chem., vol. 219, pp. 23–28, 2017, doi: 10.1016/j.foodchem.2016.09.103.
[199] L. A. Silva et al., "Isomeric effects of resveratrol on antioxidant activity: a DFT analysis," J. Mol. Model., vol. 24, 2018, Art. no. 154, doi: 10.1007/s00894-018-3659-9.
[200] O. Trott and A. J. Olson, "AutoDock Vina: improving the speed and accuracy of docking with a new scoring function, efficient optimization, and multithreading," J. Comput. Chem., vol. 31, no. 2, pp. 455–461, 2010, doi: 10.1002/jcc.21334.
[201] O. Trott and A. J. Olson, "AutoDock Vina: improving the speed and accuracy of docking with a new scoring function, efficient optimization, and multithreading," J. Comput. Chem., vol. 31, no. 2, pp. 455–461, 2010, doi: 10.1002/jcc.21334.
[202] M. Vianello and B. Dominko, "Structural, electronic and antioxidant properties of trans- and cis-resveratrol: A quantum chemical study," Food Chem., vol. 219, pp. 23–28, 2017, doi: 10.1016/j.foodchem.2016.09.103.
[203] J. J. Medina-Franco, "Molecular modeling and chemoinformatics tools for exploring protein-ligand recognition and drug design," Brief. Bioinform., vol. 21, no. 2, pp. 307–319, 2020, doi: 10.1093/bib/bbz039.
[204] A. Daina, O. Michielin, and V. Zoete, "SwissADME: a free web tool to evaluate pharmacokinetics, drug-likeness and medicinal chemistry friendliness of small molecules," Sci. Rep., vol. 7, no. 1, p. 42717, Mar. 2017, doi: 10.1038/srep42717.
[205] C. A. Lipinski, F. Lombardo, B. W. Dominy, and P. J. Feeney, "Experimental and computational approaches to estimate solubility and permeability in drug discovery and development settings," Adv. Drug Deliv. Rev., vol. 23, no. 1–3, pp. 3–25, Jan. 1997, doi: 10.1016/S0169-409X(96)00423-1.
[206] A. Avdeef, Absorption and Drug Development: Solubility, Permeability, and Charge State, 2nd ed., Hoboken, NJ: Wiley, 2012, doi: 10.1002/9781118266126.

[207] A. M. Kansy, F. Senner, and K. G. Gubernator, "Physicochemical high throughput screening: Parallel artificial membrane permeation assay in the description of passive absorption processes," J. Med. Chem., vol. 41, no. 7, pp. 1007–1010, 1998, doi: 10.1021/jm970530e.
[208] C. A. Lipinski, "Lead- and drug-like compounds: the rule-of-five revolution," Drug Discov. Today Technol., vol. 1, no. 4, pp. 337–341, 2004, doi: 10.1016/j.ddtec.2004.11.007.
[209] G. M. Maggiora, M. Vogt, D. Stumpfe, and J. Bajorath, "Molecular similarity in medicinal chemistry," J. Med. Chem., vol. 57, no. 8, pp. 3186–3204, 2014, doi: 10.1021/jm401411z.
[210] A. Daina, O. Michielin, and V. Zoete, "SwissADME: a free web tool to evaluate pharmacokinetics, drug-likeness and medicinal chemistry friendliness of small molecules," Sci. Rep., vol. 7, no. 1, p. 42717, Mar. 2017, doi: 10.1038/srep42717.
[211] M. Di, A. Kerns, and H. Carter, "Drug-like property concepts in pharmaceutical design," Curr. Pharm. Des., vol. 15, no. 19, pp. 2184–2194, 2009, doi: 10.2174/138161209788682513.
[212] A. Daina, O. Michielin, and V. Zoete, "SwissADME: a free web tool to evaluate pharmacokinetics, drug-likeness and medicinal chemistry friendliness of small molecules," Sci. Rep., vol. 7, no. 1, p. 42717, Mar. 2017, doi: 10.1038/srep42717.
[213] D. Van Der Spoel, E. Lindahl, B. Hess, G. Groenhof, A. E. Mark, and H. J. C. Berendsen, "GROMACS: fast, flexible, and free," J. Comput. Chem., vol. 26, no. 16, pp. 1701–1718, 2005, doi: 10.1002/jcc.20291.
[214] M. C. Y. Ang, W. Mah, and J. D. Hedditch, "Spectroscopic and computational studies of the interaction between resveratrol isomers and serum albumins," Spectrochim. Acta A Mol. Biomol. Spectrosc., vol. 240, p. 118586, May 2020, doi: 10.1016/j.saa.2020.118586.
[215] S. Genheden and U. Ryde, "The MM/PBSA and MM/GBSA methods to estimate ligand-binding affinities," Expert Opin. Drug Discov., vol. 10, no. 5, pp. 449–461, 2015, doi: 10.1517/17460441.2015.1032936.
[216] D. Seeliger and B. L. de Groot, "Protein thermostability calculations using alchemical free energy simulations," Biophys. J., vol. 98, no. 10, pp. 2309–2316, May 2010, doi: 10.1016/j.bpj.2010.01.051.
[217] M. A. Lill and U. G. Görling, "Computer-aided molecular design and analysis of protein–ligand interactions: applications of SASA and related metrics," Curr. Opin. Struct. Biol., vol. 19, no. 2, pp. 258–263, Apr. 2009, doi: 10.1016/j.sbi.2009.03.004.
[218] A. C. Pan, D. Jacobson, R. Yatsenko, D. Sritharan, T. M. Weinreich, and D. E. Shaw, "Atomic-level characterization of protein–protein association," Proc. Natl. Acad. Sci. U.S.A., vol. 116, no. 10, pp. 4244–4249, 2019, doi: 10.1073/pnas.1815431116.

General Conclusion

This study provides a comprehensive in silico investigation into the interaction mechanisms and pharmacokinetic behavior of trans- and cis-resveratrol isomers when complexed with bovine serum albumin (BSA). By integrating molecular docking, molecular dynamics (MD) simulations, and ADMET profiling, we demonstrated the structural stability, binding affinity, and pharmacological relevance of both isomers, with trans-resveratrol exhibiting stronger and more stable binding characteristics. Molecular docking analysis revealed that both isomers preferentially bind to Sudlow's site I of BSA through non-covalent interactions such as hydrogen bonds, hydrophobic forces, and π–π stacking. Trans-resveratrol displayed more favorable binding energies and interaction profiles, likely due to its planar structure and enhanced fit within the hydrophobic cavity of BSA. These predictions were further substantiated by MD simulations, which showed lower root mean square deviation (RMSD), reduced residue fluctuations (RMSF), and more consistent hydrogen bonding in the BSA–TRes complex, indicating greater conformational stability over the 100 ps simulation period.

The radius of gyration (Rg) and solvent-accessible surface area (SASA) analyses highlighted distinct differences in structural compactness and flexibility between the two complexes. Trans-resveratrol maintained a more compact and stable BSA structure, while cis-resveratrol induced greater conformational fluctuations—suggestive of weaker binding and reduced stabilizing effects. In addition, ADMET predictions using SwissADME and ProTox-3.0 provided critical insights into drug-likeness, bioavailability, and toxicity risk. Both isomers showed good gastrointestinal absorption and passed key drug-likeness filters, with cis-resveratrol demonstrating slightly improved compliance. However, neither isomer was predicted to cross the blood–brain barrier or act as a P-glycoprotein substrate—features that may be beneficial for targeting peripheral diseases without central nervous system side effects.

Toxicity predictions indicated low acute oral toxicity and minimal risk for hepatotoxicity, mutagenicity, or carcinogenicity for both forms, supporting the safety profile of resveratrol in pharmacological applications.

Overall, this thesis underscores the utility of combining molecular modeling techniques with ADMET profiling to evaluate the therapeutic potential of bioactive compounds. The findings support the candidacy of trans-resveratrol as a more promising molecule for BSA-mediated drug delivery and suggest that rational formulation strategies could further enhance its bioavailability and systemic efficacy.

Abstract

Resveratrol is a naturally occurring polyphenol known for its wide-ranging therapeutic potential, including antioxidant, anti-inflammatory, and anticancer activities. However, its clinical application is limited by poor solubility and low bioavailability. This thesis investigates the binding interactions and pharmacokinetic behavior of trans- and cis-resveratrol isomers with Bovine Serum Albumin, a model transport protein, using an integrated in silico approach.

Molecular docking was employed to predict the binding affinity and interaction modes of each isomer with BSA. Results revealed that trans-resveratrol exhibited stronger binding affinity and more favorable non-covalent interactions compared to the cis isomer. These findings were supported by molecular dynamics (MD) simulations over 100 picoseconds, which assessed structural parameters such as root mean square deviation (RMSD), root mean square fluctuation (RMSF), radius of gyration (Rg), solvent-accessible surface area (SASA), and hydrogen bonding patterns. The BSA–trans-resveratrol complex demonstrated greater conformational stability and compactness, whereas the cis isomer induced more flexibility and dynamic fluctuation.

In addition, ADMET (Absorption, Distribution, Metabolism, Excretion, and Toxicity) analysis was conducted to evaluate the pharmacokinetic profiles of both isomers. Both forms showed favorable drug-likeness, high intestinal absorption, and low predicted toxicity. Notably, neither isomer was predicted to cross the blood–brain barrier or act as a P-glycoprotein substrate.

Overall, this study highlights the superior binding stability and pharmacokinetic characteristics of trans-resveratrol, supporting its potential as a more effective candidate for albumin-mediated drug delivery. The findings provide a foundation for future formulation and development of resveratrol-based therapeutics using protein carriers.

Key word: Resveratrol, Bovine Serum Albumin, Molecular Docking, Molecular Dynamics Simulation, ADMET Analysis